

# DEVELOPMENT OF A NOVEL HUMIDIFIER FOR AIR BREATHING DEVICES

By

Pablo Joaquín Brizio

A thesis submitted to



Auckland University of Technology

in fulfilment of the requirements of the degree of

Master of Philosophy

January 2011

School of Engineering

Primary Supervisor: Professor Ahmed Al-Jumaily

This is a confidential commercially sensitive thesis and any copying or duplication of any of the material in this work is prohibited.

# TABLE OF CONTENTS

|   |       |
|---|-------|
| TABLE OF CONTENTS.....                      | I     |
| LIST OF FIGURES .....                       | VII   |
| LIST OF TABLES .....                        | XVII  |
| ATTESTATION OF AUTHORSHIP .....             | XVIII |
| ACKNOWLEDGEMENTS .....                      | XIX   |
| ABSTRACT .....                              | XX    |
| CHAPTER 1: INTRODUCTION .....               | 1     |
| 1.1 BACKGROUND.....                         | 1     |
| 1.2 OBJECTIVES .....                        | 2     |
| CHAPTER 2: LITERATURE SURVEY.....           | 4     |
| 2.1 INTRODUCTION.....                       | 4     |
| 2.2 ATOMIZATION PROCESSES .....             | 5     |
| 2.2.1 CENTRIFUGAL ATOMIZATION.....          | 6     |
| 2.2.2 PRESSURE ATOMIZATION .....            | 7     |
| 2.2.3 TWO-FLUID ATOMIZATION.....            | 9     |
| 2.2.4 ELECTROHYDRODYNAMIC ATOMIZATION ..... | 9     |

|   |   |    |
|---|---|----|
| 2.2.5                                       | ULTRASONIC ATOMIZATION .....  | 10 |
| 2.2.6                                       | COMBINATION OF DIFFERENT ATOMIZATION PROCESSES.....                       | 13 |
| 2.3   | DROPLET SIZE DISTRIBUTION MEASUREMENT .....                               | 16 |
| -   | Photographic methods .....  | 16 |
| -   | Impact methods .....  | 16 |
| -   | Thermal methods .....   | 16 |
| -   | Electrical methods .....  | 16 |
| -   | Optical methods.....  | 16 |
| 2.4   | WATER DROPLET VAPORIZATION .....  | 18 |
| 2.5   | PATHOGEN CONTROL.....   | 21 |
| CHAPTER 3: EXPERIMENTAL INVESTIGATION ..... |   | 23 |
| 3.1   | INTRODUCTION .....  | 23 |
| 3.2   | EXPERIMENTAL SETUP .....  | 23 |
| 3.2.1                                       | ATOMIZATION RATE .....  | 23 |
| 3.2.2                                       | DROPLET SIZE DISTRIBUTION .....   | 26 |
| 3.2.3                                       | DROPLET SIZE DISTRIBUTION AT DIFFERENT LENGTHS FROM<br>THE ATOMIZER ..... | 31 |
| 2.2.4                                       | EVAPORATION DISTANCE.....   | 33 |
| 3.3   | EXPERIMENTAL PROCEDURES .....   | 35 |



|            |   |    |
|------------|---|----|
| 3.3.1      | ATOMIZATION RATE .....  | 35 |
| 3.3.2      | DROPLET SIZE DISTRIBUTION .....   | 36 |
| 3.3.3      | DROPLET SIZE DISTRIBUTION AT DIFFERENT LENGTHS FROM<br>THE ATOMIZER ..... | 39 |
| 3.3.4      | EVAPORATION DISTANCE.....   | 40 |
| CHAPTER 4: | EXPERIMENTAL RESULTS .....  | 41 |
| 4.1        | INTRODUCTION.....   | 41 |
| 4.2        | ATOMIZATION RATE.....   | 41 |
| 4.2.1      | POWER CONSUMPTION.....  | 41 |
| 4.2.2      | EFFECT OF EXCITATION .....  | 44 |
| 4.3        | HEATING DURING ATOMIZATION.....   | 49 |
| 4.3.1      | EFFECT OF NUMBER OF PULSES .....  | 49 |
| 4.3.2      | EFFECT OF DUTY CYCLE .....  | 51 |
| 4.3.3      | EFFECT OF WAVE-SHAPE .....  | 52 |
| 4.4        | OBTAINING DROPLET SIZE DISTRIBUTION .....                                 | 53 |
| 4.4.1      | PHOTOGRAPHIC METHOD.....  | 53 |
| 4.4.2      | IMPACT METHOD .....   | 54 |
| 4.4.3      | OPTICAL METHOD.....   | 55 |

|  |  |    |
|--|--|----|
| 4.5  | DROPLET SIZE DISTRIBUTION AT DIFFERENT LENGTHS FROM THE ATOMIZER ..... | 64 |
| 4.6  | FINDING EVAPORATION DISTANCE .....                                     | 65 |
| CHAPTER 5: IMPROVEMENT OF HUMIDIFICATION ..... |  | 67 |
| 5.1  | INTRODUCTION .....   | 67 |
| 5.2  | NARROWING THE DROPLET SIZE DISTRIBUTION .....                          | 67 |
| 5.2.1  | INTRODUCTION .....   | 67 |
| 5.2.2  | DESIGN OF GEOMETRIES.....  | 68 |
| 5.2.3  | MATHEMATICAL EVALUATION OF THE GEOMETRIES .....                        | 70 |
| 5.2.4  | MIXER PERFORMANCE .....  | 74 |
| 5.3  | VAPORIZATION OF WATER DROPLETS.....                                    | 75 |
| 5.3.1  | INTRODUCTION .....   | 75 |
| 5-3-2  | ASSUMPTIONS OF THE MODEL.....  | 75 |
| 5.3.3  | GEOMETRY .....   | 76 |
| 5.3.4  | MESHING .....  | 77 |
| 5.3.5  | SET UP .....   | 78 |
| 5.3.6  | RESULTS .....  | 79 |
| CHAPTER 6: DISCUSSION AND CONCLUSION .....     |  | 87 |
| 6.1  | INTRODUCTION .....   | 87 |

|                    |   |     |
|--------------------|---|-----|
| 6.2                | ATOMIZATION PROCESS SELECTION .....       | 87  |
| 6.3                | PERFORMANCE OF ULTRASONIC ATOMIZERS ..... | 88  |
| 6.4                | VAPORIZATION OF WATER DROPLETS .....      | 89  |
| 6.5                | GENERAL OBSERVATIONS .....                | 90  |
| 6.6                | CONCLUSIONS .....                         | 91  |
| 6.7                | FUTURE WORK .....                         | 92  |
| APPENDIX A .....   |   | 94  |
| APPENDIX A.1 ..... |   | 94  |
| APPENDIX A.2 ..... |   | 95  |
| APPENDIX B .....   |   | 96  |
| APPENDIX C .....   |   | 98  |
| APPENDIX D .....   |   | 102 |
| APPENDIX D.1 ..... |   | 102 |
| APPENDIX D.2 ..... |   | 111 |
| APPENDIX D.3 ..... |   | 113 |
| APPENDIX D.4 ..... |   | 115 |
| APPENDIX D.5 ..... |   | 117 |
| APPENDIX D.6 ..... |   | 119 |
| APPENDIX D.7 ..... |   | 122 |

|                  |     |
|------------------|-----|
| APPENDIX E ..... | 125 |
| REFERENCES.....  | 128 |

## LIST OF FIGURES

|  |    |
|--|----|
| Figure 2-1: Layout to control the humidity and temperature. ....   | 5  |
| Figure 2-2: Atomization processes classification. ....   | 6  |
| Figure 3-1: Schematic of the setup for atomization rate experiments. ....  | 24 |
| Figure 3-2: Setup for atomization rate experiments.....  | 25 |
| Figure 3-3: Experimental Setup. ....   | 27 |
| Figure 3-4: High speed camera mounted into the microscope.....   | 27 |
| Figure 3-5: Water droplets above the lens. ....  | 27 |
| Figure 3-6: Water droplets being captured between sampling slides. ....  | 28 |
| Figure 3-7: Microscope with camera connected to a computer for the measurement of water droplets with an impact method. ....           | 28 |
| Figure 3-8: Schematic diagram of the principle used by the Spraytec RTSizer [92]. ....   | 29 |
| Figure 3-9: Experimental set up for the generation and measurement of water droplets with an optical method. ....                      | 30 |
| Figure 3-10: Schematic of the setup for the measurement of the droplet size distribution at different distances from the atomizer..... | 31 |
| Figure 3-11: Setup for the measurement of the droplet size distribution at different distances from the atomizer. ....                 | 32 |
| Figure 3-12: Custom-made heater used in the setup.....   | 33 |

|   |    |
|---|----|
| Figure 3-13: Detail of the tube with the housing structure and sensors.....   | 34 |
| Figure 3-14: Measurement of Current (V1/Req) and Voltage (V2) on the transducer...35  |    |
| Figure 3-15: Image of particles magnified 400X (photographic method). ....  | 37 |
| Figure 3-16: Background showing particles deposited on the glass (photographic method). ....  | 37 |
| Figure 3-17: Difference image showing the droplets without the background (photographic method). ....   | 37 |
| Figure 3-18: Difference binary image showing the droplets (photographic method).....  | 37 |
| Figure 3-19: Image of particles magnified 400X (impact method). ....  | 38 |
| Figure 3-20: Background showing particles deposited on the glass.....   | 38 |
| Figure 3-21: Difference image showing the droplets without the background (photographic method). ....   | 38 |
| Figure 3-22: Water droplets flowing into the tube. Relative humidity and temperature were measured to determine the water vapour content..... | 40 |
| Figure 4-1: Voltage on the terminals of a 1.5 MHz transducer when a square wave is applied.....   | 42 |
| Figure 4-2: Current on a 1.5 MHz transducer when a square wave is applied. ....   | 42 |
| Figure 4-3: Atomization rate of an ultrasonic transducer excited 25% of the time. Bars indicate standard deviation.....                       | 45 |
| Figure 4-4: Atomization rate of an ultrasonic transducer excited 50% of the time. Bars indicate standard deviation.....                       | 45 |

|  |    |
|--|----|
| Figure 4-5: Atomization rate of an ultrasonic transducer excited 75% of the time. Bars indicate standard deviation.....                                    | 46 |
| Figure 4-6: Atomization rate versus power consumption of a 1.5 MHz transducer excited at different duty cycles. Bars indicate standard deviation. ....     | 47 |
| Figure 4-7: Atomization rate versus power consumption for a 1.5 MHz transducer excited with sine (green) and square (blue) pulses at four duty cycles..... | 48 |
| Figure 4-8: Temperature versus power consumption of an ultrasonic transducer excited with a duty cycle of 25%. Bars indicate standard deviation. ....      | 49 |
| Figure 4-9: Temperature versus power consumption of an ultrasonic transducer excited with a duty cycle of 50%. Bars indicate standard deviation. ....      | 50 |
| Figure 4-10: Temperature versus power consumption of an ultrasonic transducer excited with a duty cycle of 75%. Bars indicate standard deviation. ....     | 50 |
| Figure 4-11: Temperature of a 1.5 MHz transducer when it was excited with sine (green) and square (blue) pulses at different powers and duty cycles. ....  | 51 |
| Figure 4-12: Temperature versus power consumption of a 1.5 MHz transducer. Bars indicate standard deviation.....   | 52 |
| Figure 4-13: Droplet size distribution for a 1.7 MHz transducer (photographic method) .....  | 53 |
| Figure 4-14: Droplet size distribution for a 1.7 MHz transducer (impact method, 699 droplets measured using 400X lens) .....                               | 54 |
| Figure 4-15: Droplet size distribution for a 2.78 MHz transducer (impact method, 279 droplets measured using 400X lens) .....                              | 55 |

|  |    |
|--|----|
| Figure 4-16: Droplets size distribution of transducers of different frequencies excited with sine pulses. ....   | 56 |
| Figure 4-17: Droplets size distribution of transducers of different frequencies excited with square pulses. ....   | 56 |
| Figure 4-18: Droplet size distribution for ultrasonic transducers of different frequencies continuously excited with square (green) and sine (blue) waves..... | 58 |
| Figure 4-19: Droplet size distribution of a 1.7 MHz transducer continuously excited with a square wave. ....   | 59 |
| Figure 4-20: Droplet size distribution of a 1.7 MHz transducer continuously excited with a sine wave. ....   | 59 |
| Figure 4-21: Droplet size distribution of a 1.7 MHz transducer excited with bursts of 5000 sine-shaped pulses. ....  | 61 |
| Figure 4-22: Droplet size distribution of a 1.7 MHz transducer excited with bursts of sine pulses. The duty cycle was 25%. ....                                | 63 |
| Figure 5-1: One of the geometries designed (left) and simulated (right) in SolidWorks™ .....   | 68 |
| Figure 5-2: Mixer 1 which offers no opposition to the pass of big droplets. ....   | 69 |
| Figure 5-3: Mixer 2 has a planar disk in the centre.....   | 69 |
| Figure 5-4: Mixer 3 has a conic structure in the centre.....   | 69 |
| Figure 5-5: Simulation of the air flow surrounding the transducer and water reservoir and leaving through mixer 1. ....  | 71 |



|  |    |
|--|----|
| Figure 5-6: Simulation of the air flow surrounding the transducer and water reservoir and leaving through mixer 2. ....  | 72 |
| Figure 5-7: Simulation of the air flow surrounding the transducer and water reservoir and leaving through mixer 3. ....  | 73 |
| Figure 5-8: Droplet size distribution of a spray generated by ultrasonic transducers using either mixer 1 (blue) or mixer 2 (green). ....  | 74 |
| Figure 5-9: Geometry of a 1/8 section of the cylinder. ....  | 76 |
| Figure 5-10: Meshing of the geometry. ....   | 77 |
| Figure 5-11: Result of the simulation with initial droplets of 5 $\mu\text{m}$ , water temperature of 50°C and air temperature of 25°C. ....                                     | 79 |
| Figure 5-12: Result of the simulation with initial droplets of 5 $\mu\text{m}$ , water temperature of 50°C and air temperature of 50°C. ....                                     | 80 |
| Figure 5-13: Result of the simulation with initial droplets of 5 $\mu\text{m}$ , water temperature of 50°C and air temperature of 100°C. ....                                    | 81 |
| Figure 5-14: Result of the simulation with initial droplet size distribution characteristic of a 1.5 MHz transducer, water temperature of 50°C and air temperature of 25°C. .... | 82 |
| Figure 5-15: Result of the simulation with initial droplet size distribution characteristic of a 1.7 MHz transducer, water temperature of 50°C and air temperature of 25°C. .... | 83 |
| Figure 5-16: Result of the simulation with initial droplet size distribution characteristic of a 2.1 MHz transducer, water temperature of 50°C and air temperature of 25°C. .... | 84 |
| Figure 5-17: Result of the simulation with initial droplet size distribution characteristic of a 2.6 MHz transducer, water temperature of 50°C and air temperature of 25°C. .... | 85 |

|  |     |
|--|-----|
| Figure 5-18: Result of the simulation with initial droplet size distribution characteristic of a 3.0 MHz transducer, water temperature of 50°C and air temperature of 25°C. .... | 86  |
| Figure D-1: Voltage on the terminals of a 1.5 MHz transducer when a sine wave is applied.....  | 102 |
| Figure D-2: Current on a 1.5 MHz transducer when a sine wave is applied. ....  | 102 |
| Figure D-3: Voltage on the terminals of a 1.7 MHz transducer when a square wave is applied.....  | 103 |
| Figure D-4: Current on a 1.7 MHz transducer when a square wave is applied. ....  | 103 |
| Figure D-5: Voltage on the terminals of a 1.7 MHz transducer when a sine wave is applied.....  | 104 |
| Figure D-6: Current on a 1.7 MHz transducer when a sine wave is applied. ....  | 104 |
| Figure D-7: Voltage on the terminals of a 2.1 MHz transducer when a square wave is applied.....  | 105 |
| Figure D-8: Current on a 2.1 MHz transducer when a square wave is applied. ....  | 105 |
| Figure D-9: Voltage on the terminals of a 2.1 MHz transducer when a sine wave is applied.....  | 106 |
| Figure D-10: Current on a 2.1 MHz transducer when a sine wave is applied. ....   | 106 |
| Figure D-11: Voltage on the terminals of a 2.6 MHz transducer when a square wave is applied.....   | 107 |
| Figure D-12: Current on a 2.6 MHz transducer when a square wave is applied. ....   | 107 |
| Figure D-13: Voltage on the terminals of a 2.6 MHz transducer when a sine wave is applied.....   | 108 |

|   |     |
|---|-----|
| Figure D-14: Current on a 2.6 MHz transducer when a square wave is applied. ....  | 108 |
| Figure D-15: Voltage on the terminals of a 3.0 MHz transducer when a square wave is applied. ....   | 109 |
| Figure D-16: Current on a 3.0 MHz transducer when a square wave is applied. ....  | 109 |
| Figure D-17: Voltage on the terminals of a 3.0 MHz transducer when a sine wave is applied. ....   | 110 |
| Figure D-18: Current on a 3.0 MHz transducer when a sine wave is applied. ....  | 110 |
| Figure D-19: Atomization rate versus power consumption of a 1.7 MHz transducer excited at different duty cycles. Bars indicate standard deviation. ....   | 111 |
| Figure D-20: Atomization rate versus power consumption of a 2.1 MHz transducer excited at different duty cycles. Bars indicate standard deviation. ....   | 111 |
| Figure D-21: Atomization rate versus power consumption of a 2.6 MHz transducer excited at different duty cycles. Bars indicate standard deviation. ....   | 112 |
| Figure D-22: Atomization rate versus power consumption of a 3.0 MHz transducer excited at different duty cycles. Bars indicate standard deviation. ....   | 112 |
| Figure D-23: Atomization rate versus power consumption for a 1.7 MHz transducer excited with bursts of 5000 sine pulses (green), 10000 sine pulses (cyan), 20000 sine pulses (brown), 5000 square pulses (blue), 10000 square pulses (red) and 20000 square pulses (magenta) of different duty cycles. .... | 113 |
| Figure D-24: Atomization rate versus power consumption for a 2.1 MHz transducer excited with sine (blue) and square (green) pulses at four duty cycles. ....  | 113 |
| Figure D-25: Atomization rate versus power consumption for a 2.6 MHz transducer excited with sine (green) and square (blue) pulses at four duty cycles. ....  | 114 |

|   |     |
|---|-----|
| Figure D-26: Atomization rate versus power consumption for a 3.0 MHz transducer excited with sine (green) and square (blue) pulses at four duty cycles..... | 114 |
| Figure D-27: Temperature of a 1.7 MHz transducer when it was excited with sine (green) and square (blue) pulses at different powers and duty cycles. ....   | 115 |
| Figure D-28: Temperature of a 2.1 MHz transducer when it was excited with sine (green) and square (blue) pulses at different powers and duty cycles. ....   | 115 |
| Figure D-29: Temperature of a 2.6 MHz transducer when it was excited with sine (green) and square (blue) pulses at different powers and duty cycles. ....   | 116 |
| Figure D-30: Temperature of a 3.0 MHz transducer when it was excited with sine (green) and square (blue) pulses at different powers and duty cycles. ....   | 116 |
| Figure D-31: Temperature versus power consumption of a 1.7 MHz transducer. Bars indicate standard deviation.....  | 117 |
| Figure D-32: Temperature versus power consumption of a 2.1 MHz transducer. Bars indicate standard deviation.....  | 117 |
| Figure D-33: Temperature versus power consumption of a 2.6 MHz transducer. Bars indicate standard deviation.....  | 118 |
| Figure D-34: Temperature versus power consumption of a 3.0 MHz transducer. Bars indicate standard deviation.....  | 118 |
| Figure D-35: Droplet size distribution of a 1.7 MHz transducer excited with bursts of 10000 sine-shaped pulses.....   | 119 |
| Figure D-36: Droplet size distribution of a 1.7 MHz transducer excited with bursts of 20000 sine-shaped pulses.....   | 119 |

|  |     |
|--|-----|
| Figure D-37: Droplet size distribution of a 1.7 MHz transducer excited with bursts of 5000 square-shaped pulses.....             | 120 |
| Figure D-38: Droplet size distribution of a 1.7 MHz transducer excited with bursts of 10000 square-shaped pulses.....            | 120 |
| Figure D-39: Droplet size distribution of a 1.7 MHz transducer excited with bursts of 20000 square-shaped pulses.....            | 121 |
| Figure D-40: Droplet size distribution of a 1.7 MHz transducer excited with bursts of sine pulses. The duty cycle was 50%.....   | 122 |
| Figure D-41: Droplet size distribution of a 1.7 MHz transducer excited with bursts of sine pulses. The duty cycle was 75%.....   | 122 |
| Figure D-42: Droplet size distribution of a 1.7 MHz transducer excited with bursts of square pulses. The duty cycle was 25%..... | 123 |
| Figure D-43: Droplet size distribution of a 1.7 MHz transducer excited with bursts of square pulses. The duty cycle was 50%..... | 123 |
| Figure D-44: Droplet size distribution of a 1.7 MHz transducer excited with bursts of square pulses. The duty cycle was 75%..... | 124 |
| Figure E-1: Droplet size distribution of a spray generated by a 1.5 MHz transducer using a mixer.....                            | 125 |
| Figure E-2: Droplet size distribution of a spray generated by a 1.7 MHz transducer using a mixer.....                            | 125 |
| Figure E-3: Droplet size distribution of a spray generated by a 2.1 MHz transducer using a mixer.....                            | 126 |

|  |     |
|--|-----|
| Figure E-4: Droplet size distribution of a spray generated by a 2.6 MHz transducer using a mixer. .... | 126 |
| Figure E-5: Droplet size distribution of a spray generated by a 3.0 MHz transducer using a mixer. .... | 127 |

## LIST OF TABLES

|   |    |
|---|----|
| Table 2-1: Atomization processes comparison .....   | 14 |
| Table 4-1: RMS values when a given voltage peak to peak is applied to transducer of different frequencies.....    | 43 |
| Table 4-2: Burst frequency for different duty cycles (bursts of 20000 pulses). ....                               | 47 |
| Table 4-3: Sauter mean diameter of transducers of different frequencies excited with sine and square pulses ..... | 57 |
| Table 4-4: Effect of the power on the Sauter mean diameter. ....  | 60 |
| Table 4-5: Sauter mean diameter of a spray produced by a 1.7 MHz trasnducer .....                                 | 62 |
| Table 4-6: Sauter mean diameter of a spray produced by a 1.7 MHz trasnducer .....                                 | 64 |
| Table 4-7: Water content in air that carries water droplets and flows inside a tube. ....                         | 65 |

## **ATTESTATION OF AUTHORSHIP**

I hereby declare that this submission is my own work and that, to the best of my knowledge and belief, it contains no material previously published or written by another person (except where explicitly defined in the acknowledgements), nor material which to a substantial extent has been submitted for the award of any other degree or diploma of a university or other institution of higher learning.

Pablo Joaquín Brizio

January 2011



## **ACKNOWLEDGEMENTS**

Firstly, I would like to express my profound gratitude to my supervisor Professor Ahmed Al-Jumaily, who not only opened me the doors of AUT and guided me in this research but also gave me support in difficult personal moments that I had during this time. He made this thesis possible.

I would also like to say thanks to Dr. Gijs Ipjma, Mohammad Al-Rawi, Dr. Robert Paxton and David White for their comments, suggestions and help in the research and IBTec for the financial support.

Lastly, my thanks to my family who gave me support from afar and my fiancée Guillermina.

## ABSTRACT

Continuous positive pressure of air on the airways (CPAP) is the most common treatment for the obstructive sleep apnea syndrome. Humidification of the air applied to the patient improves patient compliance by preventing congestion and nasal and throat dryness. Most humidifiers used in CPAP systems are traditional heating-type humidifiers which consume large amount of energy.

In this thesis, a non-traditional humidification technique was developed to be used in various respiratory supportive device applications such as CPAP therapy. Atomization processes were reviewed and ultrasonic atomizers were found to be the most suitable in terms of power consumption, droplets size distribution of the spray generated and size of the device. Four setups were used for experiments with these atomizers using five frequencies (1.5, 1.7, 2.1, 2.6 and 3.0 MHz). The experiments demonstrated that excitation with sine pulses has better efficiency than square pulses. In order to avoid overheating of the ultrasonic atomizer, the pulses must be sent in bursts and the frequency at which this bursts are sent (duty cycle) was proportional to the heating of the transducer. The droplet size distribution was measured by three different methods (photographic, impact and optic) and it did not have a significant change with the power applied to the transducer. The power did have a direct relationship with the atomization rate. Ultrasonic transducers with resonant frequency of 1.5 MHz are recommended for this application since the generated droplets have a small diameter (which facilitates its evaporation). The complexity of a driving circuit also increases with the frequency.

Ideally there should be no water droplets in the air supplied to the patient. The evaporation of the droplets was mathematically modelled and experimentally tested to determine if the air that will be supplied needs to be heated to reach the fully evaporation. With an airflow rate of 60 L/min, the full evaporation of the droplets was

reached in a relatively short distance (0.05 m) compared with the normal separation between the equipment and the patient (1.50m). There is no need to use a heater achieve such evaporation of the droplets. In this device, the pathogen risk could be reduced with the use of hydrophobic filters.

This work demonstrates that ultrasonic transducers are capable of atomizing sufficient quantities of water for this application with low power consumption.

# CHAPTER 1: INTRODUCTION

## 1.1 BACKGROUND

This chapter outlines the background and objectives of this research.

Obstructive sleep apnea syndrome (OSAS) is a common disorder which affects a significant part of the population, for instance 4% of men and 2% of women in middle aged US population [1], 4.1-7.5% of men and 2.1-3.2% of woman in the same age-ranged Asian population [2, 3] and 7.5% in Indian men [4]. OSAS is linked with anatomic or functional narrowing of the upper airway during sleeping time [5]. The consequences include respiratory disturbances from significant obstruction with or without reduced airflow (hypopnea and snoring) to total absence of airflow (apnea)[6].

Continuous positive pressure of air on the airways maintained by mechanical ventilation is the preferred treatment for OSAS [7-9]. The pressurized air inside of the airway produces the restitution of airflow and it represents an effective therapy for OSAS in many patients[10] by improving the sleep quality of patients [11].

Mechanical ventilation can be applied to the patient through an oral, nasal or full facial mask. When oral masks are used, the nose is bypassed and, as consequence of this, humidification is required [12]. Full facial masks are not comfortable and present lower patient compliance than nasal masks [13]. When using the nasal mask, most patients also breathe through the mouth, which requires a higher flow rate. The respiratory system does not provide sufficient humidification at high flow, making the use of humidifiers imperative to prevent congestion, nasal and throat dryness [14, 15].

Most humidifiers used in breathing systems are traditional heating-type humidifiers, which can result in overheating of air on hot days. Additionally, this kind of humidifier consumes a large amount of energy. Furthermore, the size of the current humidifiers presents a problem as patients require mobility to maintain their treatment.

The main goal of this research is to develop a non-traditional humidification technique which could be implemented in various respiratory supportive device applications such as continuous positive airway pressure (CPAP) therapy. The project entails the modelling, simulation, fabrication and testing of a novel humidification system.

## **1.2 OBJECTIVES**

This thesis aims to develop a novel humidifier for breathing assistive devices and aims to achieve the following objectives:

- Develop a miniaturized atomizer that will form the first stage of a humidifier with low power consumption and small droplet size distribution.
  - a- Decide on the optimal atomization method by performing a comprehensive literature review of different atomization processes. Techniques will be compared based on various parameters such as droplet size distribution, energy consumption, fabrication and electronic implementation complexity.
  - b- Experimentally evaluate the performance of the chosen atomization method for air humidification purposes.
  - c- Test different excitation modes to determine energy efficiency.
  - d- Characterize different transducers in terms of power consumption and droplet size distribution of the spray generated.

- Analyze the need for a second stage to fully evaporate the droplets produced on the first stage
  - a- Analyze of the required conditions to fully evaporate the droplets. Define the power requirements.
  - b- Design a housing structure that enhances the mixing of the air and water droplets generated by the atomizer and force the large droplets to fall back into the atomization chamber.
  - c- Formulate a mathematical model of the evaporation of water droplets in a tube to determine the length required for full evaporation in response to variables such as initial droplet size distribution, air temperature, water temperature.
- Define the final characteristics of the humidifier such as water storage, water feeding system and pathogen control technique.

## CHAPTER 2: LITERATURE SURVEY

### 2.1 INTRODUCTION

When mechanical ventilation is applied to a patient, humidification of the air is needed in order to prevent functional and morphological damage to the ciliary cells of the trachea-bronchial tree caused by the loss of moisture [16].

The humidification of air can be separated into two categories:

- Isothermal
- Adiabatic

In *isothermal humidification*, an external heat source is used to change liquid water into water vapour which is added into the air supply. *Adiabatic humidification* does not involve the contribution of thermal energy from an external source. The water is evaporated with the heat supplied by the air that is being humidified (evaporative humidifiers) or the water is atomized (disintegrated into small drops or droplets [17]) by the addition of mechanical energy and then the water droplets are injected into the air supply [18] (atomizers).

Both isothermal humidifiers and adiabatic humidifiers (without considering atomizers) need a large water surface area to be effective. Since this condition makes miniaturization difficult, it has been decided to atomize the water and then vaporize the droplets.

Figure 2-1 shows the details of the proposed layout for the control of the humidity and temperature at the output of the system. Air at the input passes through the component 1 “heater” and component 2 “atomizer” where heat and water droplets are added. Then,

the “vaporization process” takes place in component 4. Component 3 feeds water to the atomizer and the bacteria risk is reduced by component 6. The function of all the components is regulated by an appropriate control.

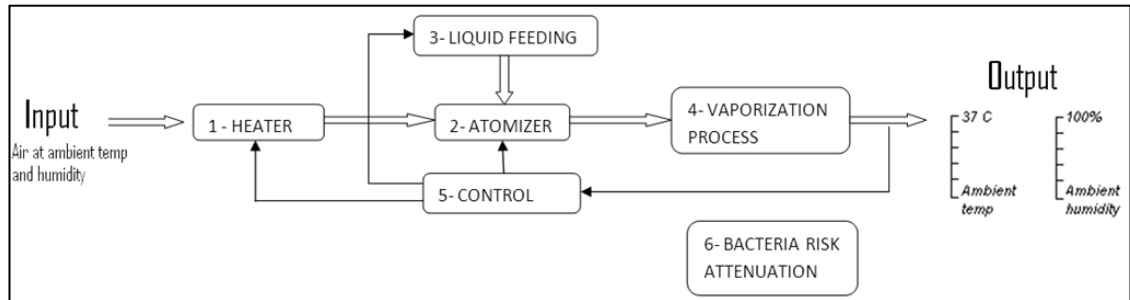


**Figure 2-1: Layout to control the humidity and temperature.**

This literature review will focus on the following subjects:

- Atomization processes (to define the atomizer)
- Droplet Size Distribution Measurement (to define the atomizer)
- Water Droplet Vaporization (to define the heater)
- Pathogen Control (to define the attenuation method)

## 2.2 ATOMIZATION PROCESSES

This section will evaluate atomizers in terms of different parameters such as droplet size distribution, energy consumption and fabrication and electronic implementation complexity.

The main methods of water atomization processes are: rotary, pressure, two-fluid, electrohydrodynamic and ultrasonic [19], see Figure 2.2



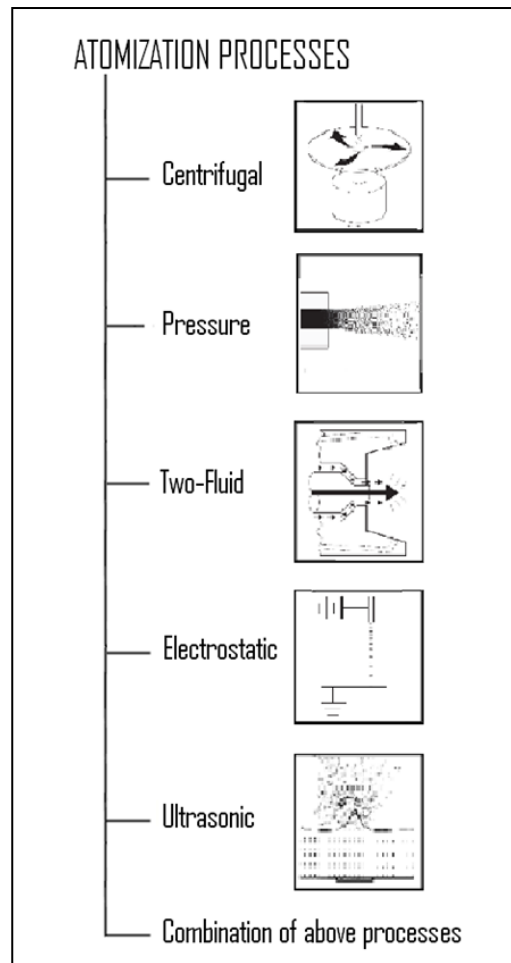


**Figure 2-2: Atomization processes classification.**

### **2.2.1 CENTRIFUGAL ATOMIZATION**

Water is fed to a rotating surface that spreads droplets due to centrifugal force [20]. The atomization occurs as a result of unstable aerodynamic waves normal to the direction of flow. This can be achieved using flat disks, vaned disks, cups, slotted wheels [19]. The opening conditions of the atomizer will determine the flow regimes [21]. The droplet size depends, amongst others, on the disk rotational speed and diameter and geometry parameters of the vanes [19, 22-25]. A narrow droplet size distribution is a characteristic of small disks, high rotational speeds and low liquid flow rates. As the

tangential velocity increases, a direct droplet formation mode changes to a ligament formation and then atomization and film formation [19, 25].

The exit velocity of water from this kind of atomizers can be predicted by analyzing the energy balance and there are theoretical equations of the trajectory of the droplets in the plane perpendicular to the atomizer's rotation axis [22]. Rotation multi-nozzle system would also be a centrifugal atomizer such as that designed by Masayuky [23]. He had predicted the parameters from the data of the experiment of a single nozzle.

The energy needed for atomization would be the energy required to accelerate the water to the tangential velocity. Roughly, mass flow rate times the half of the square rotational velocity [26]. Although the energy consumption is a good point to consider a centrifugal atomizer as a candidate, the droplets are ejected from the atomizer at high speed and are likely to impinge any close surface which makes its miniaturization difficult.

### **2.2.2 PRESSURE ATOMIZATION**

When liquid is forced through an orifice by a pressure differential, four break modes are possible: Rayleigh, First wind-induced, Second wind-induced and Atomization. These break modes depend on the Weber number ( $We$ ) of the liquid jet which is the ratio of the inertia force to surface tension force acting on the jet. This may be written as:

$$We = \rho d \mu^2 / \sigma \quad (2.1)$$

where  $\rho$  is the density of the liquid  $d$  the diameter of the stream  $\mu$  the velocity of the liquid and  $\sigma$  is the liquid surface tension respect to the air. If the Weber number is higher than 40.3, atomization of the liquid is achieved [27, 28].

Manufacturing techniques for integrated circuits (which allow the pattern and etching of tiny holes/nozzles on wafers of silicon), make possible the fabrication of pressure

atomizers for ink-jet print-head applications. The ink droplets are ejected through a nozzle by the propagation of a pressure wave generated by the growth and collapse of a gas bubble (thermal print-heads) or by the deformation of a piezoceramic material (piezoelectric print-heads). The droplet size can be manipulated by modifying the geometry of the chamber and nozzle, the excitation pulses and the quantity of water before compression (fill-before-fire level) [29]. This concept also applies to the generation of water droplets and they can be as small as 3  $\mu\text{m}$  in diameter [30]. Compared with piezoelectric print-heads, thermal print-heads have the advantage of speed and easy fabrication but also with increased power consumption [31]. Nebulizers are usually based on piezoelectric actuation due to the risk of thermal degradation of medicines that are to be nebulized [32]. Moreover, the heater has a short lifetime because of cavitation damage [33].

Instead of having an actuator pushing the liquid against the holes, some nebulizers have a vibration plate with holes that extrudes the liquid that is underneath through its holes [34]. The vibration plate is moved upwards and downwards by the action of a piezoelectric transducer that is surrounding the plate. A commercial aerosol generator can convert more than 0.75 ml/min of water in water droplets of 3-4  $\mu\text{m}$  [35]. It is important to note that a rate of 2.3 ml/min is needed to humidify 60 L/min of air from 50 % RH at 10°C to 100 % RH at 37°C. Manufacturers recommend 60 L/min of air as appropriate therapy for OSAS.

These atomizers can work in any orientation. The main drawback of this method is the possible clogging of the hole/nozzles. This problem could be solved by using distilled water.

### **2.2.3 TWO-FLUID ATOMIZATION**

Two-fluid atomization is produced by the interaction of a gas jet (usually air) and the liquid that is to be atomized. Frictional shearing forces on the surface of the liquid assist the split of droplets [36].

When the gas stream is faster, laminar and coaxial to the liquid jet and Weber number is between 1 and 40, a monodispersed droplet size distribution [37]. Coaxial gas jet is not the only configuration. Other atomizers use micro jets crossing a film of the fluid. The film of liquid is on a surface that has 7  $\mu\text{m}$  holes from which air is coming at high pressure ( $\sim 400$  KPa)[38]. The droplets produced were  $\sim 20$   $\mu\text{m}$  diameter and no smaller droplets were obtained with smaller holes [38, 39].

None of these configurations seem to be suitable for a miniaturized humidifier since they need a compressed air source.

### **2.2.4 ELECTROHYDRODYNAMIC ATOMIZATION**

A certain value of charge in a droplet generates electric forces that are stronger than those of surface tension, which promotes instability of a droplet [40]. Liquid is usually supplied by a narrow capillary/nozzle that is at a given voltage. An annular ground electrode helps the atomization. The charging of the liquid can be done by direct contact, induction and conduction [41]. Five modes of liquid disintegration can be identified in electrohydrodynamic atomization: Cone jet, Micro-dripping, Spindle, Simple jet and Dripping. Cone jet mode is the one that presents smaller droplet sizes. The size distribution is also considered monodisperse when compared with the other 3 modes [42]. This mode is the result of extremely small flow rate ( $\sim \mu\text{l/min}$ ) exposed to high DC voltage ( $\sim \text{KV}$ ). The droplet size doesn't depend on nozzle diameters, but is related to the liquid properties (electric conductivity, electric permittivity and surface

tension) [43]. Atomization of water in this mode is not common due to its high surface tension and conductivity. However, Lastow and Balachandran [44] have successfully atomized water in this mode with relatively low voltage (~4 KV). The flow rate was in the range of 0.5-4.0  $\mu\text{L}/\text{min}$ . For humidification purposes in medical devices, ~2300  $\mu\text{L}/\text{min}$  of water has to be atomized. Moreover, a power supply that provides high voltages would not be easy to miniaturize.

### **2.2.5 ULTRASONIC ATOMIZATION**

Large volumes of water aerosol can be generated by small devices with ultrasonic techniques. This techniques are also being used in medical applications generating medical solution aerosols for respiratory therapy [45]. When liquid is vibrated at high frequencies (higher than 20 KHz), a combination of capillary waves and cavitation take place and minute droplets break the surface tension of the water and quickly dissipate into the air forming fog or mist. Lang has formulated an equation that relates the droplet size with the forcing sound frequency based on Kelvin's equation and its modification by Rayleigh [46, 47].

$$D = 0.34 * \left( \frac{8 * \pi * \sigma}{\rho * F^2} \right)^{1/3} \quad (2.2)$$

Where D is the number-median diameter of the spray (drop diameter such that 50% of the number of drops in the spray have smaller diameter), F the forcing sound frequency,  $\sigma$  and  $\rho$  the surface tension and density of water respectively [48]. It seems that the diameter does not depend on the amplitude of oscillation of the transducer [49]. In the experiments, water atomized at one specific frequency results in droplets of a wide range of sizes. This can be due to phenomena of coalescence and evaporation of the droplets just after they break the surface tension [47] or because the pattern of the capillary waves on the surface of the liquid becomes chaotic a little onset of atomization

[50]. If the phenomena are the cause, the maximum entropy formulation can be used to theoretically predict the droplet size distribution [51].

There are two approaches to generate droplets by ultrasonic atomization: passing flow across a standing ultrasonic wave or depositing the liquid over an ultrasonic transducer. The first method involves a channel that works as a mechanical amplifier of the vibrations generated by circular piezoceramic plates. Experimental geometries have been tested in order to detect important design parameters such as shape, size and number of circular piezoceramic plates. By increasing atomizer size and wave amplitude, the flow rate was increased. Resonant surface area has also affected the flow rate but in less proportion [52]. Tsai et al. [53] have micromachined a 3-Fourier horn silicon nozzle that works at 0.5 MHz and produced droplet sizes smaller than those produced by other conventional ultrasonic atomizers at three times higher frequency.

Barreras, et al. [46] have focused on the second approach to atomize volumes of water of 0.2-0.4 ml. The frequency used was 1.65 MHz yielding micron-range droplets. Considering the characteristic length of the perturbations on the liquid surface was different to the droplet size, the origin of the spray droplets could be attributed to cavitation instead of capillary waves. Atomization rate was increased with increments of oscillation amplitude (proportional to voltage increments). Droplet velocities were also found to increase with the voltage. Currently, most of the atomizers have flat transducers, however, Wolf-Dietrich et al. [54] have patented an ultrasonic liquid atomizer with a continuously concave surface adapted to the liquid quantity and liquid surface tension. The atomizer was able to atomize volumes up to 15  $\mu$ l in less than 3 seconds requiring up to 30 W of power. The frequency was in the range of 1-5 MHz and most of the generated droplets had diameters smaller than 5  $\mu$ m. The atomizer could also be based on silicon membrane vibrated by a piezoelectric ZnO layer at ultrasonic frequency [55].

A pulsed excitation system is required to avoid heating the ceramic over its Curie temperature, otherwise, it is depolarized. Still, it is not easy to excite these transducers since driving circuits that provide voltages of 50-60 V and powers around 10 W are not common [56]. In order to use lower voltages, more than one transducer could be arranged to focus at the same point, considering that the intensity of the ultrasonic waves reaches a maximum at the natural focal point of the ultrasound beam [57]. To control the output, some variables such as current, voltage or power supplied to the transducer could be used as a feedback to maintain a stabilized atomization rate [58].

The excitation frequency has a limit due to resonance models and piezoelectric materials. The maximum driving frequencies that have been found in the literature are 5 and 8 MHz to yield sub-micron droplets [59, 60]. However, **Surface Acoustic Wave (SAW) devices** could work at higher frequencies [61]. These atomizers have an interdigit transducer (IDT) that, in response to an electric signal, generates a Rayleigh type SAW that is propagated on a piezoceramic plate. The energy of the SAW is radiated into liquid if it is placed in the propagation path producing the atomization of the liquid (SAW streaming) [62]. Even though ultrasonic atomizers have high energy density, good energy-conversion efficiency and small size in comparison with those produced by other methods, SAW atomizers could be 5 times smaller. Contrary to ultrasonic atomization, in which the droplet size is not related to the voltage, SAW atomizers present a relation between droplet diameter and driving voltage [63]. Chono et al. [62] have worked on continuous generation of mist by a SAW-based atomizers. A filter paper was used to keep the thin liquid layer on the surface [62]. Kurosawa et al. [64] have worked on a pumping system to be used in SAW water atomizers. The pumping effect is due to the wave motion of the elastic material and viscosity of the fluid. There is a SAW atomizer that works at 78 MHz and continuously generates droplets of 1.5  $\mu\text{m}$ . The device was constituted by an IDT, reflector, and a Rayleigh wave beam compressor [65].

Ultrasonic atomizers usually need to work in a horizontal position since the water has to be on the surface to be atomized.

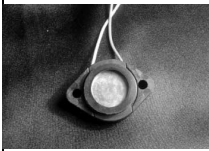
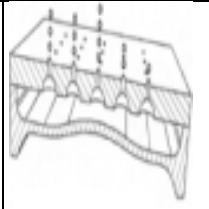
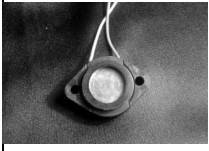
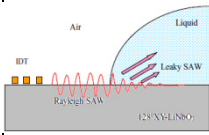
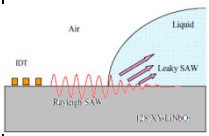
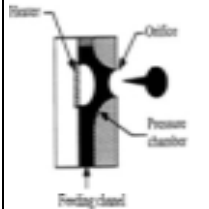
#### **2.2.6 COMBINATION OF DIFFERENT ATOMIZATION PROCESSES**

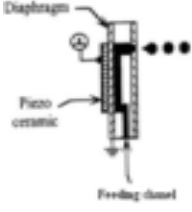
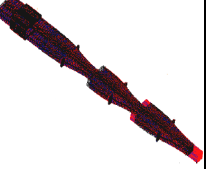
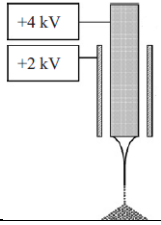
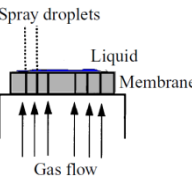
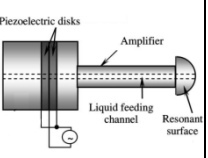
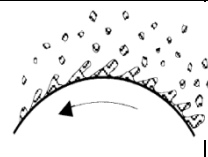
There are combinations of the mentioned atomization processes. An example of this is the ultrasound-modulated two-fluid (UMTF) atomization that utilizes air to assist the ultrasonic atomization. By ultrasound, capillary waves are produced on the liquid surface and air helps the split of small droplets from the crests [66]. Tsai et al. [67] have compared three precursor drop generation systems, namely an ultrasonic atomizer working at 120 KHz that presented low output and narrow drop size distribution, an UMTF at 120 KHz which has shown high throughput, narrow size distribution and small peak drop diameter and an ultrasonic nebulizer (1.65 MHz) with the small peak drop diameter. Ultrasonic and pressure atomization are also combined. The liquid is vibrated in a micromachined horn structure that is designed to focus the acoustic wave. The thickness of the piezoelectric transducer is chosen to match the cavity resonance. Driving electronics and control of fluid level are complex and expensive to achieve [32].

Table 2-1 summarizes devices based on different atomization processes that have shown better results considering droplet size generated, flow rate, power consumption and size.



**Table 2-1: Atomization processes comparison**

| ATOMIZER                                  |   | ATOMIZATION PRINCIPLE                           | FREQ [MHz] | DEVICE SIZE [mm <sup>2</sup> ] | DROPLET DIAMETER [μm] | POWER [W] | ATOM. RATE [ml/min] | ATOM. RATE / POWER |
|---|---|---|------------|--------------------------------|-----------------------|-----------|---------------------|--------------------|
| Ultrasonic Atomizers (Flat transd.) [56]  |    | Vibration causes capillary waves and cavitation | 1.65       | $\pi \times 10.0^2 \times 5.5$ | 3.5                   | 10.0      | 18.00               | 1.80               |
| Pressure Atomizer [68]                    |    | Vibration plate extruding water                 | 0.12       | 18.0 x 32.0 x 35.0             | 4.0                   | 1.2       | 0.50                | 0.41               |
| Ultrasonic Atomizers (Flat transd.) [46]  |   | Vibration causes capillary waves and cavitation | 1.65       | $\pi \times 10.0^2 \times 5.5$ | 3.5                   | 30.0      | 6.67                | 0.22               |
| Ultrasonic Atomizers (SAW) [63]           |  | Surface waves cause capillary waves             | 48.00      | 4.0 x 8.0 x 0.6                | 3.0                   | 2.3       | 0.17                | 0.07               |
| Ultrasonic Atomizers (SAW) [65]           |  | Surface waves cause capillary waves             | 78.00      | -                              | 1.5                   | 1.0       | 0.04                | 0.04               |
| Pressure Atom. (Thermal print-heads) [30] |  | Liquid is pushed through a nozzle               | NA         | 10.0 x 20.0 x ~0.1             | 3.0                   | -         | -                   | -                  |

|   |   |  |      |                                      |      |     |        |   |
|---|---|--|------|--------------------------------------|------|-----|--------|---|
| Pressure Atom. (Piezoelectric print-heads) [33] |    | Liquid is pushed through a nozzle                    | 3.50 | 10.0 x 10.0 x ~0.1                   | 4.0  | -   | ~3.5   | - |
| Ultrasonic Atom. (standing wave) [53]           |    | Vibration causes capillary waves and cavitation      | 0.50 | 3.8 x 1.5 x 36.6                     | 7.1  | -   | 0.05   | - |
| EHD Low Voltage Atomizer [44]                   |    | Electric charges cause cavitation of a narrow stream | NA   | $\pi \times 2.0^2 \times \sim 40.0$  | 2.5  | -   | 0.04   | - |
| Gas-Assisted Atomizers [38]                     |   | Gas jet through liquid film                          | NA   | $\pi \times 11.5^2 \times \sim 10.0$ | 20.0 | -   | -      | - |
| UMTF Atomizers [67]                             |  | Air and capillary waves                              | 0.12 | $\pi \times 18.3^2 \times 45.2$      | 44.0 | 2.3 | -      | - |
| Centrifugal Atomizers [25]                      |  | Spray due to centrifugal forces                      | NA   | $\pi \times 66.1^2 \times 12.7$      | 45.0 | -   | 365.00 | - |

The information about the size does not include the driving circuit. The higher the frequency, the more difficult the electronic implementation.

## 2.3 DROPLET SIZE DISTRIBUTION MEASUREMENT

The measurement of droplets in an aerosol presents many difficulties, primarily because aerosol droplets are not static in volume and location. Determining droplet sizes is important in many applications such as agriculture (irrigation and application of pesticide), spray combustion and energy systems, atmospheric measurements (fog formation, visibility, cloud studies and formation of rain and storm) and industrial. Medical applications such as characterization of medicinal aerosol in development of administration devices and prospective medications also require droplet size determination [69-71].

In order to measure droplet's sizes, several methods have been developed:

- **Photographic methods** which could be obtained with relatively simply techniques and equipment, although, possible errors are related to the illumination utilized, the measurement of the images and focus issues [72, 73].
- **Impact methods** are based on the fact that drops could be sized by microscopic examination after they are captured on sampling slides or cascade samplers [72].
- **Thermal methods** can be sub classified in evaporation and freezing methods. The first ones are based on the fact that evaporation times of droplets on a hot surface are a direct indication of droplet sizes. On the other hand, freezing methods consist in freezing the droplets and analyzing them like particles. These methods are not accurate for small droplets [72, 73].
- **Electrical methods** use the electrical properties of the droplet (resistance or capacitance) and relate them to their size [72].
- **Optical methods** achieve the measurement by means of processing either light scattered by the droplets or the obscuration, extinction and turbidity of a light beam passing through the aerosol. Diffraction sizers are based on the

diffraction pattern produced when a spherical particle is illuminated by a low power laser. The light beam is scattered by a droplet when its wavelength is smaller than the droplet's diameter [69]. Laser-doppler anemometers also use an optical method to measure the size distribution and they make use of the frequency of the scattered light to determine the velocity of the droplets [72].

Photographic and Optical methods are techniques often used to analyze droplet sizes in sprays [74].

The decision of which method should be used, depends on the characteristics of the spray to be measured [73]. Corcoran et al. [71] have compared a phase Doppler interferometer, a time-of-flight instrument and three diffraction instruments by testing mono-sized polystyrene latex spheres and several sprays. When measuring water sprays from nebulizers, phase doppler interferometer and diffraction instruments showed similar results but the time-of-flight instrument showed higher mass median aerodynamic diameters.

In this thesis, an impact method with sampling slides has been attempted to measure droplets produced by ultrasonic transducers at different frequencies. Hedrih et al. [75] have described this technique as easy for the measurement of water droplets smaller than 10  $\mu\text{m}$ . Yuan et al. [76] have mentioned that a technique based on this method had high accuracy and low cost, however, it presents limitations to measure small droplets as they might bypass the sampler [73]. Hedrih et al. [75] explained that there are two main problems when a glass plate is used to capture droplets, one of them is the spherical shape of the droplet changes when is in contact with the glass and the second one is the quickly evaporation of the small droplets. This technique eliminates the first problem by using a thin film of paraffin oil covering the glass surface. The second problem is solved by covering the glass with settled droplets with another thin oiled plate. There would be partial resorption of liquid drops in paraffin oil but this process is

significant after 10 or 15 minutes. They declared that this technique was easy and gave good results with small droplets.

However, when this method was used, the processing of the images was difficult since it was not possible to easily distinguish the droplets to be measured from the droplets that also appeared in the images and belonged to other planes different from the focal plane. Not even the use of filters helped to get rid of these unwanted droplets. A device based on an optical method was used, the Malvern Spraytec Laser Diffractometer because it is sensitive, accurate and available.

## 2.4 WATER DROPLET VAPORIZATION

Regardless droplets with a diameter smaller than 5 micrometers would reach the deeper lung region [77], they might not be desirable for mechanical ventilation. A water vaporization stage has to be implemented to assure that the droplets are fully vaporized into the airstream.

The difference in vapour's concentration between the free stream and the droplet surface is the driving force for small droplets to be evaporated [78]. The main mechanism of vapour transport to or from an inactive gas is diffusion. Maxwell and Langmuir have obtained the mass flux of water vapour (considering ideal gas behaviour  $\rho_i = p_i M_i / R T_i$ ) for a diffusion-controlled isothermal evaporation of a sphere [79-81]

$$j_i = \frac{D_{ij} M_i}{d} \left( \frac{p_i}{R T_a} - \frac{p_{i\infty}}{R T_\infty} \right) \quad (2.3)$$

Where  $D_{ij}$  is a diffusion coefficient for the gas mixture,  $d$  the diameter of the sphere,  $p_i$  the vapour pressure of the evaporating liquid  $i$  at the surface temperature  $T_a$ ,  $M_i$  the molecular weight,  $R$  the universal gas constant,  $p_{i\infty}$  and  $T_\infty$  the partial vapour pressure and temperature at a long distance from the surface of the evaporating liquid and. [81]

Considering that the vapour pressure at the surface is in equilibrium (due to the fast departure of molecules from the surface) and  $T_d = T_\infty$  (thanks to the high rate of heat transfer), the rate at which the diameter is decreasing is

$$\frac{dd}{dt} = \frac{4 D_v M}{R \rho d} \left( \frac{p_\infty}{T_\infty} - \frac{p_d}{T_d} \right) \phi \quad (2.4)$$

Where  $p_d$  and  $T_d$  are the pressure and temperature of the droplet respectively,  $\rho$  is the density of the liquid,  $\phi$  is a factor correction given by Fuchs for droplets smaller than  $1.0 \mu\text{m}$  [80].

The equation (2.4) can be integrated to obtain the time required to completely evaporate a droplet

$$t = \frac{R \rho d^2}{8 D_v M \left( \frac{p_\infty}{T_\infty} - \frac{p_d}{T_d} \right)} \quad (2.5)$$

Maxwell assumed that the vapor pressure at  $T_d$  is equal to the partial pressure at the surface of the droplet (vapor concentration at the surface = concentration of saturated vapor) [79]. This assumption is valid as long as the water droplet diameter is bigger than  $0.1 \mu\text{m}$ . For droplets smaller than  $0.1 \mu\text{m}$ , Kelvin equation associates the increase in vapour pressure with the surface curvature

$$p_d = p_\infty e^{\frac{4 \gamma M}{\rho R T d}} \quad (2.6)$$

$p_d$  is the vapour pressure over a curved surface,  $p_\infty$  the vapor pressure over a flat surface and  $\gamma$  the surface tension of the liquid [79-81].

An empirical expression for the saturation vapour pressure of water is

$$p_d = e^{18.72 - \frac{4062}{T-37}} [\text{mmHg}] \quad (2.7)$$

Equation (2.6) has good agreement with experimental data for  $T$  between 273 and 373°K [80]

Values of diffusion coefficient can be found for various gas mixtures at 0 °C and 760 mmHg. They can be scaled to other temperatures with the equation (1.7).

$$D \approx D_0 \left( \frac{T}{T_0} \right)^{1.94} \quad (2.8)$$

$D_0$  and  $T_0$  are the diffusion coefficient and temperature for the gas mixture at 0 °C and 760 mmHg [79].

On the other hand, the temperature of the droplet  $T_d$  can be obtained from the balance between the heat lost due to the evaporation and that gained by conduction with the surrounding air

$$T_d - T_\infty = \frac{D_v M H}{R k_v} \left( \frac{p_d}{T_d} - \frac{p_\infty}{T_\infty} \right) \quad (2.9)$$

$H$  is the latent heat of evaporation and  $k_v$  is the thermal conductivity of the gas.

Equation (2.9) cannot be evaluated explicitly (dependence of  $p_d$  on  $T_d$ ), and the following equation has good results for specific humidities ( $w$ ) between 0 and 0.5 and ambient temperatures between 0 and 20°C [80]

$$T_d - T_\infty = \frac{(6.65 + 0.345 T_\infty + 0.0031 T_\infty^2) (w - 1)}{1 + (0.082 + 0.00782 T_\infty) w} \quad (2.10)$$

## 2.5 PATHOGEN CONTROL

Sanner et al. [82] have concluded that CPAP therapy increases the risk of upper airway infection either with or without heated humidity. Yet when patients are not intubated (less exposed to pathogen), water pretreatment is recommended for ultrasonic humidifiers as any dissolved solids present will become airborne [83].

Although microbial contamination of new and used CPAP machines might be minimal [84], a report of United States Environmental Protection Agency stated that ultrasonic and impeller humidifiers can disperse microorganism and minerals present in the water used for humidification and the use of tap water in these humidifiers poses a serious health risk [85]. It also mentioned the importance of the proper care and cleaning of humidifiers in the reduction of the exposure to microorganisms. Any particle between 0.02 and 3.00 micrometers are optimal in size for depositing in the bronchi, trachea and pharynx [86]. Moreover, while dead microbial cells may not be infectious, their protein content could trigger allergic responses [87]. Convection-type humidifiers don't have this problem since bacteria present in the water do not become air-borne [88].

Rodriguez et al. [89] have investigated the bacterial contamination in noninvasive home ventilators of two brands. The most frequent microorganism was *Staphylococcus aureus* and they have concluded that the degree of cleaning and disinfection seems to affect contamination.

Even though ultrasound in the range 1-3 MHz was shown to kill bacteria in biofilms both *in vitro* and in animal models, different bacteria appeared to have different response to ultrasound waves and lower frequencies could be more effective [90].

Filtering the humid air that goes into the patient could be the solution. Ortolano et al. [91] have studied the performance of hydrophobic filters to reduce contamination risk in CPAP therapy when humidifiers are used. They have stated that hygroscopic materials would retain water and increase the pressure drop. They concluded, after analyzing the



water produced by the condensation of the humid air in the patient tube, that there may be a risk for respiratory infection when heated humidifiers are used with contaminated water and no filters. On the other hand, hydrophobic filters between humidifier and mask may reduce the risk.

## **CHAPTER 3: EXPERIMENTAL INVESTIGATION**

### **3.1 INTRODUCTION**

In this chapter, the details of the experimental investigation are presented. This includes the experimental setup and methodology.

The main purposes of the experimental investigation are to determine:

1. The atomization rate of ultrasonic transducers
2. The droplet size distribution generated by ultrasonic transducers
3. The droplet size distribution at different distances from the atomizer
4. The length of the tube and the heat required to fully evaporate the droplets produced by the atomizer

### **3.2 EXPERIMENTAL SETUP**

To fulfil the above objectives, four experimental setups were developed. In this section, these setups will be explained.

#### **3.2.1 ATOMIZATION RATE**

In order to obtain air with a relative humidity (RH) in the range of 70-100% at 37 °C at the output of the humidifier, it is necessary to find the proper excitation signal which can generate an atomization rate from 0.46 ml/min (enough to increase the humidity of 30 L/min of air with 65% RH at 25 °C to 70% at 37 °C) to 2.23 ml/min (enough to increase the humidity of 60 L/min of air with 40% RH at 20 °C to 100% at 37 °C).

Ultrasonic transducers that work at different resonant frequencies (1.5, 1.7, 2.1, 2.6 and 3.0 MHz, datasheets I and II) were tested. A precision scale (AND HF-3000G) was used to record the difference of mass of water before and after the atomization in a fixed period of time (one and two minutes). A precision in the atomization rate of 2.5% RH at 37 °C was also desirable. This is 0.03 g/min when the air flow rate is 30 L/min and 0.06 mg/min when the air flow rate is 60 L/min. Consequently, the scale was required to measure down to 0.01 g.

Figures 3-1 and 3-2 show the setup used to determine the atomization rate of the ultrasonic transducers in response to different excitation signals. The ultrasonic transducer (element 1) atomizes the water and the air flow takes away the generated water droplets. The atomization is produced inside a Y-shaped structure (part 2) and air is blown into it by a fan (Sanyo Denki 40 mm, 12 V DC Axial Fan) (element 3) to pick up the small droplets. The big droplets hit the walls of the structure and fall back on the atomizer. K-type thermocouples (Labfacility Z2-K-1M) are located outside (element 4) and inside (element 5) in contact with the water 1 cm above the transducer to measure to ambient and transducer temperatures respectively. The weight of the setup before and after the atomization was measured with a precision scale (element 6).

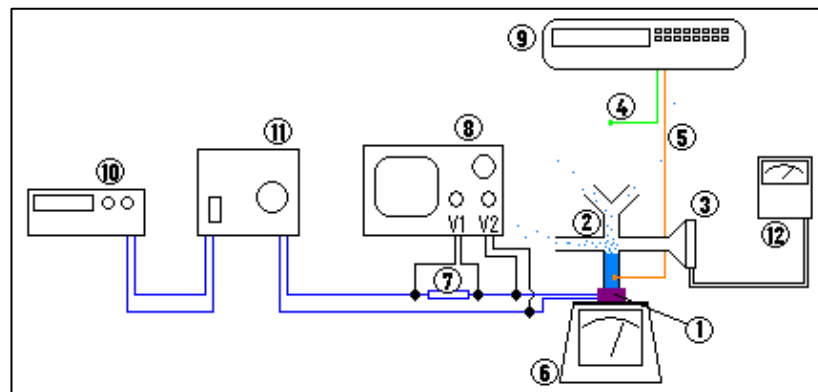


**Figure 3-1: Schematic of the setup for atomization rate experiments. Element 1- Ultrasonic transducer. 2- Y-shaped structure. 3- Fan. 4- Thermal couple measuring ambient temp. 5- Thermal couple measuring water temp. 6- Precision scale. 7- Resistances. 8- Oscilloscope. 9- Data logger. 10- Function generator. 11- Amplifier. 12- Power supply.**

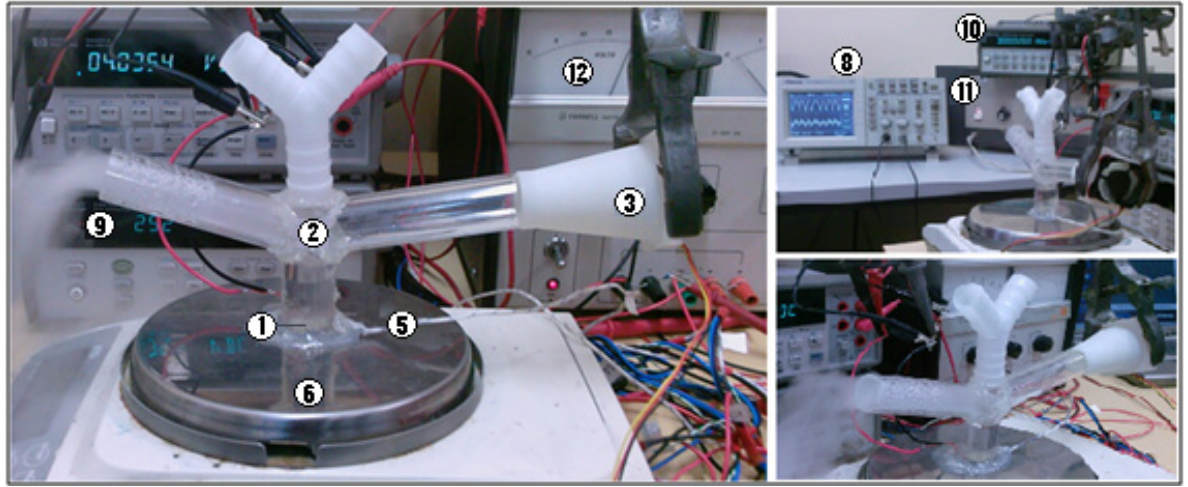


**Figure 3-2: Setup for atomization rate experiments.**

The excitation signal was produced with a function generator (Hewlett Packard 33120A) (element 10) connected to an amplifier (Amplifier Research 40A12) (element 11).

To measure the current in the transducer, four  $10\ \Omega$  resistances in parallel ( $R_{eq} = 2.5\ \Omega$ ) (element 7) were connected in series with the transducer and the voltage across these resistances was divided into the value of  $R_{eq}$ . Both the voltage across the resistances (to calculate the current) and across the transducer were recorded with an oscilloscope (Tektronix TDS 1012) (element 8) and the associated software (Open Choice Desktop Tek) to save the data. The RMS values were calculated using MATLAB<sup>TM</sup> from the measured wave shape.

Temperature was measured with a eight K-type thermocouples (Labfacility Z2-K-1M) and the humidity was measured with Honeywell HIH-4000-004 resistive sensors. These values were recorded with a data logger (Hewlett Packard 34970A) (element 9).

Experiments were conducted in order to investigate the effect of different variables such as the number of pulses, the frequency at which they are sent (duty cycle) and peak to peak voltage.

In this setup, big droplets hitting and staying on the wall did not affect the measurement of the atomization rate since they tended to return to the water reservoir (due to self weight).

### **3.2.2 DROPLET SIZE DISTRIBUTION**

Different methods (with different results) were chosen to determine the droplet size distribution generated by ultrasonic atomization at different frequencies.

Droplets to be measured were created due to the vibration of ultrasonic transducers excited with signals produced by a function generator (Hewlett Packard 33120A) (Fig 3-3, element 1) connected to an amplifier (Amplifier Research 40A12) (Fig 3-3, element 2). Three methods were used to determine the droplet size distribution.

- **Photographic Method:** Droplets were forced to fly through the focal length of an inverted microscope (Olympus IX71) (Fig 3-3, element 3). A high speed camera (PHOTRON FASTCAM-1024PCI) (Fig 3-3, element 4) was mounted to the microscope with a 400X magnification lens to capture images of the droplets at 500 frames per second.

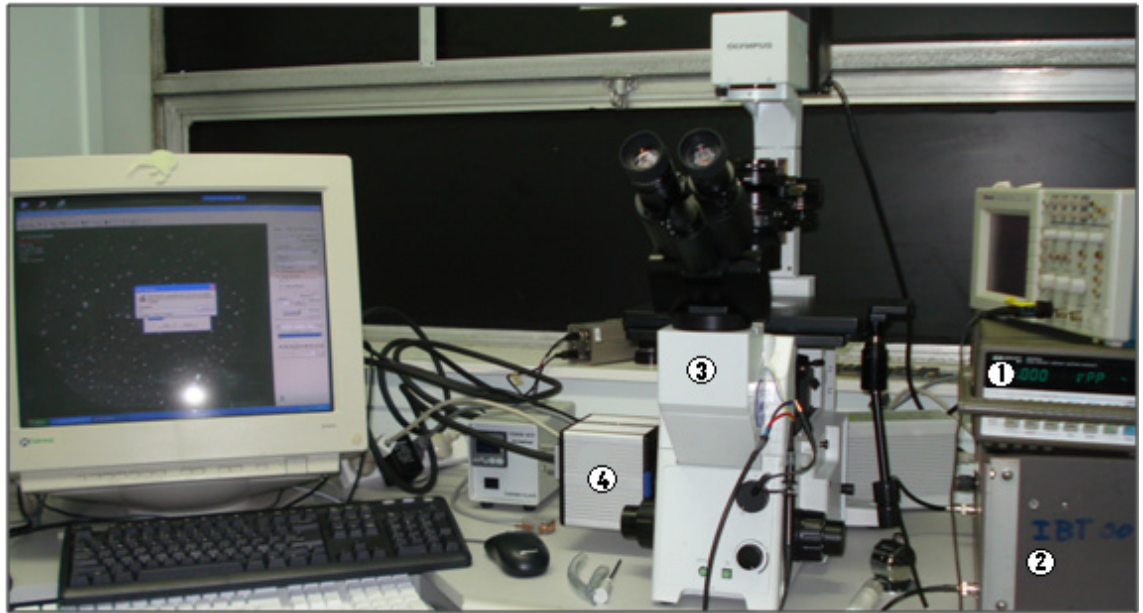


**Figure 3-3: Experimental Setup. Element 1- Function generator. 2- Amplifier. 3- Microscope. 4- High speed camera.**

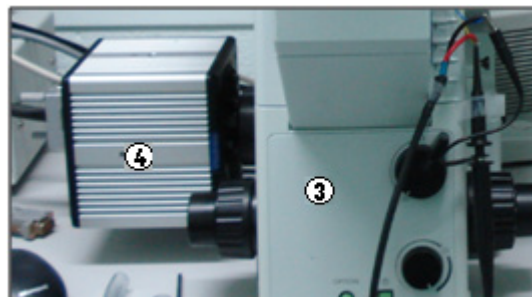


**Figure 3-4: High speed camera mounted into the microscope.**



**Figure 3-5: Water droplets above the lens.**

The images were then imported into MATLAB<sup>TM</sup> and analyzed.

- **Impact Method:** The water droplets to be measured were captured with sampling slides (Figure 3-6). Paraffin oil was on the surface of the slides to prevent the droplets from making contact with them. Hence, the captured droplets retain their spherical shape and evaporation is slowed.

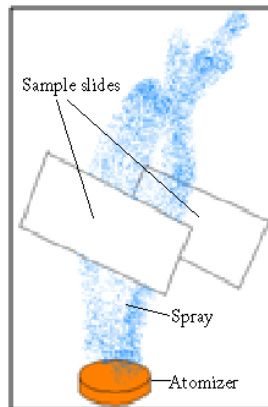


**Figure 3-6: Water droplets being captured between sampling slides.**

The slides containing the droplets were then placed on a microscope (Meiji MT6000 Epi-Fluorescence Series) with magnifications of 40X, 100X, 400X and 1000X and pictures were taken with a camera. Then the images were processed with MATLAB<sup>TM</sup>



**Figure 3-7: Microscope with camera connected to a computer for the measurement of water droplets with an impact method.**

- **Optical Method**: A Malvern Spraytec RTSizer was used for this method. This machine calculates the droplet size distribution using a laser technique (laser diffraction patterning). The spray, which is formed by droplets to be measured is passed through a laser beam and the scattering pattern is recorded and analyzed [92].

Figure 3-8 shows the laser of the Spraytec RTSizer and its path being altered by spatial filters, lens and particles or droplets to be measured. Once it is detected, the data is amplified and sent to a PC [93].

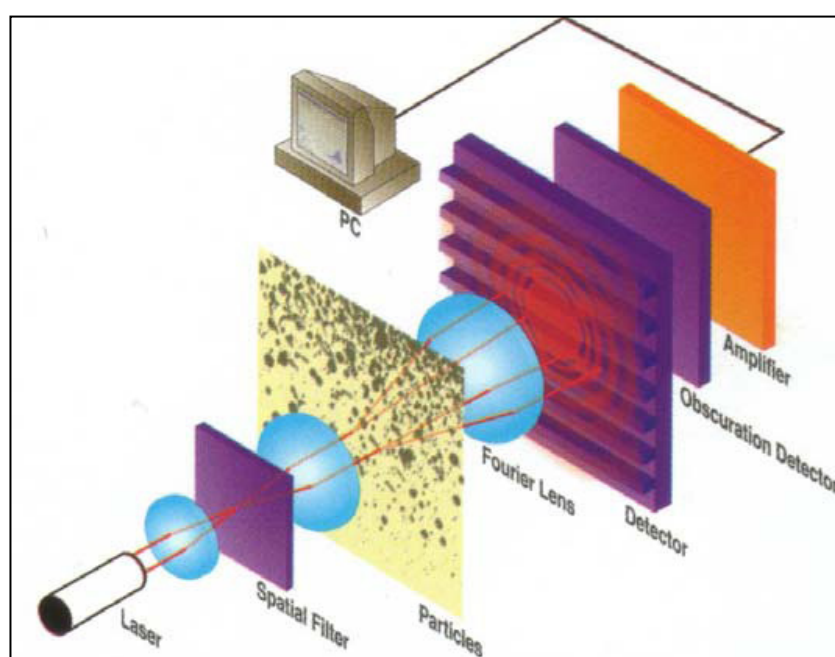


**Figure 3-8: Schematic diagram of the principle used by the Spraytec RTSizer [92].**

The Spraytec can be used in two different configurations - inhalation cell and open head. In the inhalation cell, the total flow of droplets is confined to a specific diameter pipe and the absolute volume can be measured. With the open head, the droplet size distribution will give a relative measurement of the drop size for the total spray.



The open head method was used for this experiment because it allows the laser beam to be pointed just above the atomizer. To make the droplets pass through the laser beam, a custom-made housing structure was also used (for details see Chapter 5).

Figure 3-9 shows the set up for the measurement of the droplets generated by an ultrasonic transducer (element 1) which is excited with a signal generated by a function generator (Hewlett Packard 33120A) (element 2) amplified by an amplifier (Amplifier Research 40A12) (element 3) and measured with an oscilloscope (Tektronix TDS 1012) (element 4). The laser emitter (element 5), receiver (element 6) and electronic interface (element 7) of the RTSizer can also be clearly. Compressed air is connected (element 8) to the emitter and receiver to avoid deposition of water droplets on the lens. A fan (Sanyo Denki 40 mm, 12 V DC Axial Fan) (element 9) passes air underneath the transducer to help the droplets to pass through the laser's path.

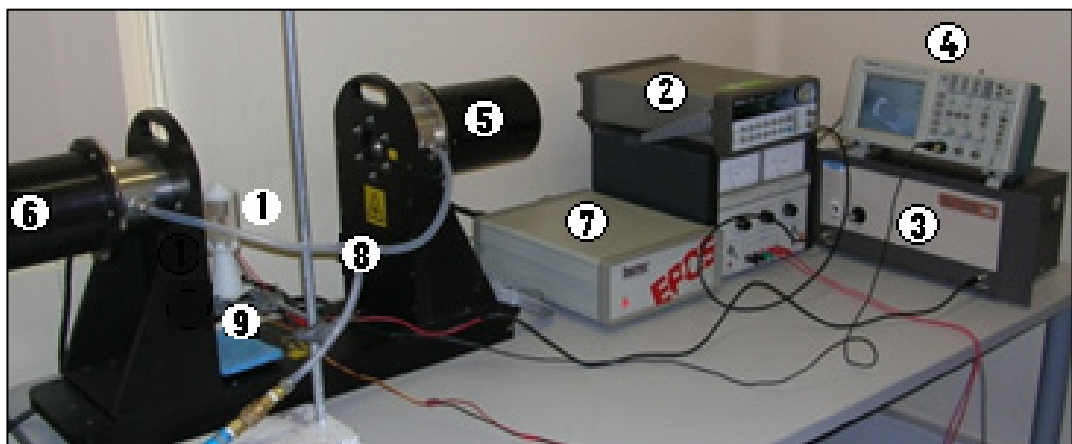


**Figure 3-9: Experimental set up for the generation and measurement of water droplets with an optical method. Element 1- Ultrasonic transducer. 2- Function generator. 3- Amplifier. 4- Oscilloscope. 5- Laser emitter. 6- Laser detector. 7- Electronic interface. 8- Compressed air connection. 9- Fan.**

### **3.2.3 DROPLET SIZE DISTRIBUTION AT DIFFERENT LENGTHS FROM THE ATOMIZER**

The following setup was built to measure the droplet size distribution of the spray of droplets at different locations. The droplets generated by the atomizer were forced to pass through a diffractometer (Malvern Spraytec RTSizer) which measures the droplet size distribution. The setup has the possibility of changing the distance between the atomizer and the RTSizer.

Figures 3-10 and 3-11 show the layout of the experimental setup. Air is blown underneath the atomizer and heated before passing through the atomizer picking up the droplets generated and transporting them to the laser diffractometer in a closed space. Another fan helped to maintain the flow.

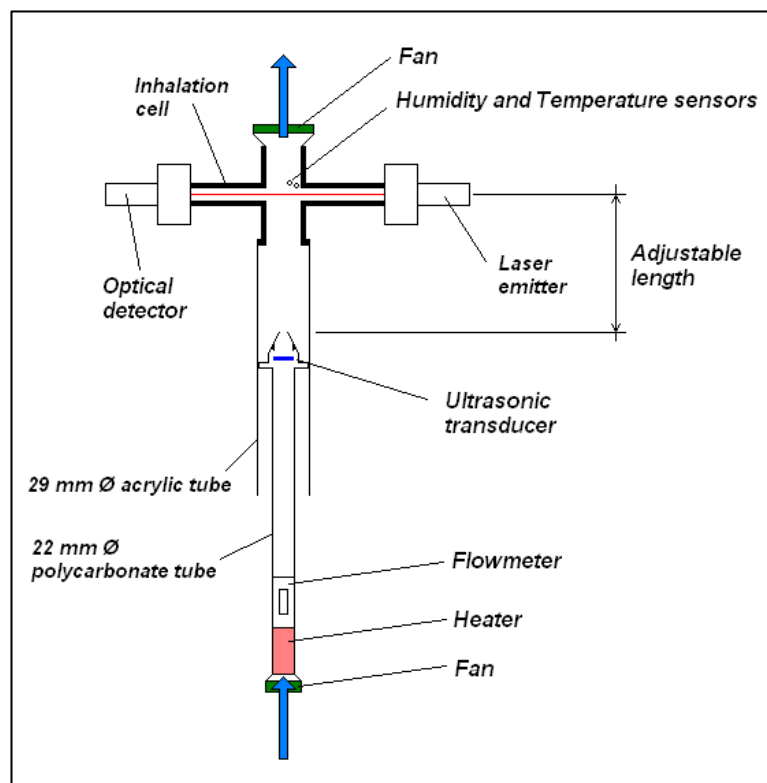


**Figure 3-10: Schematic of the setup for the measurement of the droplet size distribution at different distances from the atomizer.**

A 29-mm diameter acrylic tube was attached to the inhalation cell of the laser diffractometer. A 1.7 MHz ultrasonic transducer was fixed to a custom made base which fits inside the 29-mm tube and was connected to a 22-mm diameter polycarbonate tube. Through the 22-mm polycarbonate tube, air was supplied by a fan (Sanyo Denki 40 mm, 12 V DC Axial Fan). The air was warmed up with a custom made heater (Figure 3-12) and a flow meter (TSI 4000) was also connected to provide readings of the flow rate. The position of the atomizer was manually regulated to verify the droplet size distribution at different distances from the RTSizer.

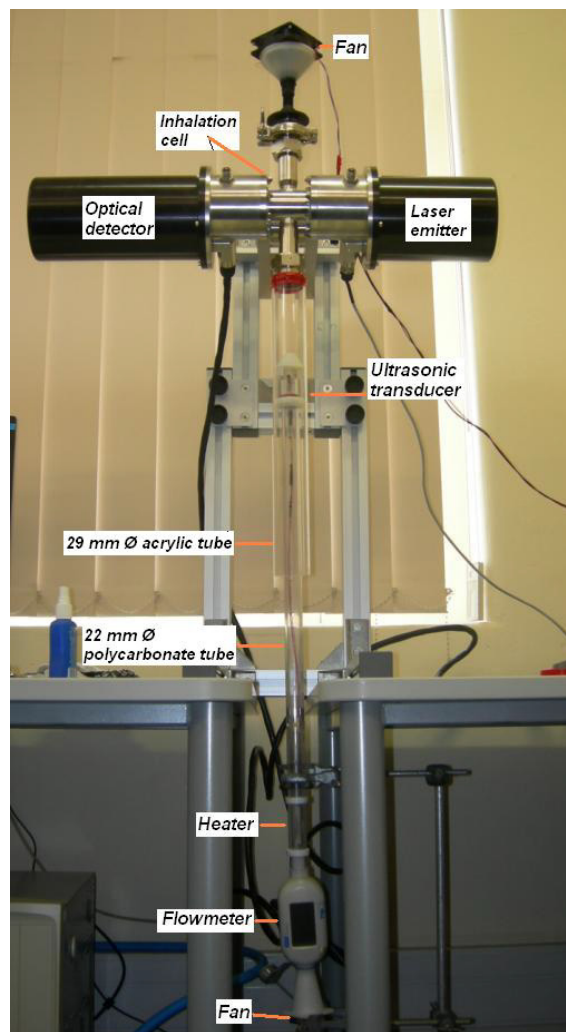


**Figure 3-11: Setup for the measurement of the droplet size distribution at different distances from the atomizer.**

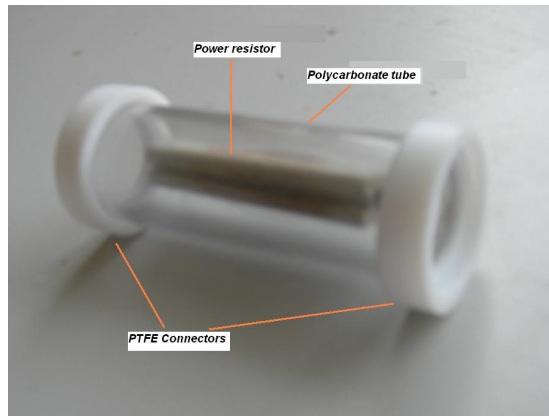


**Figure 3-12: Custom-made heater used in the setup.**

The heater was a high power resistor (Nte Electronics 25W4D7) encased in a polycarbonate tube (which melts at 120°C) as shown in figure 3 -12. It was designed to heat up to 30 L/min of air from 15 to 37°C ( ~12.5 Watts given a specific heat capacity of 1.012 J/(g °K) and a density of 1.204 Kg/m<sup>3</sup> at 20°C). The resistor was not in contact with the polycarbonate, and the heater had connectors at both ends manufactured from polytetrafluoroethylene (PTFE) with a maximum working temperature of approximately 300 °C. The resistance was connected to a power supply and an electrical current was passed through it to generate heat.

#### **2.2.4 EVAPORATION DISTANCE**

Experiments were performed to analyze the evaporation of the water droplets in a tube as they travel away from the atomizer. Knowing the amount of water in liquid state added to the air per unit of time, relative humidity and temperature (to work out the absolute humidity) were measured before the atomizer and at different distances from the atomizer. Considering that the absolute humidity is the amount of water in vapour state, it was possible to calculate the amount of water in liquid state changing to vapour state as it goes away from the atomizer with the air flow. The results were shown as percentage of water in liquid state over the total amount of water in the air flow. This

percentage was expected to be decreasing to zero as the distance from the atomizer increased. A zero percentage would represent the fully evaporation of the water present in the air flow.

Different water droplet size distributions were produced with ultrasonic sensors at different frequencies (1.4, 1.7, 2.0, 2.5 and 3.0 MHz, datasheets I and II) combining them with a custom made housing structure (Fig 3-13, element 1, for more detail, see chapter 5). The flow rate was generated by a fan (Sanyo Denki 40 mm, 12 V DC Axial Fan) (Fig 3-13, element 2).

The temperature was measured with 8 K-type thermocouples (Labfacility Z2-K-1M) (Fig 3-13, element 3) and eight Honeywell HIH-4000-004 humidity sensors (Fig 3-13, element 3). Data was recorded using an HP 34970A data logger (Hewlett Packard 34970A) (Fig 3-13, element 4). All of the calculations were performed with MATLAB<sup>TM</sup>. As shown in Figures 3-13, the temperature and humidity sensors were located above the atomizer, at 4, 8, 16, 32, 50 cm and outside the tube to register the atmospheric conditions.

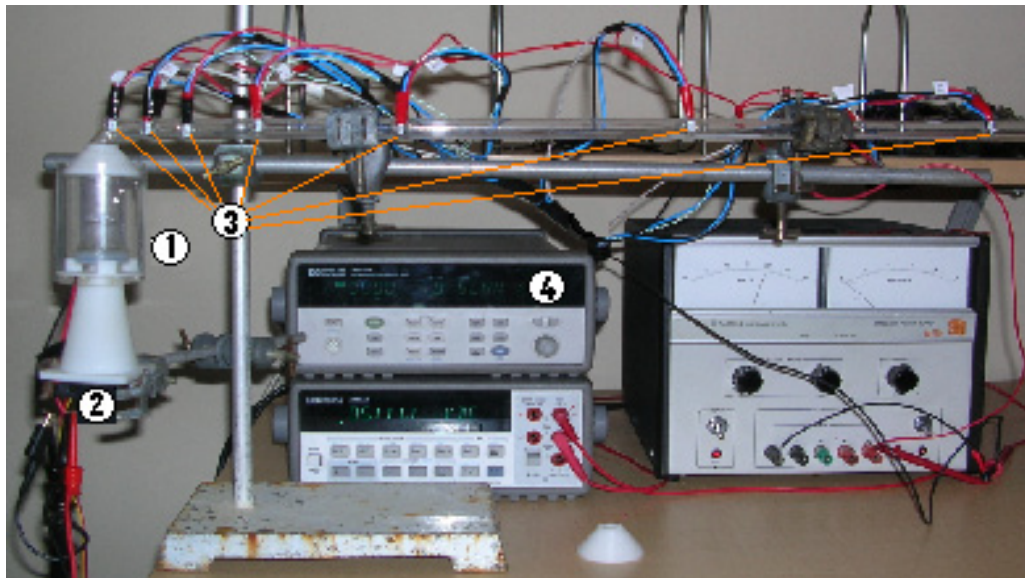


**Figure 3-13: Detail of the tube with the housing structure and sensors. Element 1- Housing structure with atomizer. 2- Fan. 3- Humidity and Temperature sensors. 4- Data logger.**

### 3.3 EXPERIMENTAL PROCEDURES

To address the four objectives given in section 3.1, the procedures used in the experiments will be explained.

#### 3.3.1 ATOMIZATION RATE

The atomization rate was related to the power absorbed by the transducer which was obtained as follow. Four  $10\ \Omega$  resistances in parallel ( $R_{eq} = 2.5\ \Omega$ ) were connected in series with the transducer (Figure 3-14) and the potential across the resistance  $V1$  was detected with an oscilloscope. At the same time, the voltage on the terminals of the oscilloscope  $V2$  was also recorded on the oscilloscope.

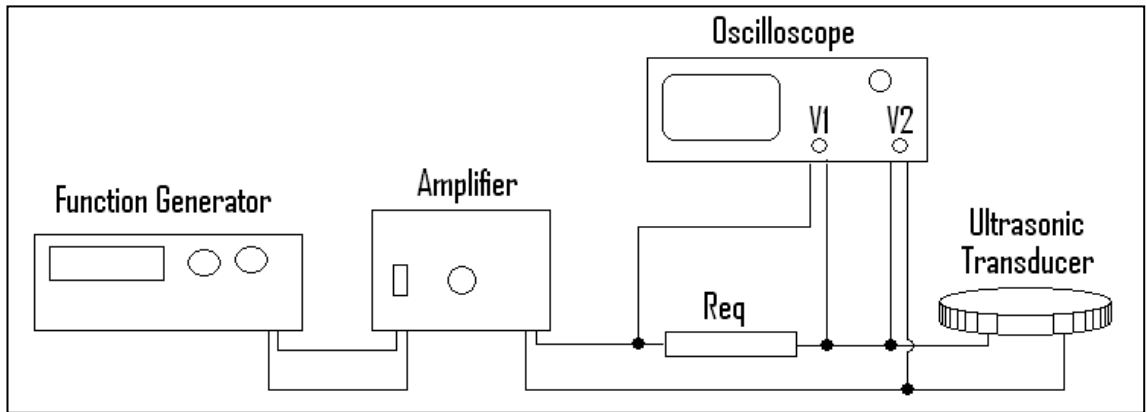


**Figure 3-14: Measurement of Current ( $V1/R_{eq}$ ) and Voltage ( $V2$ ) on the transducer.**

Then,  $V1/R_{eq}$  is the current and  $V2$  the voltage applied to the transducer. The transducers were excited with sine and square waves. Sine waves were used because of its simplicity of generation and amplification. On the other hand, square waves impart the highest power density to the transducer but, they are not easy to be generated and amplified. From the oscilloscope it was seen that the shape of the signals applied to the transducer were distortionated and the RMS value had to be calculated from the  $V1$  and

$V/2$  signals. This procedure was repeated for square and sine signals of 80  $V_{p-p}$ , 100  $V_{p-p}$ , 120  $V_{p-p}$ , 140  $V_{p-p}$  and 160  $V_{p-p}$ . The signals obtained with the oscilloscope were then processed with MATLAB<sup>TM</sup>.

The atomization rate was measured for each one of the above signals. The first transducer had a resonant frequency of the 1.7 MHz (datasheet on appendix A.1). Firstly, a 4-cm column of water was above the transducer and it was weighted before exciting the transducer. Then the transducer was excited for 2 minutes and the transducer with column of water was weighted again. The difference between these two values was the water that had been converted into droplets and blown away. This measurement was repeated 3 times for each excitation signal. And the excitation signals consisted of bursts of 5000, 10000 and 20000 pulses at 25, 50, 75 and 100% of duty cycle for square and sine shapes. The temperature of the water above the transducer was also measured.

Since the pulses did not have major effect on the result, the transducers with other frequencies (1.4, 2.0, 2.5 and 3.0 MHz, datasheets on appendix A.2) were tested with square and sine signals of 20000 pulses at 25, 50, 75 and 100% of duty cycle for 80, 100, 120, 140 and 160  $V_{p-p}$ . The results are fitted with MATLAB<sup>TM</sup> code.

### **3.3.2 DROPLET SIZE DISTRIBUTION**

- In the **photographic method**, images containing the droplets to be measured and images with the background were read with MATLAB<sup>TM</sup>. Subsequently, the background was subtracted from the images with droplets to eliminate all particles deposited on the glass and the resulting images were then converted into binary images with the right threshold for the calculation of the Sauter Mean Diameter (diameter of a hypothetical spherical drop which has and equivalent surface to volume ratio as the whole spray field) and representation in percentage of the total volume (Appendix B).

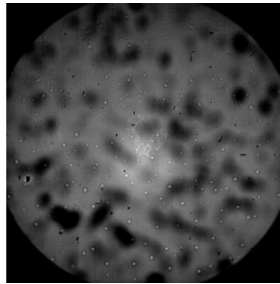


**Figure 3-15: Image of particles magnified 400X (photographic method).**

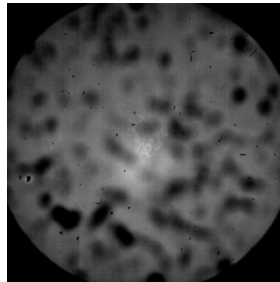


**Figure 3-16: Background showing particles deposited on the glass (photographic method).**

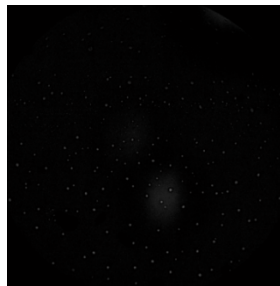


**Figure 3-17: Difference image showing the droplets without the background (photographic method).**

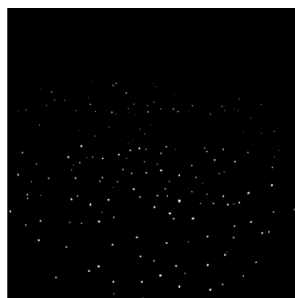


**Figure 3-18: Difference binary image showing the droplets (photographic method).**



- With the **impact method**, a sampling slide was located for ~2 seconds above the atomizer so the droplets generated were deposited on it. This slide had a thin film of paraffin oil covering the contact surface to avoid the deformation of the small water droplets. Then, the surface containing the droplets was covered with other oiled plate. The “sandwich” of plates was located on the microscope and images were taken with 400X and 1000X lenses. These images were sent to the computer to follow the same analysis as the one previously explained for the photographic method (MATLAB code in Appendix B).



**Figure 3-19: Image of particles magnified 400X (impact method).**



**Figure 3-20: Background showing particles deposited on the glass (impact method).**



**Figure 3-21: Difference image showing the droplets without the background (photographic method).**

- When the **optical method** was used to determine the droplet size distribution, the following steps were followed to prepare the equipment before starting the measurement. To start with, the reference noise and the background scattering were recorded. The sample details were set (details of how the sample was going to be measured). The reduction control parameters were chosen to make sure that correct analysis settings were applied during the measurement. The process variables were configured. Dv10 (droplet diameter below which 10% of the sample volume is detected) and Dv90 (droplet diameter below which 90% of the sample volume is detected) were selected.

Droplet size distributions for different frequencies with and without use of a custom made housing structure (for more detail, see chapter 5) were obtained for 4 min approximately and the average was calculated with the RTSizer software. The results were exported in text files and, then, read and compared with a code in MATLAB<sup>TM</sup>.

### **3.3.3 DROPLET SIZE DISTRIBUTION AT DIFFERENT LENGTHS FROM THE ATOMIZER**

The droplets to be measured in this experiment were produced by a 1.7MHz ultrasonic transducer (see datasheet in appendix A).

Firstly, the atomizer was located 50 cm away from the laser diffractometer. Atomization rates of 0.20 and 0.40 g/min and air flow rates of 30 and 60 L/min with and without the heater being on. Temperature, humidity, droplet size distribution were recorded for 15 minutes for every setting. Afterwards, the distance between atomizer and laser diffractometer was changed to 40, 30 and 20 cm.

### **3.3.4 EVAPORATION DISTANCE**

The fan was set to provide 60 L/min of air. This flow was directed underneath the atomizer and surrounding it taking the droplets generated. For every frequency, the transducers were excited to atomize 0.2 mL/min of water. The air with the droplets was directed into the tube so relative humidity and temperature were measured every 20 seconds.

The system was run with air for 5 minutes to obtain the initial conditions. Then, the atomizer was excited for another 5 minutes to provide the water droplets. This experiment was performed for frequencies of 1.5, 1.7, 2.1, 2.6 and 3.0 MHz.

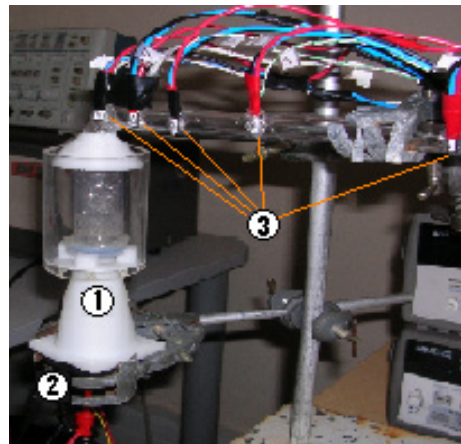


**Figure 3-22: Water droplets flowing into the tube. Relative humidity and temperature were measured to determine the water vapour content. Element 1- Housing structure with atomizer. 2- Fan. 3- Humidity and Temperature sensors.**

The data was processed with MATLAB<sup>TM</sup> (appendix C) to determine the content of water in vapour and in liquid state at different locations of the tube.

## **CHAPTER 4: EXPERIMENTAL RESULTS**

### **4.1 INTRODUCTION**

Four sets of experiments were performed and their results will be presented in this chapter. The results are presented in the same sequence as the objectives given in section 3.1.

The experiments were to determine:

1. The atomization rate of ultrasonic transducers
2. The droplet size distribution generated by ultrasonic transducers
3. The droplet size distribution at different distances from the atomizer
4. The length of tube and heat required to reach the fully evaporation of the droplets produced by the atomizer

### **4.2 ATOMIZATION RATE**

The atomization rate is influenced by different parameters which are considered as follow.

#### **4.2.1 POWER CONSUMPTION**

The shape of the excitation wave (sinusoidal or square) suffers a distortion when it is applied to the transducer due to the impedance mismatch (low transducer's impedance). Hence, the RMS values at different peak-to-peak voltages for different transducers had to be calculated for every transducer.

Figures 4-1 and 4-2 show the distortion of voltage and current respectively of a 1.5 MHz ultrasonic transducer when a square shape excitation is applied.

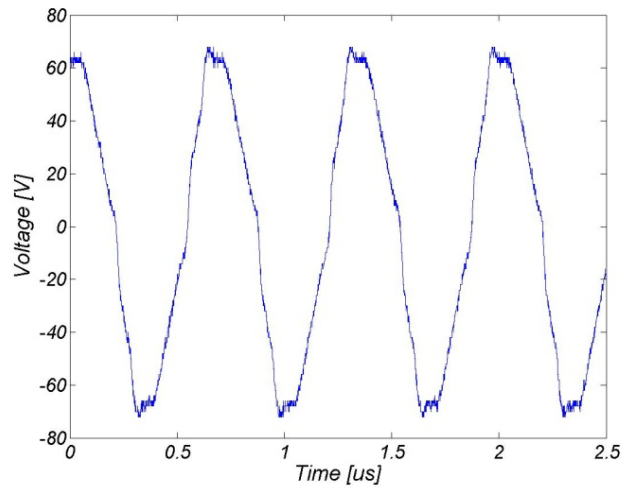


**Figure 4-1: Voltage on the terminals of a 1.5 MHz transducer when a square wave is applied.**

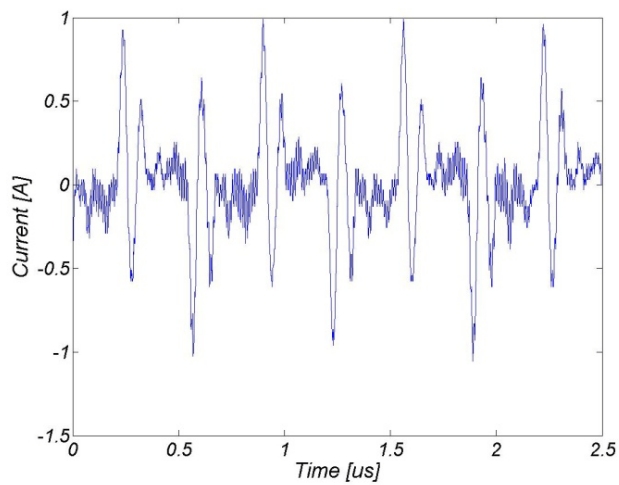


**Figure 4-2: Current on a 1.5 MHz transducer when a square wave is applied.**

The above two figures are samples of the data. The distortion of square and sine waves on transducers of 1.7, 2.1, 2.6 and 3.0 MHz are in appendix D.1

The resonant frequencies experimentally found for the transducers were different to the values reported by their manufacturer (datasheets in appendixes A.1 and A.2).

The RMS values were calculated for the square and sine shapes with MATLAB<sup>TM</sup>. The transducers of 1.5, 1.7, 2.1 and 2.6 MHz were excited with signals of 100, 120, 140 and 160 V<sub>p-p</sub> and the transducer of 3.0 MHz with signals of 80, 100 and 120 V<sub>p-p</sub> since it was no possible to get a good amplification at this frequency.

Table 4-1 shows the values obtained for 1.5, 1.7, 2.1, 2.6 and 3.0 MHz transducers in response to different excitation signals.

**Table 4-1: RMS values when a given voltage peak to peak is applied to transducer of different frequencies.**

| Excitation signal                | 1.50 MHz<br>(reported<br>1.40 ± 0.05<br>MHz)            | 1.74 MHz<br>(reported<br>1.65 ± 0.05<br>MHz)            | 2.10 MHz<br>(reported<br>2.00 ± 0.05<br>MHz)            | 2.60 MHz<br>(reported<br>2.50 ± 0.05<br>MHz)            | 3.0 MHz<br>(reported<br>3.00 ± 0.05<br>MHz)             |
|----------------------------------|---|---|---|---|---|
| 80 V <sub>p-p</sub> square wave  | *   | *   | *   | *   | V <sub>rms</sub> = 26.7347<br>I <sub>rms</sub> = 0.3182 |
| 100 V <sub>p-p</sub> square wave | V <sub>rms</sub> = 33.6544<br>I <sub>rms</sub> = 0.2774 | V <sub>rms</sub> = 31.0579<br>I <sub>rms</sub> = 0.2570 | V <sub>rms</sub> = 35.7838<br>I <sub>rms</sub> = 0.0086 | V <sub>rms</sub> = 32.3953<br>I <sub>rms</sub> = 0.0135 | V <sub>rms</sub> = 31.0921<br>I <sub>rms</sub> = 0.3752 |
| 120 V <sub>p-p</sub> square wave | V <sub>rms</sub> = 41.8844<br>I <sub>rms</sub> = 0.3168 | V <sub>rms</sub> = 36.1089<br>I <sub>rms</sub> = 0.2516 | V <sub>rms</sub> = 42.5269<br>I <sub>rms</sub> = 0.0106 | V <sub>rms</sub> = 39.8392<br>I <sub>rms</sub> = 0.0140 | V <sub>rms</sub> = 36.7988<br>I <sub>rms</sub> = 0.4551 |
| 140 V <sub>p-p</sub> square wave | V <sub>rms</sub> = 47.4767<br>I <sub>rms</sub> = 0.3398 | V <sub>rms</sub> = 34.6727<br>I <sub>rms</sub> = 0.3065 | V <sub>rms</sub> = 49.5397<br>I <sub>rms</sub> = 0.0126 | V <sub>rms</sub> = 46.1055<br>I <sub>rms</sub> = 0.0155 | *   |
| 160 V <sub>p-p</sub> square wave | V <sub>rms</sub> = 58.4596<br>I <sub>rms</sub> = 0.3603 | V <sub>rms</sub> = 46.9981<br>I <sub>rms</sub> = 0.3315 | V <sub>rms</sub> = 60.8540<br>I <sub>rms</sub> = 0.0173 | V <sub>rms</sub> = 50.0768<br>I <sub>rms</sub> = 0.0183 | *   |
| 80 V <sub>p-p</sub> sine wave    | *   | *   | *   | *   | V <sub>rms</sub> = 27.8946<br>I <sub>rms</sub> = 0.1519 |
| 100 V <sub>p-p</sub> sine wave   | V <sub>rms</sub> = 34.2200<br>I <sub>rms</sub> = 0.0857 | V <sub>rms</sub> = 30.5000<br>I <sub>rms</sub> = 0.1029 | V <sub>rms</sub> = 33.1472<br>I <sub>rms</sub> = 0.0068 | V <sub>rms</sub> = 34.3199<br>I <sub>rms</sub> = 0.0092 | V <sub>rms</sub> = 33.8772<br>I <sub>rms</sub> = 0.2184 |
| 120 V <sub>p-p</sub> sine wave   | V <sub>rms</sub> = 40.9706<br>I <sub>rms</sub> = 0.0999 | V <sub>rms</sub> = 32.4019<br>I <sub>rms</sub> = 0.1278 | V <sub>rms</sub> = 41.3319<br>I <sub>rms</sub> = 0.0089 | V <sub>rms</sub> = 41.5762<br>I <sub>rms</sub> = 0.0101 | V <sub>rms</sub> = 40.3199<br>I <sub>rms</sub> = 0.2902 |
| 140 V <sub>p-p</sub> sine wave   | V <sub>rms</sub> = 50.0167<br>I <sub>rms</sub> = 0.1126 | V <sub>rms</sub> = 44.7699<br>I <sub>rms</sub> = 0.1521 | V <sub>rms</sub> = 48.2117<br>I <sub>rms</sub> = 0.0103 | V <sub>rms</sub> = 49.8204<br>I <sub>rms</sub> = 0.0115 | *   |
| 160 V <sub>p-p</sub> sine wave   | V <sub>rms</sub> = 56.2423<br>I <sub>rms</sub> = 0.1528 | V <sub>rms</sub> = 46.6084<br>I <sub>rms</sub> = 0.2222 | V <sub>rms</sub> = 56.8789<br>I <sub>rms</sub> = 0.0121 | V <sub>rms</sub> = 57.3641<br>I <sub>rms</sub> = 0.0143 | *   |

#### **4.2.2 EFFECT OF EXCITATION**

The ultrasonic transducers were excited with square and sine pulses at the resonant frequency of the transducers. These pulses were applied either continuously or in bursts of certain amount of pulses. These bursts were sent at a specific frequency as to excite the transducer for a fraction of time. Duty cycle is defined as the time in which the transducer is being excited with the burst divided the period at which the bursts are sent.

In this section, the atomization rate versus power consumption is presented for the analysis of the effect of bursts with different number of pulses, different frequencies, and with different shapes.

##### **Effect of number of pulses per burst**

The experiments were done with the 1.7 MHz transducer at different duty cycles. Bursts of 5000, 10000 and 20000 pulses were used for the comparison.

For bursts of 5000 pulses, these were sent every 11.56 ms to excite the transducer for 25% of the time, every 5.78 ms for a duty cycle of 50% and 3.85 ms for a duty cycle of 75%. For bursts of 10000 pulses, these were sent every 23.12, 11.56 and 7.71 ms for duty cycles of 25%, 50% and 75% respectively. Likewise, for bursts of 20000 pulses, these were sent every 46.30, 23.12 and 15.42 ms for duty cycles of 25%, 50% and 75%.

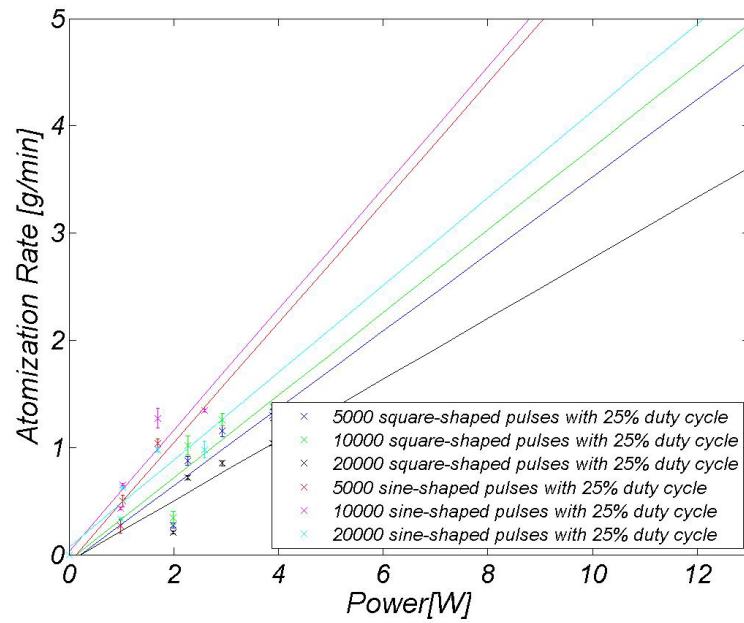


**Figure 4-3: Atomization rate of an ultrasonic transducer excited 25% of the time.  
Bars indicate standard deviation.**

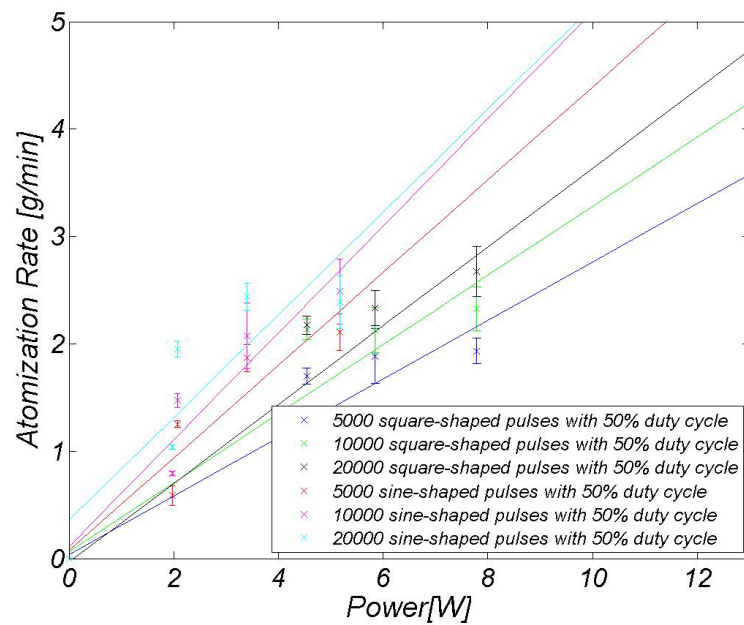


**Figure 4-4: Atomization rate of an ultrasonic transducer excited 50% of the time.  
Bars indicate standard deviation.**



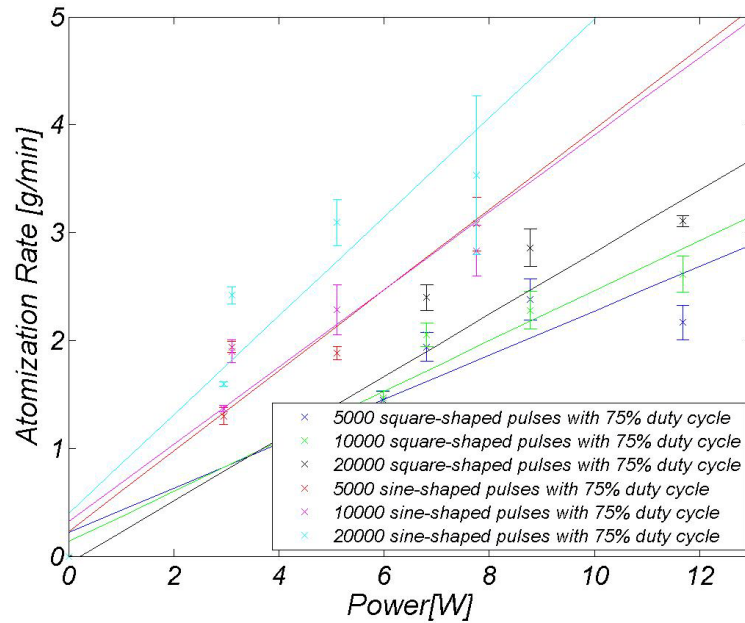


**Figure 4-5: Atomization rate of an ultrasonic transducer excited 75% of the time. Bars indicate standard deviation.**

From figures 4-3, 4-4 and 4-5, the transducer's performance seems to be similar for different number of pulses per burst of pulses of equal pulse shape (square or sine).

### Effect of duty cycle

The experiments were performed with transducers of frequencies of 1.5, 1.7, 2.1, 2.6 and 3.0 MHz. They were excited with bursts of 20000 pulses sent at different rates to create duty cycles of 25, 50 and 75% for every frequency. Table 4-2 shows the frequency at which the bursts of 20000 pulses were sent in order to create different duty cycles.

**Table 4-2: Burst frequency for different duty cycles (bursts of 20000 pulses).**

| Transducer's Frequency | 25 % Duty Cycle        | 50% Duty Cycle         | 75% Duty Cycle          |
|------------------------|------------------------|------------------------|-------------------------|
| 1.5 MHz                | 18.87 Hz (bursts freq) | 37.75 Hz (bursts freq) | 56.62 Hz (bursts freq)  |
| 1.7 MHz                | 21.60 Hz (bursts freq) | 43.25 Hz (bursts freq) | 64.87 Hz (bursts freq)  |
| 2.1 MHz                | 26.25 Hz (bursts freq) | 52.50 Hz (bursts freq) | 78.75 Hz (bursts freq)  |
| 2.6 MHz                | 32.50 Hz (bursts freq) | 65.00 Hz (bursts freq) | 97.50 Hz (bursts freq)  |
| 3.0 MHz                | 37.50 Hz (bursts freq) | 75.00 Hz (bursts freq) | 112.50 Hz (bursts freq) |

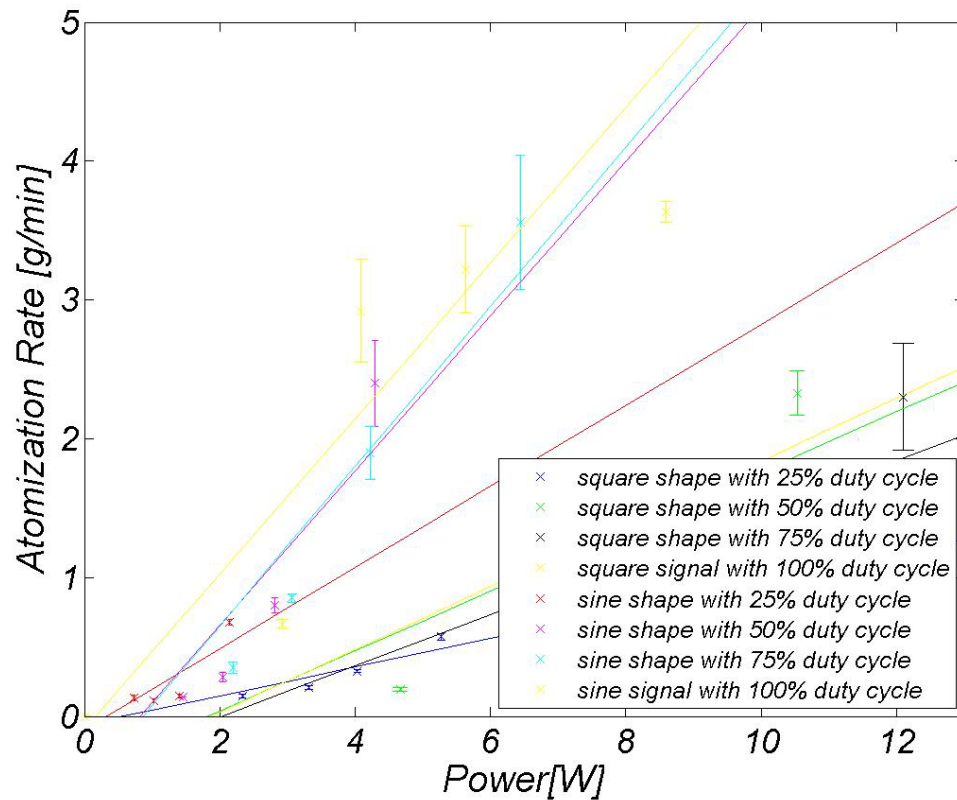


**Figure 4-6: Atomization rate versus power consumption of a 1.5 MHz transducer excited at different duty cycles. Bars indicate standard deviation.**

The above figure was a sample of the data. Figures that show the atomization rate versus power consumption at different duty cycles for frequencies of 1.7, 2.1, 2.6 and

3.0 MHz are in appendix D.2. They all show clearly that the higher the duty cycle, the better the performance (steeper relationship) for all the frequencies.

### **Effect of wave-shape**

The transducers were excited with square and sine pulses for comparison. The transducers were of 1.5, 1.7, 2.1, 2.6 and 3.0 MHz and were excited with duty cycles of 25, 50, 75 and 100%. The bursts had 20000 pulses for all the transducers except that the 1.7 MHz was also excited with bursts of 5000 and 10000 pulses.

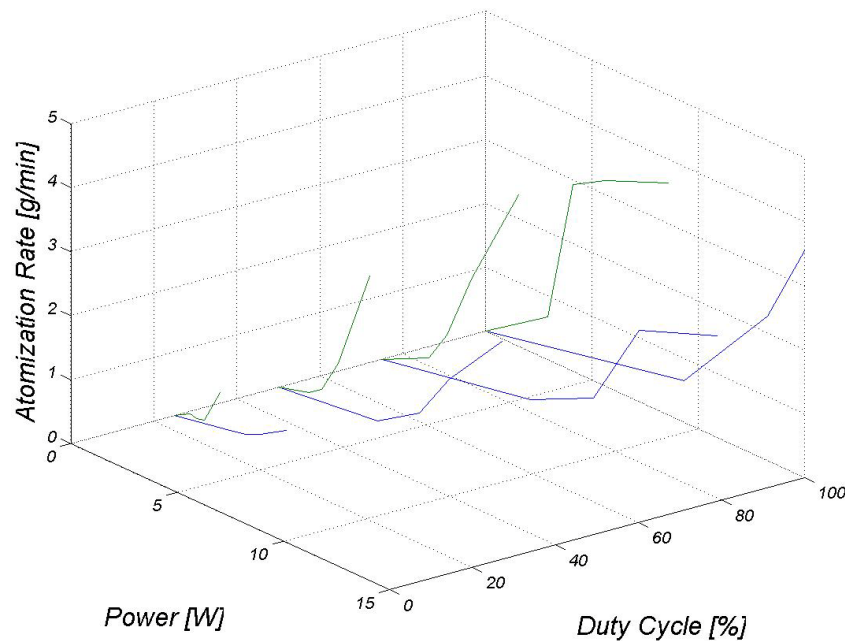


**Figure 4-7: Atomization rate versus power consumption for a 1.5 MHz transducer excited with sine (green) and square (blue) pulses at four duty cycles.**

Figures that show the atomization rate versus power consumption for different duty cycles for frequencies of 1.7, 2.1, 2.6 and 3.0 MHz are presented in appendix D.3. It is noticeable that the transducers were more effective at atomizing water (steeper lines) when they were excited with sine pulses than with square pulses.

### 4.3 HEATING DURING ATOMIZATION

The temperature of the water 1 cm above the ultrasonic transducer during the atomization was measured and is shown in this section.

The effect of the number of pulses per burst, duty cycle and shape of the pulses on the temperature of the transducer was analyzed from the following graphs.

#### 4.3.1 EFFECT OF NUMBER OF PULSES

The 1.7 MHz transducer was excited with bursts of 5000, 10000 and 20000 pulses of square and sine shape. The results were grouped for 25, 50, 75 and 100% duty cycles.

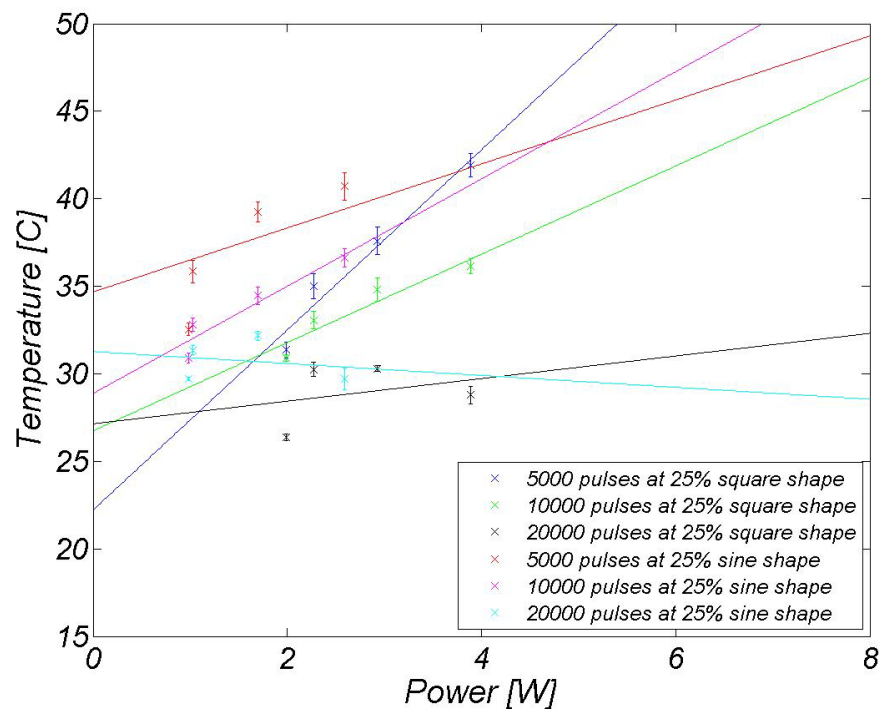


**Figure 4-8: Temperature versus power consumption of an ultrasonic transducer excited with a duty cycle of 25%. Bars indicate standard deviation.**

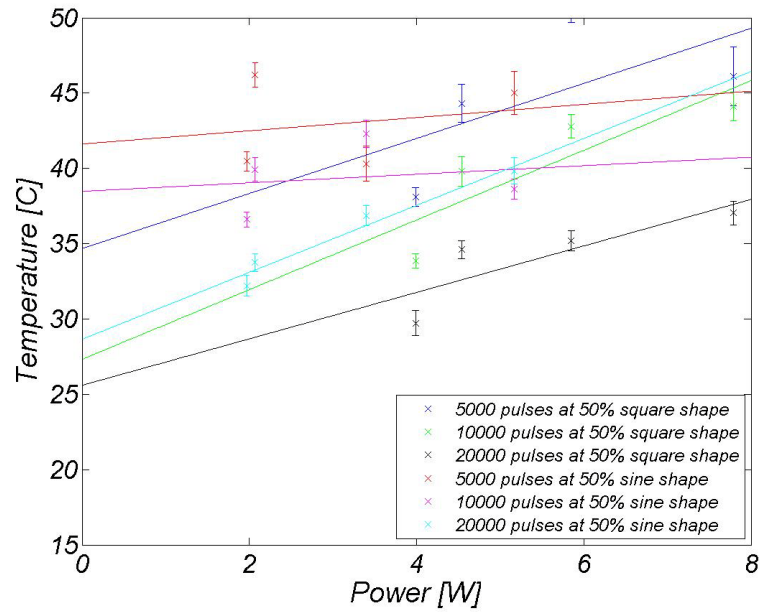


**Figure 4-9: Temperature versus power consumption of an ultrasonic transducer excited with a duty cycle of 50%. Bars indicate standard deviation.**

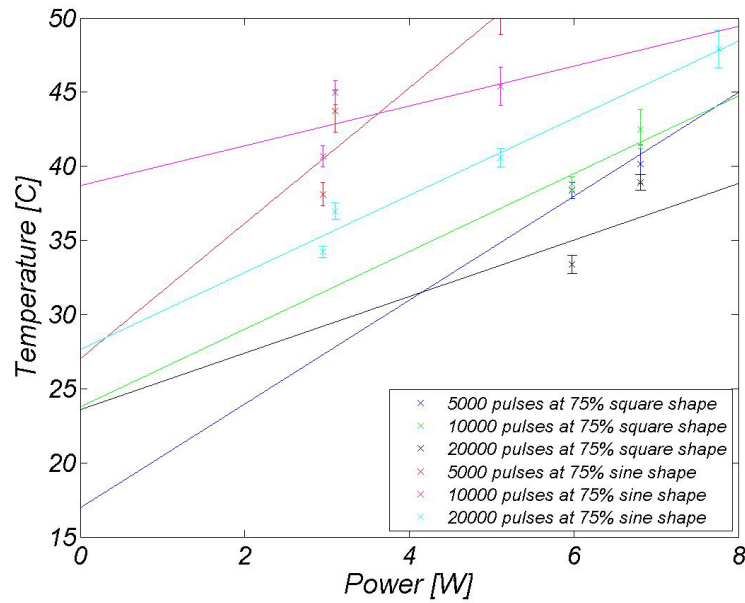


**Figure 4-10: Temperature versus power consumption of an ultrasonic transducer excited with a duty cycle of 75%. Bars indicate standard deviation.**

It is not possible to say which number of pulses per burst generates more heat in ultrasonic transducers as shown in figures 4-8, 4-9 and 4-10.

### **4.3.2 EFFECT OF DUTY CYCLE**

The experiments were carried out with transducers of 1.5, 1.7, 2.1, 2.6 and 3.0 MHz. They were excited with bursts of 20000 pulses at the frequencies shown in table 4-2.

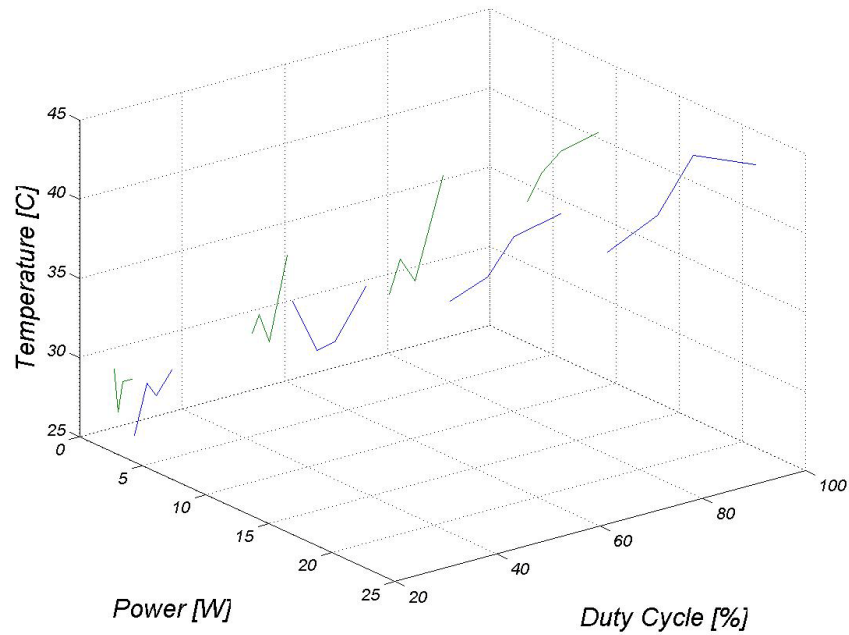


**Figure 4-11: Temperature of a 1.5 MHz transducer when it was excited with sine (green) and square (blue) pulses at different powers and duty cycles.**

Figures that show the temperature versus power consumption at different duty cycles for transducers of 1.7, 2.1, 2.6 and 3.0 MHz are presented in appendix D.4.

As the duty cycle increases, so does the heat generated on the transducers of different frequencies.

### **4.3.3 EFFECT OF WAVE-SHAPE**

In this section, the heating of ultrasonic transducers when they are excited with square and sine pulses at different settings is shown.

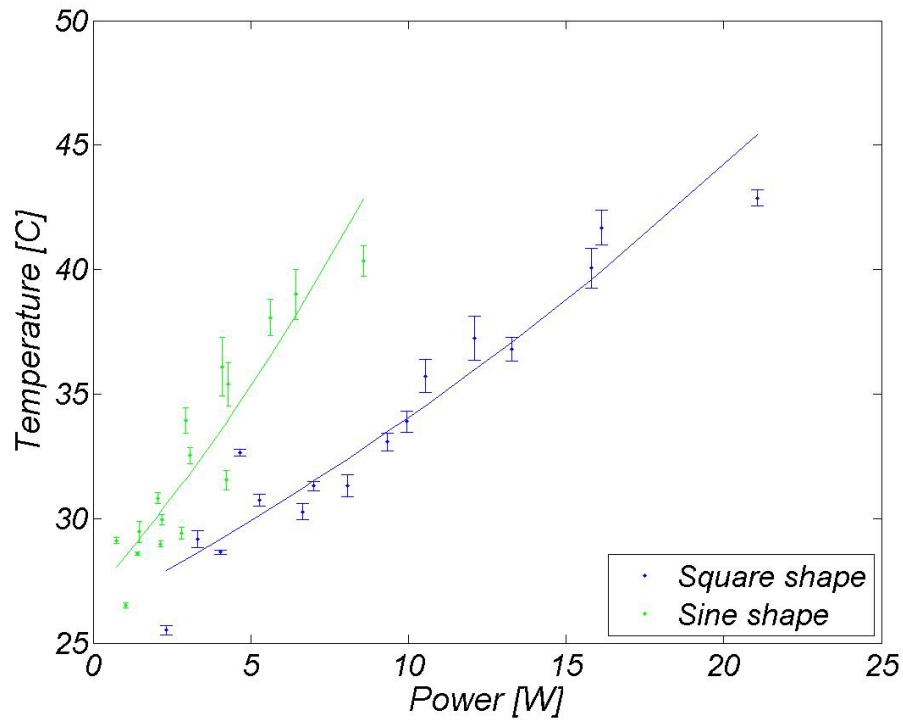


**Figure 4-12: Temperature versus power consumption of a 1.5 MHz transducer. Bars indicate standard deviation.**

Figures that show temperature versus power consumption for transducers of 1.7, 2.1, 2.6 and 3.0 MHz are in appendix D.5. Although the transducers consumed less power when they were excited with sine pulses, they generated as much heat as when they were excited with square pulses.

## 4.4 OBTAINING DROPLET SIZE DISTRIBUTION

### 4.4.1 PHOTOGRAPHIC METHOD

With the photographic method, the measurement of the size of the droplets generated with a transducer of 1.7 MHz was attempted. Figure 4-13 shows the percentage in volume for the different diameters of droplets generated in the spray.

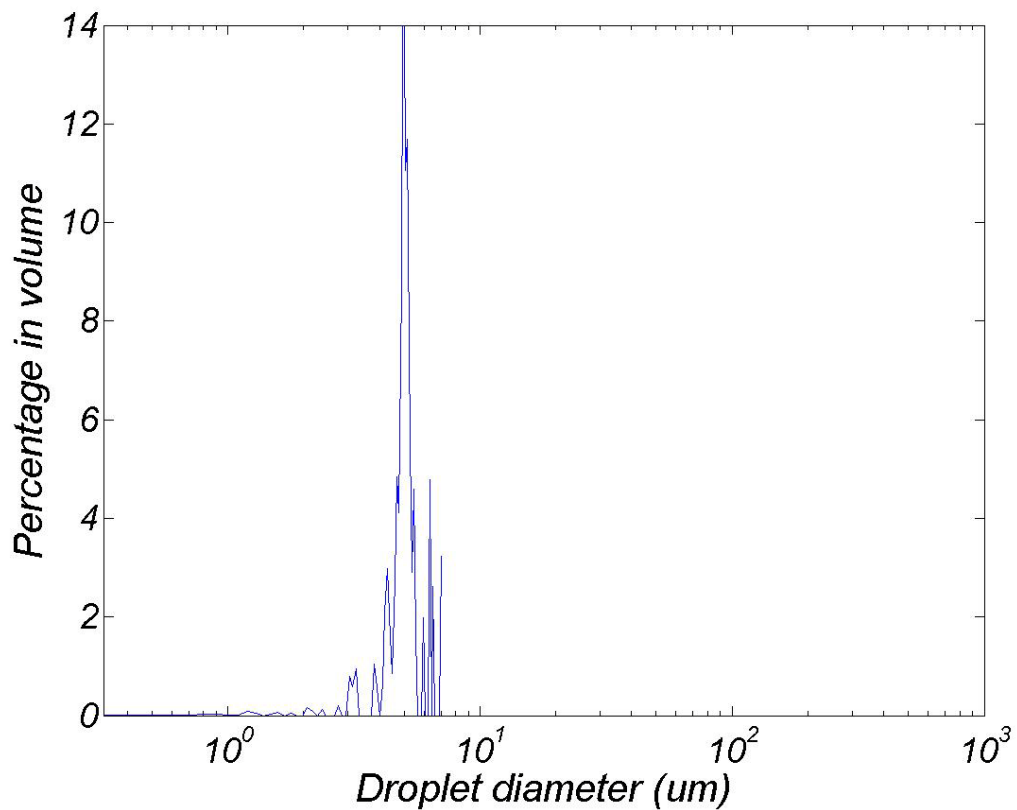


**Figure 4-13: Droplet size distribution for a 1.7 MHz transducer (photographic method)**

There were no consistent measurements. Droplets moving in different planes to the focal plane also appeared on the image and their sizes were affected. It was not possible to distinguish these droplets from the ones on the focal plane.



#### **4.4.2 IMPACT METHOD**

The following figures show the result of the droplet size distribution measurement of transducers of 1.70 and 2.78 MHz. The measurement was done with an impact technique using magnifications of 400X and 1000X.

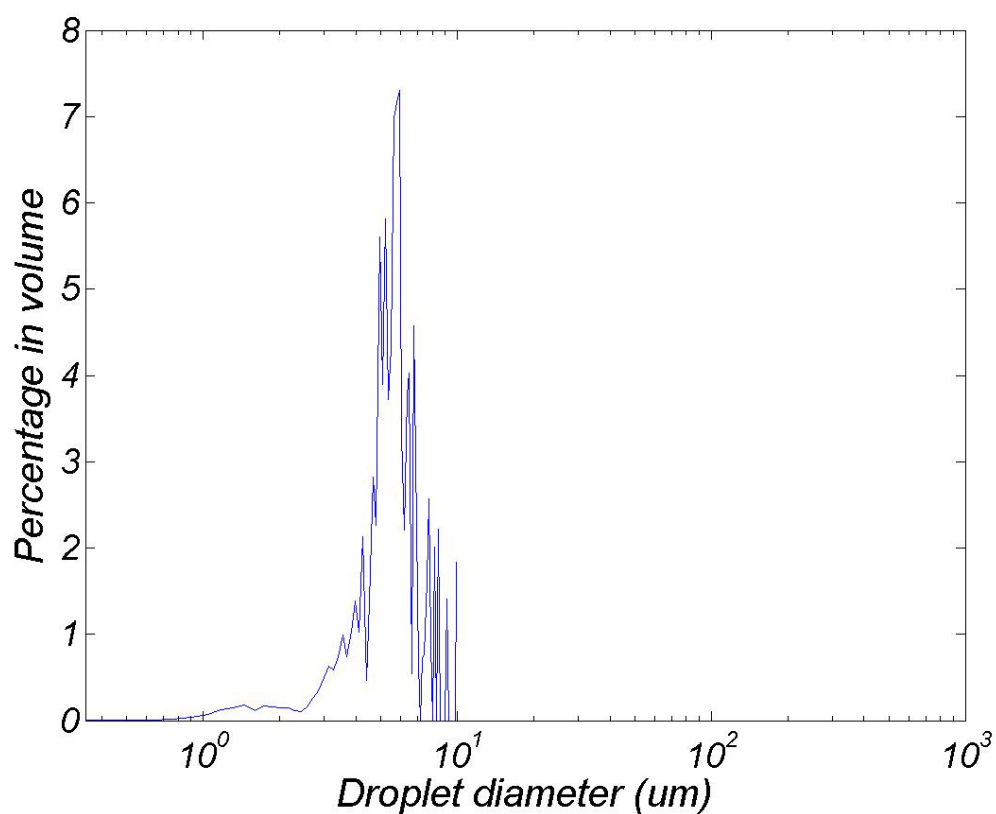


**Figure 4-14: Droplet size distribution for a 1.7 MHz transducer (impact method, 699 droplets measured using 400X lens)**

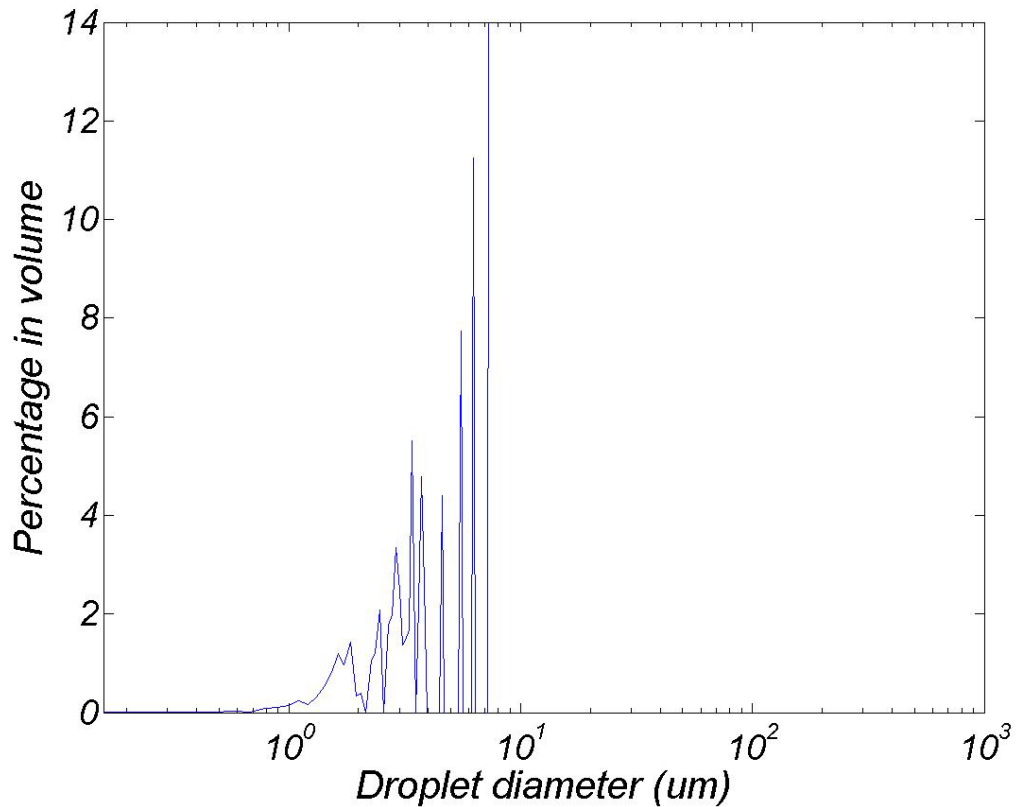


**Figure 4-15: Droplet size distribution for a 2.78 MHz transducer (impact method, 279 droplets measured using 400X lens)**

This method presented the same problems as the photographic method (droplets of different planes appearing in the images and complicating the processing of the images) and the results were not consistent.

#### **4.4.3 OPTICAL METHOD**

Droplet size distributions for different configurations were obtained using a Malvern Spraytec Laser Diffractometer. The effect of the frequency, shape, number of pulses per bursts and duty cycle on the droplet size distribution was found.

### Effect of frequency

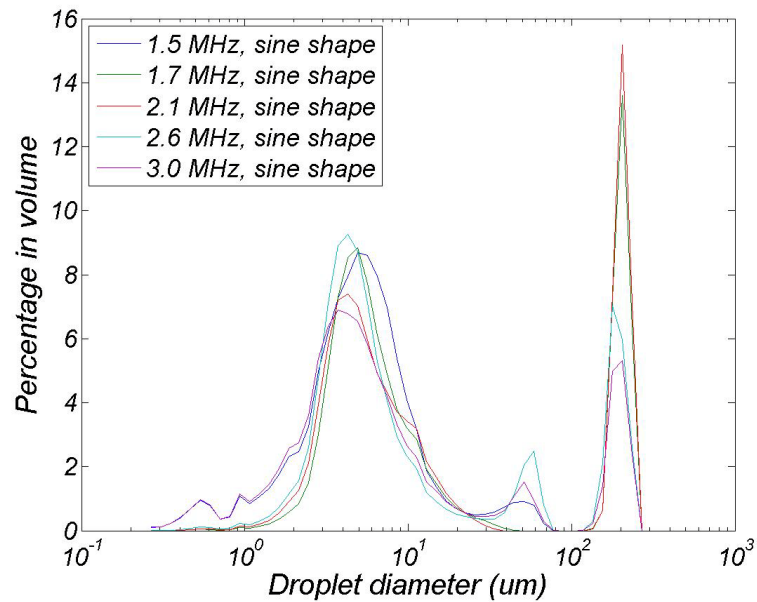


**Figure 4-16: Droplets size distribution of transducers of different frequencies excited with sine pulses.**

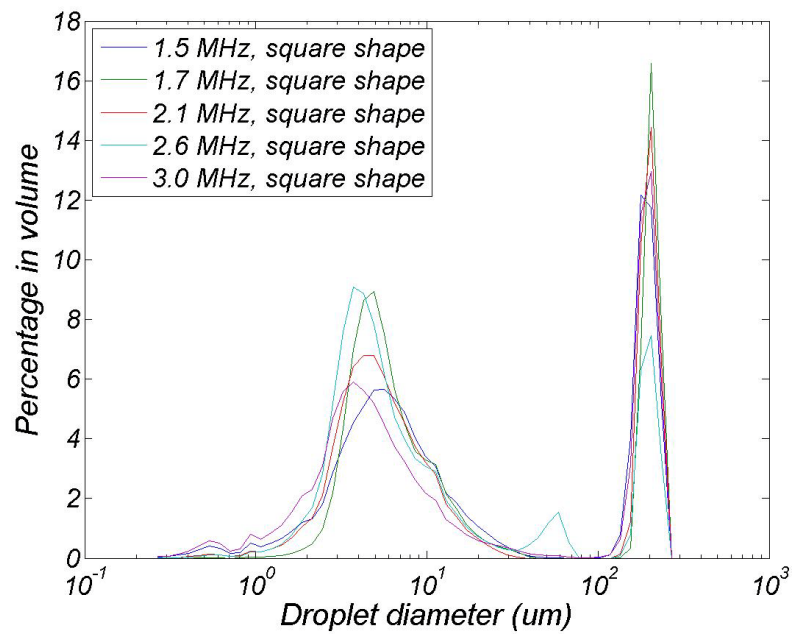


**Figure 4-17: Droplets size distribution of transducers of different frequencies excited with square pulses.**

**Table 4-3: Sauter mean diameter of transducers of different frequencies excited with sine and square pulses**

| Frequency [MHz] | Lang's predicted Diameter [ $\mu\text{m}$ ] | Sauter Mean Diameter [ $\mu\text{m}$ ] (sine shape) | Sauter Mean Diameter [ $\mu\text{m}$ ] (square shape) |
|-----------------|---|---|---|
| 1.5             | 3.17  | 3.18  | 5.61  |
| 1.7             | 2.92  | 6.50  | 6.50  |
| 2.1             | 2.54  | 6.34  | 6.15  |
| 2.6             | 2.20  | 5.28  | 5.19  |
| 3.0             | 2.00  | 3.34  | 4.42  |

Figures 4-16 and 4-17 show a similar droplet size distribution for transducers of different frequencies. From Table 4-3 it is not possible to make a statement of the dependency of the Sauter mean diameter on the frequency of the transducer and the shape of the excitation signal. At the same frequency, the Sauter mean diameter of the droplets generated by a transducer excited with square or sine-shaped signals are similar.

### Effect of shape

Figure 4-18 shows the droplet size distribution for ultrasonic transducers of 1.5, 1.7, 2.1, 2.6 and 3.0 MHz continuously excited with square and sine waves.

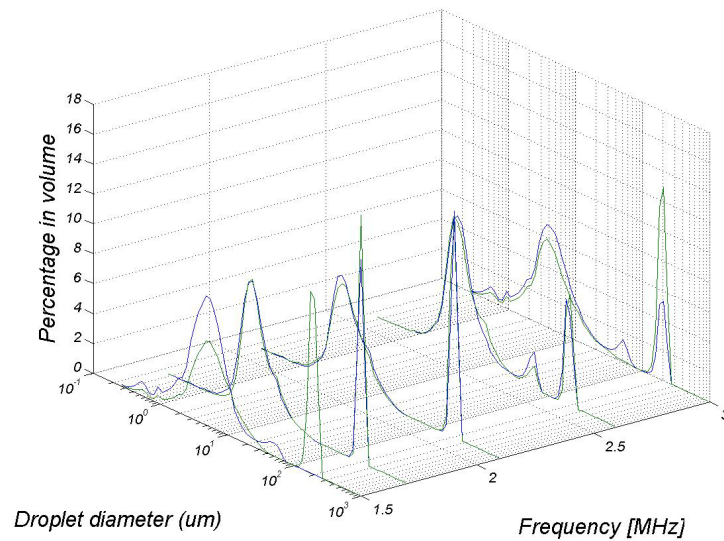


**Figure 4-18: Droplet size distribution for ultrasonic transducers of different frequencies continuously excited with square (green) and sine (blue) waves.**

As seen in figure 4-18, the shape seems to have no effect on the droplet size distribution of the generated droplets.

### **Effect of the power**

The 1.7 MHz transducer was continuously excited with square and sine waves of 100, 120, 140 and 160 V<sub>p-p</sub> to analyze the change on the droplet size distribution of the spray generated with the power.

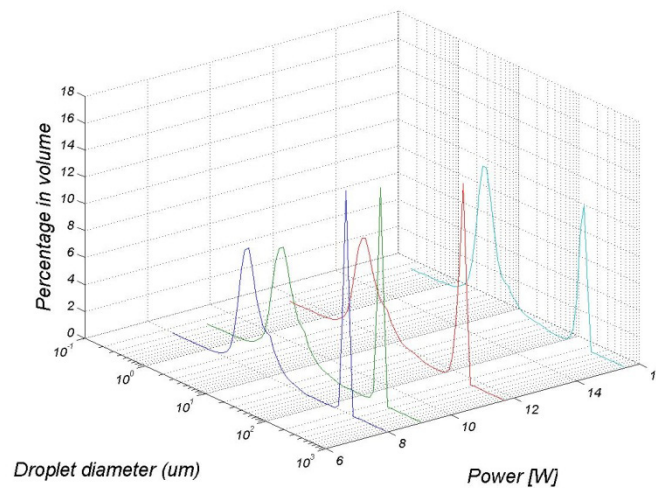


**Figure 4-19: Droplet size distribution of a 1.7 MHz transducer continuously excited with a square wave.**

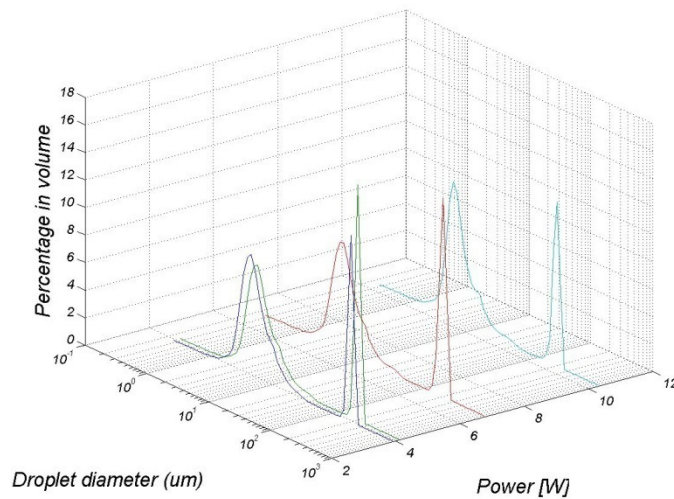


**Figure 4-20: Droplet size distribution of a 1.7 MHz transducer continuously excited with a sine wave.**

**Table 4-4: Effect of the power on the Sauter mean diameter.**

| Characteristic       | Power [W] | Sauter Mean Diameter [ $\mu\text{m}$ ] |
|----------------------|-----------|--|
| 1.7 MHz square shape | 3.94      | 6.50                                   |
| 1.7 MHz square shape | 4.14      | 7.11                                   |
| 1.7 MHz square shape | 6.18      | 6.76                                   |
| 1.7 MHz square shape | 10.35     | 6.33                                   |
| 1.7 MHz sine shape   | 7.98      | 6.50                                   |
| 1.7 MHz sine shape   | 9.08      | 7.43                                   |
| 1.7 MHz sine shape   | 11.71     | 6.88                                   |
| 1.7 MHz sine shape   | 15.57     | 7.55                                   |

Although the power had a direct relationship with the atomization rate (as shown in section 4.2), it did not affect the droplet size distribution as shown in Figures 4-19, 4-20 and Table 4-4.

### **Effect of the duty cycle**

The 1.7 MHz transducer was excited with different duty cycles and the droplet size distribution was recorded. The bursts had 5000, 10000, and 20000 sine and square pulses.

Figure 4-21 shows the percentage in volume at different sizes for duty cycles of 25, 50 and 75% when the transducer is excited with bursts of 5000 sine-shaped pulses.

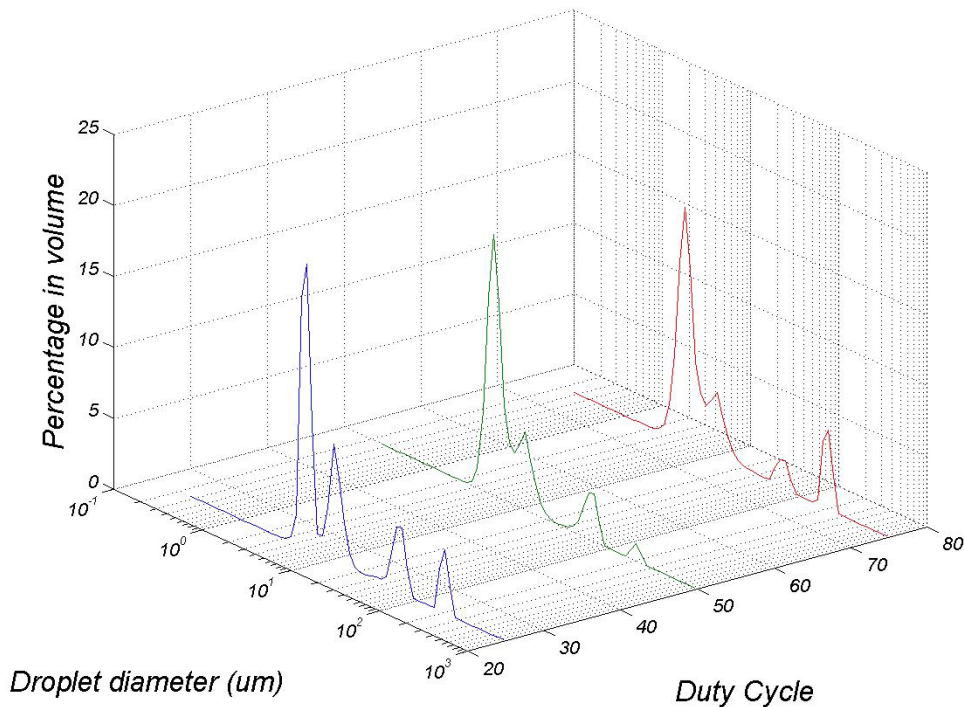


**Figure 4-21: Droplet size distribution of a 1.7 MHz transducer excited with bursts of 5000 sine-shaped pulses.**

The graphs in appendix D.6 show the same relation when the transducer is excited with bursts of 5000 square-shaped pulses, 10000 sine-shaped pulses, 10000 square-shaped pulses, 20000 sine-shaped pulses and 20000 square-shaped pulses. They do not show any dependency between the droplet size distribution and the number of pulses. Table 4-5



give the Sauter mean diameter calculated from the droplet size distributions of the sprays generated with the 1.7 MHz transducer under different number and shape of pulses.

**Table 4-5: Sauter mean diameter of a spray produced by a 1.7 MHz transducer**

| Burst               | 25% DC             | 50% DC             | 75% DC             |
|---------------------|--------------------|--------------------|--------------------|
| 5000 sine pulses    | 8.43 $\mu\text{m}$ | 6.52 $\mu\text{m}$ | 6.84 $\mu\text{m}$ |
| 10000 sine pulses   | 7.95 $\mu\text{m}$ | 6.89 $\mu\text{m}$ | 6.95 $\mu\text{m}$ |
| 20000 sine pulses   | 7.16 $\mu\text{m}$ | 7.56 $\mu\text{m}$ | 6.39 $\mu\text{m}$ |
| 5000 square pulses  | 8.39 $\mu\text{m}$ | 7.09 $\mu\text{m}$ | 6.74 $\mu\text{m}$ |
| 10000 square pulses | 7.82 $\mu\text{m}$ | 7.62 $\mu\text{m}$ | 6.46 $\mu\text{m}$ |
| 20000 square pulses | 7.56 $\mu\text{m}$ | 7.22 $\mu\text{m}$ | 6.13 $\mu\text{m}$ |

There is no a visible trend of the Sauter mean diameters with the change of duty cycle.

### **Effect of the number of pulses per burst**

The 1.7 MHz transducer was excited with bursts to analyze how the droplet size distribution of the spray produced changes with the number of pulses per burst. The experiments were performed with different duty cycles.

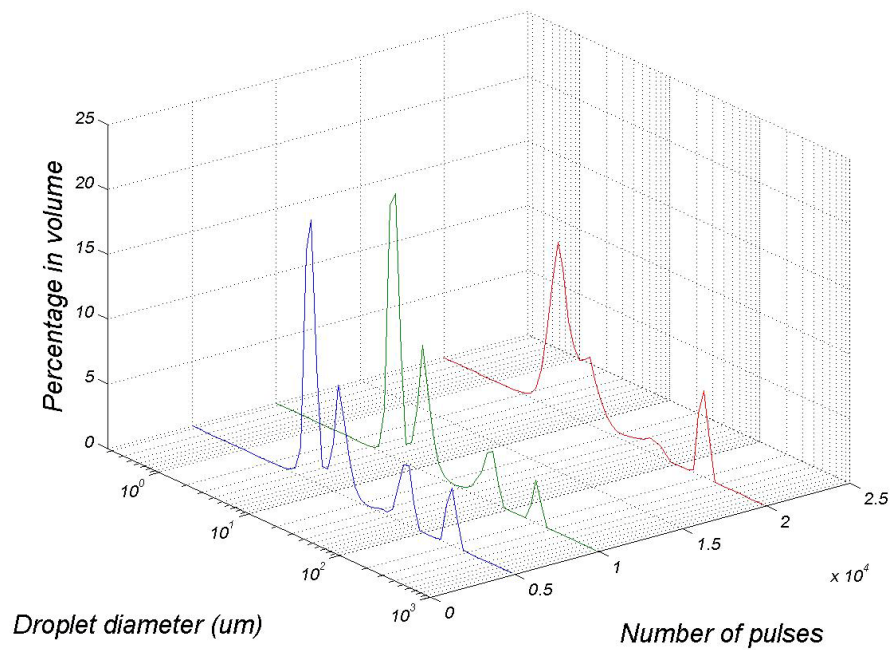


**Figure 4-22: Droplet size distribution of a 1.7 MHz transducer excited with bursts of sine pulses. The duty cycle was 25%.**

Figures that show the same relationship for duty cycles of 25, 50 and 75% duty cycle and square and sine pulses are in appendix D.7. Table 4-6 gives the Sauter mean diameter calculated for the different droplet size distributions.

**Table 4-6: Sauter mean diameter of a spray produced by a 1.7 MHz transducer**

| Burst                | 5000 pulses        | 10000 pulses       | 20000 pulses       |
|----------------------|--------------------|--------------------|--------------------|
| Sine pulses 25% DC   | 8.43 $\mu\text{m}$ | 7.95 $\mu\text{m}$ | 7.16 $\mu\text{m}$ |
| Sine pulses 50% DC   | 6.52 $\mu\text{m}$ | 6.89 $\mu\text{m}$ | 7.56 $\mu\text{m}$ |
| Sine pulses 75% DC   | 6.84 $\mu\text{m}$ | 6.95 $\mu\text{m}$ | 6.39 $\mu\text{m}$ |
| Square pulses 25% DC | 8.39 $\mu\text{m}$ | 7.82 $\mu\text{m}$ | 7.56 $\mu\text{m}$ |
| Square pulses 50% DC | 7.09 $\mu\text{m}$ | 7.62 $\mu\text{m}$ | 7.22 $\mu\text{m}$ |
| Square pulses 75% DC | 6.74 $\mu\text{m}$ | 6.46 $\mu\text{m}$ | 6.13 $\mu\text{m}$ |

Neither the droplet size distribution nor the Sauter mean diameter seem to be affected by the duty cycle or shape of the pulses.

#### **4.5 DROPLET SIZE DISTRIBUTION AT DIFFERENT LENGTHS FROM THE ATOMIZER**

The spray of droplets reaching the laser diffractometer was not dense enough to calculate a droplet size distribution. For this reason, higher atomization rates were tried. Yet this was also unsuccessful.

There was no visible change in droplet size distribution with distance from transducer and with changes in the amount of heating supplied.

It is theorised that full saturation is achieved within a few centimetres of the transducer. For this reason, there was no significant change in the droplet size distribution.

## 4.6 FINDING EVAPORATION DISTANCE

Table 4-7 show the content of water in the tube in which air with water droplets flow. Absolute humidity (water content in vapour state) is calculated from the readings of relative humidity and temperature inside the tube at different locations.

**Table 4-7: Water content in air that carries water droplets and flows inside a tube.**

| LOCATION                                 | 1.5 MHz             | 1.7 MHz             | 2.1 MHz             | 2.6 MHz             | 3.0 MHz             |
|--|---------------------|---------------------|---------------------|---------------------|---------------------|
| Initial water content in the input air   | 13.9 mg/L           | 14.1 mg/L           | 14.8 mg/L           | 15.9 mg/L           | 13.6 mg/L           |
| Water added by atomization               | 3.3 mg/L            | 3.3 mg/L            | 3.3 mg/L            | 3.3 mg/L            | 3.3 mg/L            |
| Water vapour - above the transducer      | 17.1 mg/L (99.25 %) | 14.3 mg/L (82.44 %) | 18.1 mg/L (99.96 %) | 19.2 mg/L (99.93 %) | 15.9 mg/L (94.04 %) |
| Water liquid - above the transducer      | 0.1 mg/L (0.75 %)   | 3.1 mg/L (17.56 %)  | 0.0 mg/L (0.04 %)   | 0.0 mg/L (0.07 %)   | 1.0 mg/L (5.96 %)   |
| Water vapour - 4 cm from the transducer  | 17.2 mg/L (99.95 %) | 14.6 mg/L (83.85 %) | 17.3 mg/L (95.53 %) | 18.3 mg/L (95.01 %) | 16.6 mg/L (97.77 %) |
| Water liquid - 4 cm from the transducer  | 0.0 mg/L (0.05 %)   | 2.8 mg/L (16.15 %)  | 0.8 mg/L (4.47 %)   | 0.9 mg/L (4.99 %)   | 0.0 mg/L (2.23 %)   |
| Water vapour - 8 cm from the transducer  | 16.6 mg/L (96.45 %) | 14.5 mg/L (83.34 %) | 18.0 mg/L (99.55 %) | 18.4 mg/L (95.57 %) | 16.4 mg/L (97.08 %) |
| Water liquid - 8 cm from the transducer  | 0.6 mg/L (3.55 %)   | 2.9 mg/L (16.66 %)  | 0.1 mg/L (0.45 %)   | 0.8 mg/L (4.43 %)   | 0.2 mg/L (2.92 %)   |
| Water vapour - 16 cm from the transducer | 16.5 mg/L (95.64 %) | 14.2 mg/L (81.68 %) | 17.2 mg/L (94.89 %) | 17.8 mg/L (92.60 %) | 16.5 mg/L (97.35 %) |
| Water liquid - 16 cm from the transducer | 0.7 mg/L (4.36 %)   | 3.2 mg/L (18.32 %)  | 0.9 mg/L (5.11 %)   | 1.4 mg/L (7.40 %)   | 0.1 mg/L (2.65 %)   |
| Water vapour - 32 cm from the transducer | 16.7 mg/L (96.85 %) | 14.4 mg/L (82.66 %) | 17.7 mg/L (97.91 %) | 18.5 mg/L (96.00 %) | 16.6 mg/L (98.15 %) |
| Water liquid - 32 cm from the transducer | 0.5 mg/L (3.15 %)   | 3.0 mg/L (17.34 %)  | 0.4 mg/L (2.09 %)   | 0.7 mg/L (4.00 %)   | 0.0 mg/L (1.85 %)   |
| Water vapour - 50 cm from the transducer | 16.6 mg/L (95.97 %) | 14.4 mg/L (82.43 %) | 17.9 mg/L (98.94 %) | 18.5 mg/L (96.04 %) | 16.6 mg/L (97.87 %) |
| Water liquid - 50 cm from the transducer | 0.6 mg/L (4.03 %)   | 3.0 mg/L (17.57 %)  | 0.2 mg/L (1.06 %)   | 0.7 mg/L (3.95 %)   | 0.0 mg/L (2.13 %)   |

It can be seen that for every transducer (without considering the one of 1.7 MHz), there was a quick evaporation of the droplets recorded just above the transducer. The percentages of water content in vapour and liquid stay slightly constant along the tube.

No complete evaporation was seen in the 50 cm of length of the tube under these conditions. However, it is important to mention that the accuracy of the thermocouples used in this experiment is  $\pm 1.5\%$  and for the humidity sensors,  $\pm 3.5\%$ .

A mathematical model will be presented in section 5.3 to simulate this experiment with air at different temperatures (25, 50 and 100°C).

## **CHAPTER 5: IMPROVEMENT OF HUMIDIFICATION**

### **5.1 INTRODUCTION**

There were some difficulties with the atomization of water using planar US transducers for this application: This is due to the fact that:

- The droplets were not mixed in the air
- A few big droplets were formed during the atomization

These problems were assessed by designing a housing structure to have a narrow droplet size distribution (explained in 5.2) and the length required for full evaporation to occur (5.3).

### **5.2 NARROWING THE DROPLET SIZE DISTRIBUTION**

#### **5.2.1 INTRODUCTION**

In this section, the design, mathematical evaluation and experimentation of a housing structure that keeps the big droplets (which do not move with the air flow) in the atomization chamber. The design allows these droplets to run on the walls back to the ultrasonic transducer.

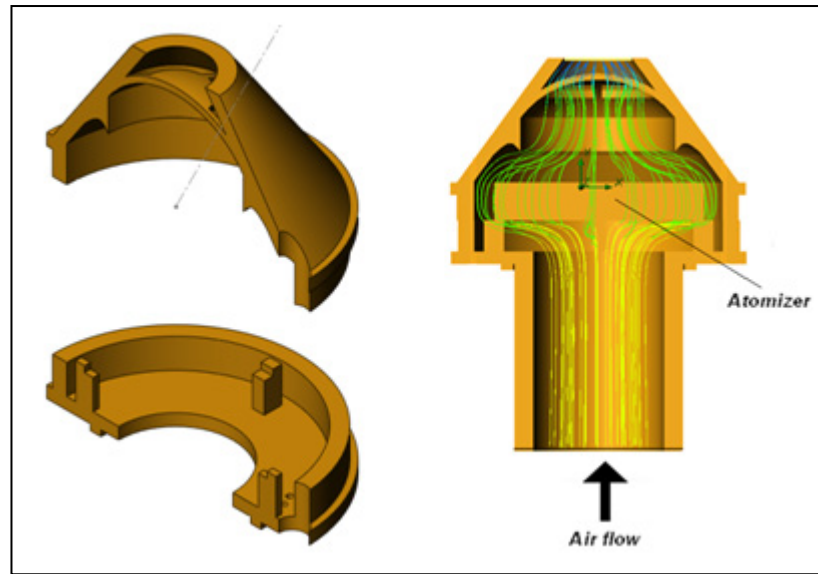


**Figure 5-1: One of the geometries designed (left) and simulated (right) in SolidWorks™**

### **5.2.2 DESIGN OF GEOMETRIES**

All the geometries force the airflow to surround underneath the transducer to then pick up the droplets and leave the structure upwards. At the same time, any droplet that collides the wall, should fall down back to the transducer surface since the structures have smaller diameter than the transducers.

The first geometry is open above the transducer and should give minimal obstruction for the big droplets to jump over the structure. The other two geometries have some structure that restricts the big droplets from exiting the chamber.

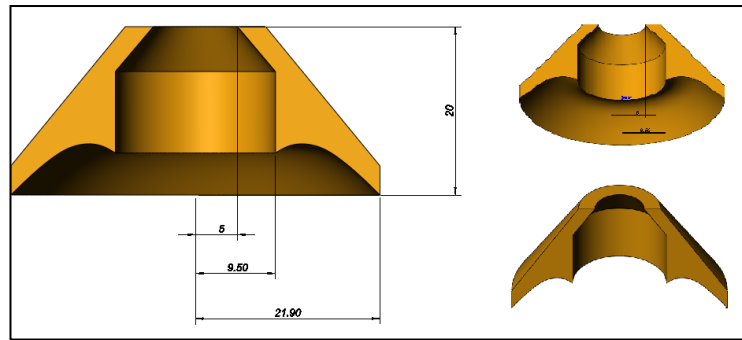


**Figure 5-2: Mixer 1 which offers no opposition to the pass of big droplets.**

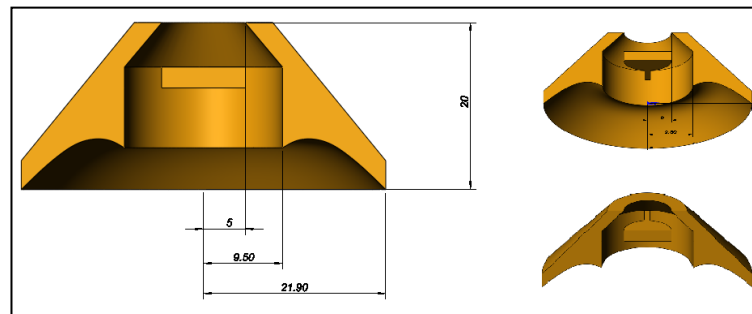


**Figure 5-3: Mixer 2 has a planar disk in the centre.**

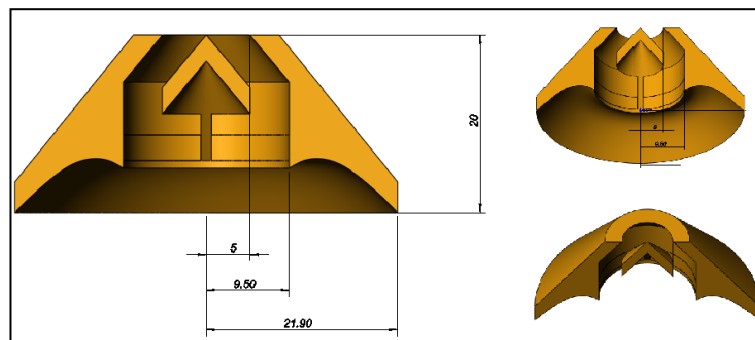


**Figure 5-4: Mixer 3 has a conic structure in the centre.**



### **5.2.3 MATHEMATICAL EVALUATION OF THE GEOMETRIES**

The flow inside the mixers has been simulated. The air inlet was set in the low part of the structure and flows upwards inside a 22-mm tube until it reaches another cavity which is cylindrical with a 43.8mm diameter and the different mixers as roof. Inside this cavity, the ultrasonic transducer disk is located with a cylinder on top of it that acts as water reservoir. The air surrounding the transducer and water reservoir leaves the cavity through the mixer.

A fan was selected to generate the air flow as in the experiments. It was an ideal device predefined as a brushless DC fan from the SolidWorks<sup>TM</sup> engineering database free of boundary conditions. The walls were set as ideal walls (adiabatic and frictionless) and the output as a pressure opening (static pressure for the outgoing flow). The global goals were pressure, temperature and velocity of the fluid.

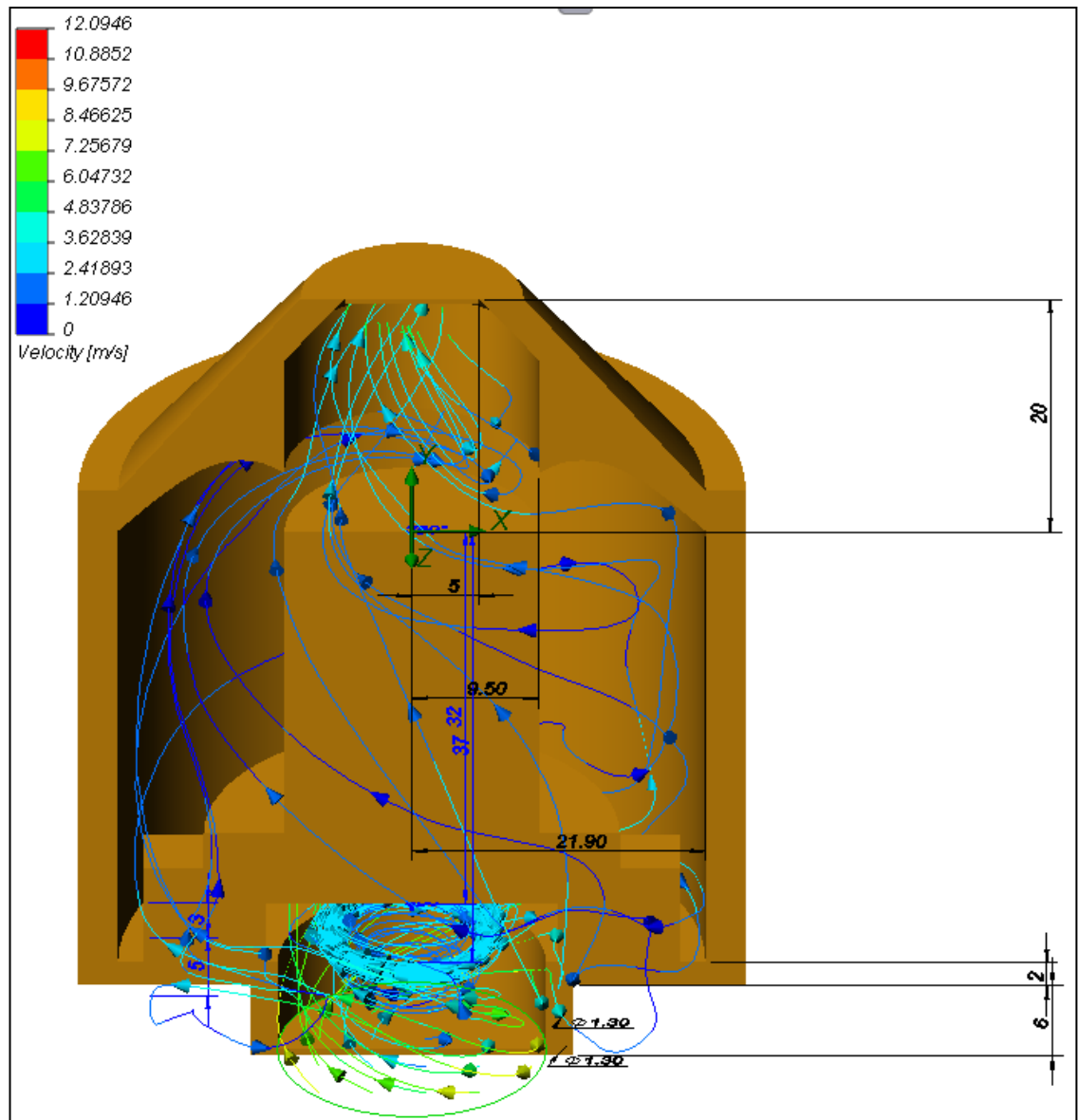


**Figure 5-5: Simulation of the air flow surrounding the transducer and water reservoir and leaving through mixer 1.**

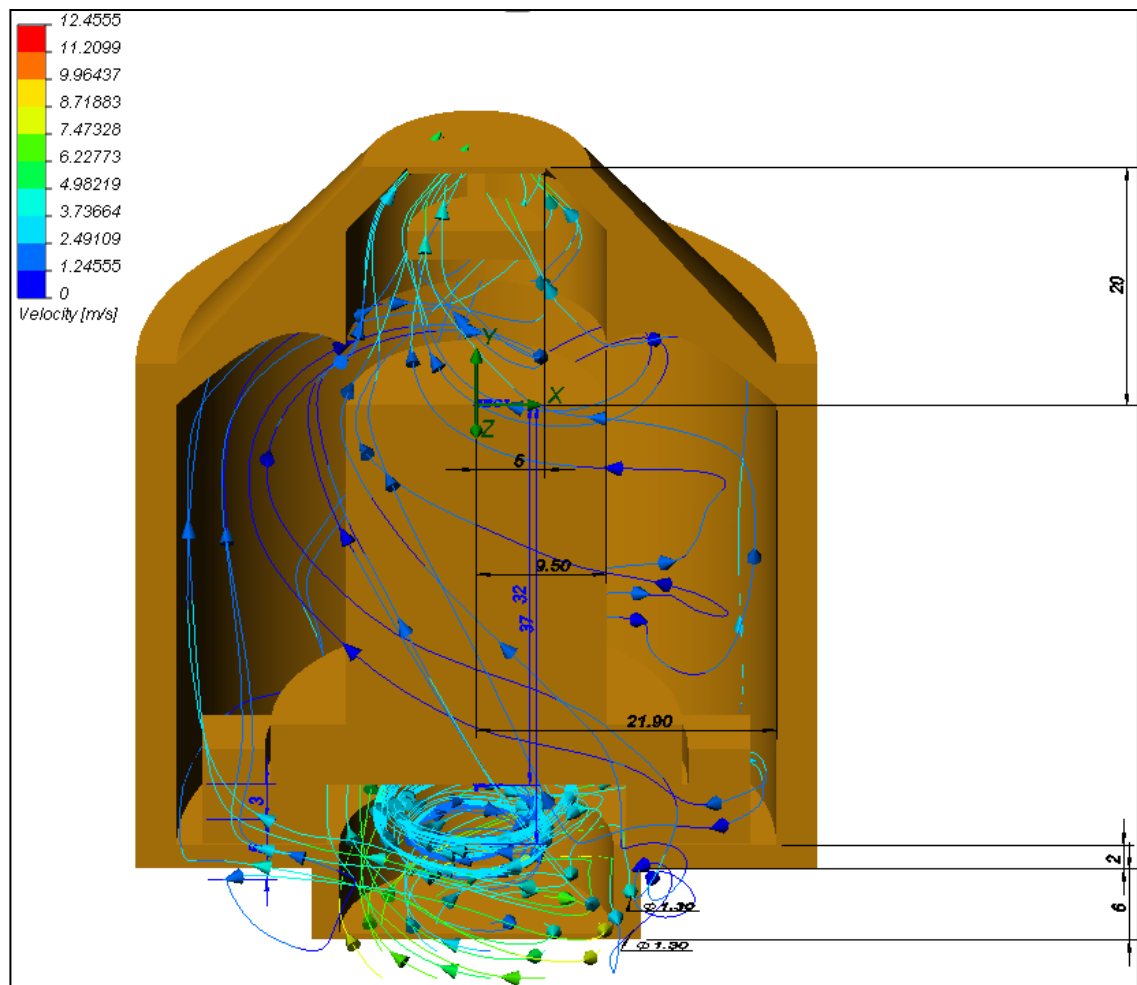


**Figure 5-6: Simulation of the air flow surrounding the transducer and water reservoir and leaving through mixer 2.**

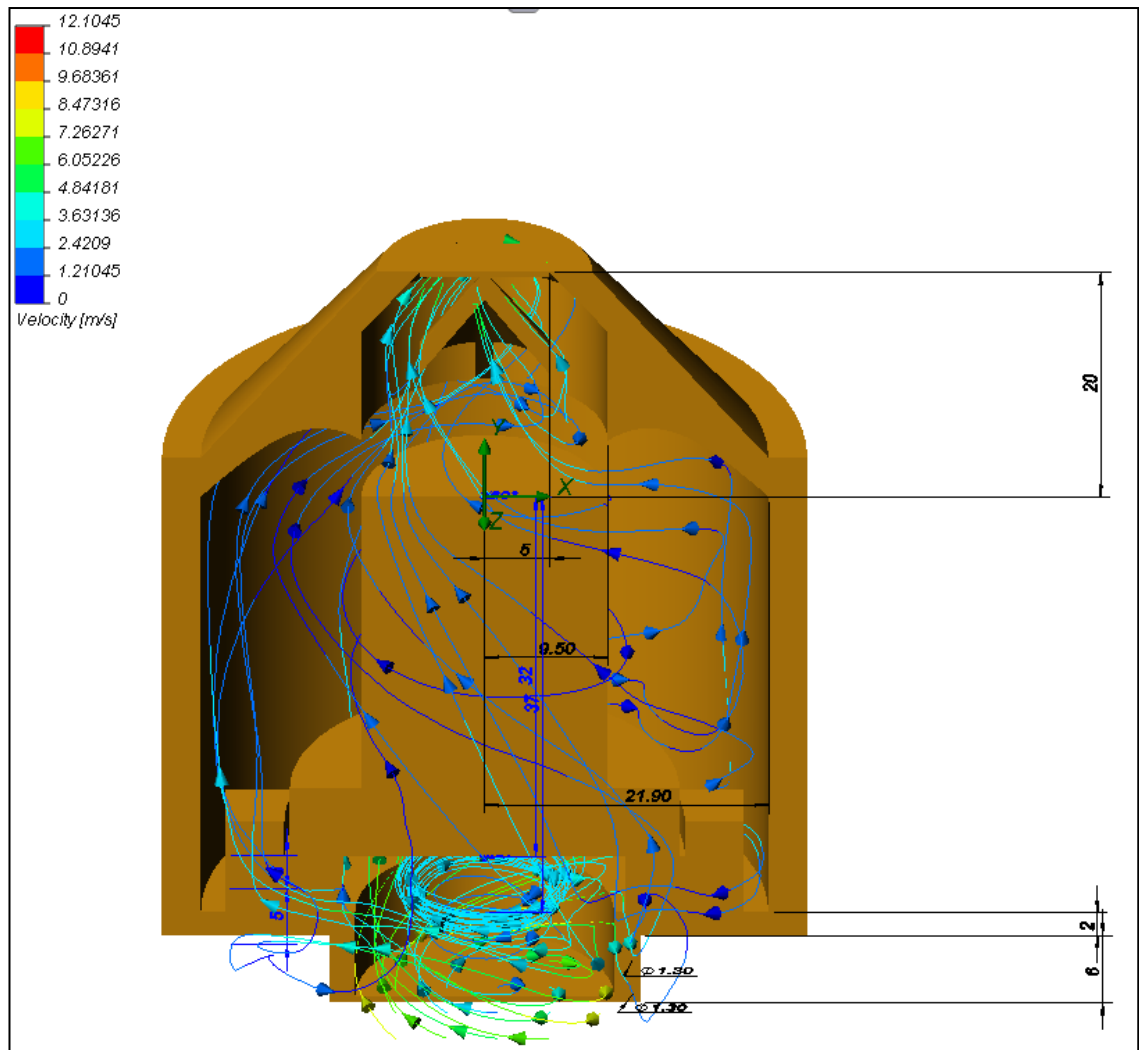


**Figure 5-7: Simulation of the air flow surrounding the transducer and water reservoir and leaving through mixer 3.**

In the three geometries the air enters at a relatively high speed ( $\sim 8$  m/s) and then slows down as it flows upwards surrounding the cylinder which represents the water reservoir. Then, as the cross-sectional area decreases, the velocity increases (flow rate is constant). At this point the mixing of water droplets and air may take place.

#### **5.2.4 MIXER PERFORMANCE**

Since the last three geometries had similar performance in the simulation, only one of them (mixer 2) was fabricated using Fused Deposition Moulding (FDM) printing. The first geometry (mixer 1) was also printed for comparison purposes. The droplet size distribution of the spray generated by ultrasonic transducers at different frequencies has been affected as Figure 5-8. For more detail, see the figures that show the same comparison for all transducers in 2D in appendix E.

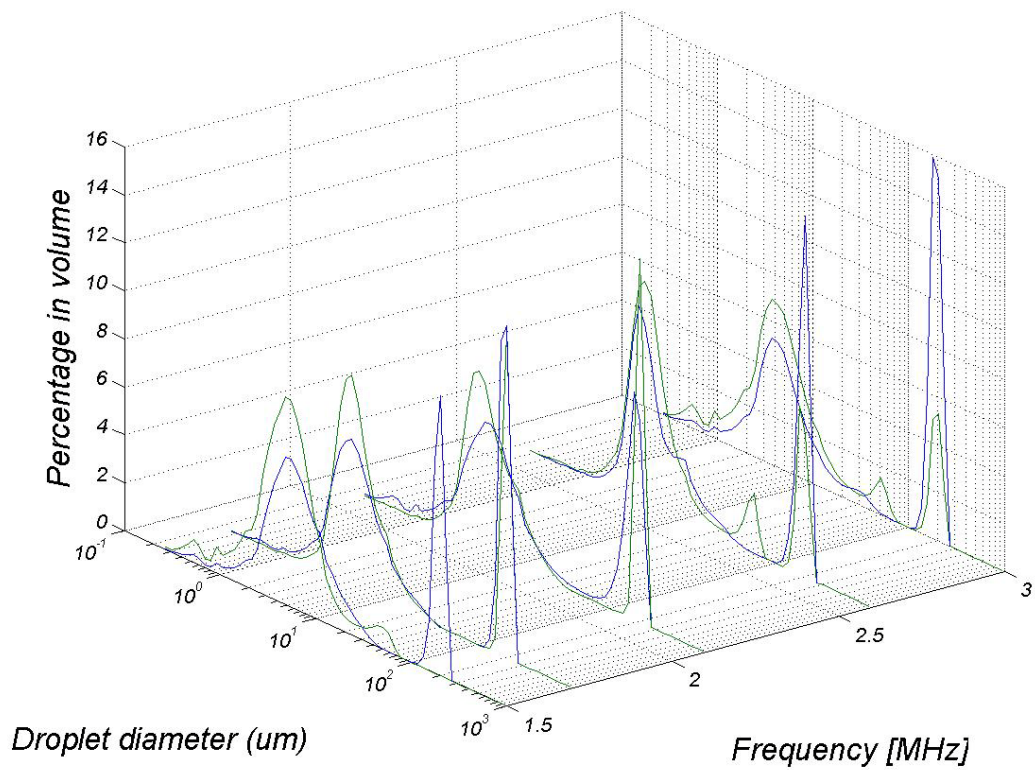


**Figure 5-8: Droplet size distribution of a spray generated by ultrasonic transducers using either mixer 1 (blue) or mixer 2 (green).**

It can be seen for all transducers that there is a higher concentration of the volume in droplets of small diameter for the mixer 2.

## 5.3 VAPORIZATION OF WATER DROPLETS

### 5.3.1 INTRODUCTION

Ideally, a humidifier has no water droplets at its output. All of the water content of the air supplied to the patient should be in vapour state. Assuming that the droplets generated from ultrasonic atomization are taken in the mixer by the air and carried away to the patient through a tube, these droplets should be evaporated in the connecting tube in a short distance without reaching the patient.

In this section, a finite volume model is used to simulate the evaporation of water droplets in a tube is described. This model was used to evaluate the conditions required for the fully evaporation of the droplets in a relatively short distance.

### 5-3-2 ASSUMPTIONS OF THE MODEL

A gas phase containing H<sub>2</sub>O and Air ideal gas (ANSYS Library), and a homogeneous binary mixture for the phase change of water were assumed. The mass transfer equation [94] used for the evaporation of the droplets was:

$$\frac{dm_c}{dt} = \pi d_p \rho_F D_F \text{Sh} \frac{W_C}{W_G} \log \left( \frac{1 - X^*}{1 - X_G} \right) \quad (5.1)$$

where  $m_c$  is the mass of water,  $\rho_F D_F$  is the dynamic diffusivity of the mass fraction in the continuum,  $W_C$  and  $W_G$  are the molecular weights of the vapour and the mixture in the continuous phase,  $X_G$  is the molar fraction in the gas phase,  $X^*$  is the equilibrium mole fraction at the droplet surface and Sh is the Sherwood number given by the equation 5.2:

$$\text{Sh} = 2 + 0.6 \text{Re}^{0.5} \left( \frac{\mu}{\rho D} \right)^{\frac{1}{3}} \quad (5.2)$$

where Re is the Reynolds number,  $\mu$  the viscosity,  $\rho$  the density and  $D$  the diameter of the water droplet.

The evaporation of the droplets was evaluated on a cylindrical tube. One of the sides had the water and air inputs. The output was on the other end.

Raoult's law was used for the interfacial equilibrium model. The resistance mass transfer on the droplet side was considered negligible. Hence Zero Resistance on the dispersed phase side and Ranz-Marshall on the continuous phase side[94].

### **5.3.3 GEOMETRY**

The geometric representation of the computational domain was set as a steady-state rotating domain. For this reason, only 1/8 of the cylinder was drawn in ANSYS Design Modeler.

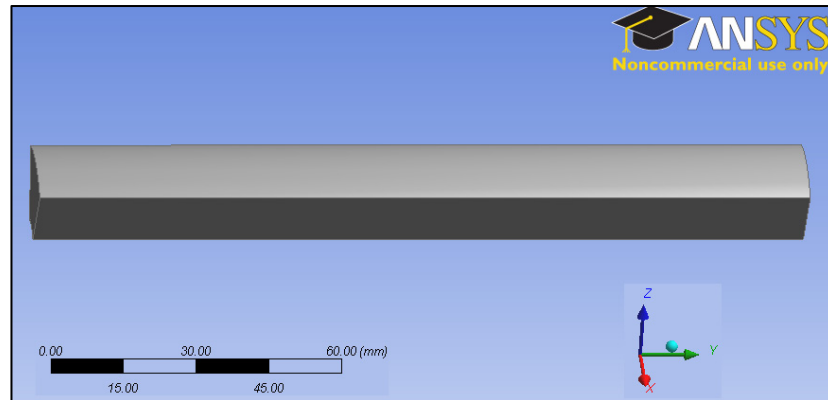


**Figure 5-9: Geometry of a 1/8 section of the cylinder.**

Water and air inputs were “printed” on one of the faces and its counterpart was set as the output. The length of the cylinder was 16 cm.

### **5.3.4 MESHING**

An accurate solution depends on the quality of the mesh. For the geometry previously mentioned, a structured layer made of high-aspect-ratio elements (prisms and structured tetrahedral) were chosen in wall boundaries. The rest of the geometry used an unstructured grid (tetrahedral elements) which permitted automation of the mesh generation procedure.

The settings for the mesh were patch independent of 0.001, face sizing of 0.0001 and edge sizing of 30. The quality of the mesh was assessed using Skewness which is one parameter available within ANSYS® 12.1. Skewness is a measure of the relative distortion of an element compared to its ideal shape and is scaled from 0 (excellent) to 1 (unacceptable). In the present work the Skewness was 0.3 which is within the acceptable range.

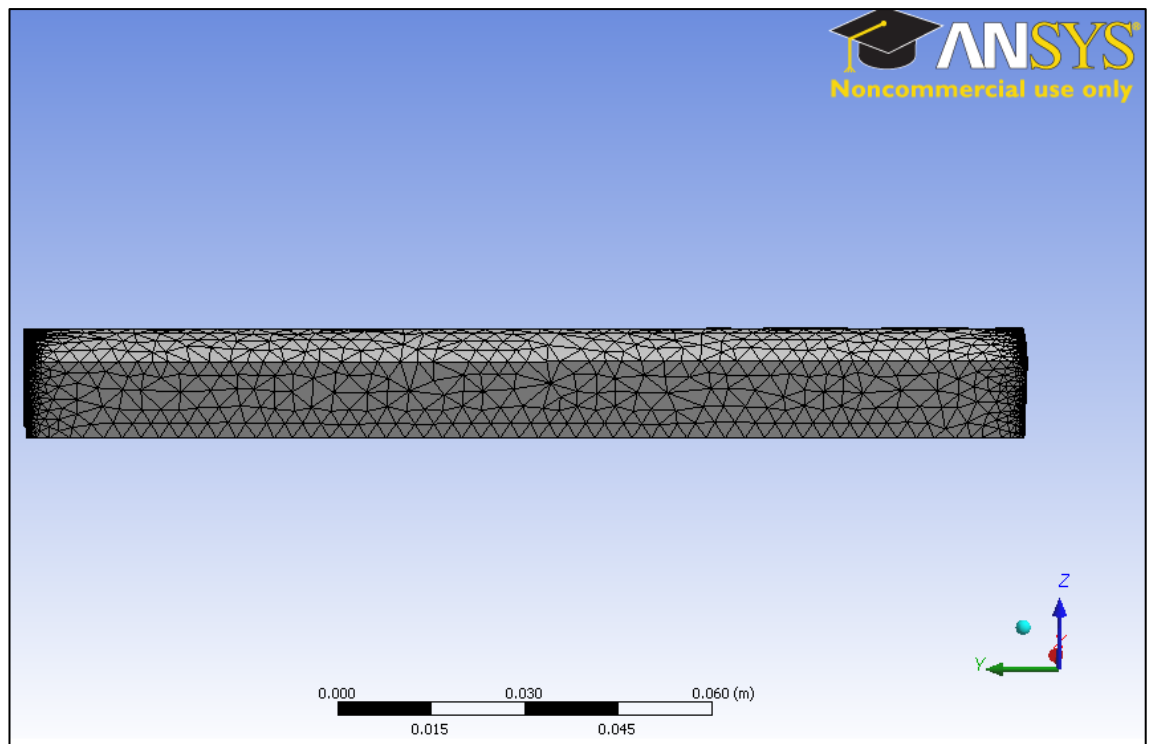


**Figure 5-10: Meshing of the geometry.**



### **5.3.5 SET UP**

For the simulation, relevant parameters were set:

- The gas mixture was set as non bouyant to neglect the natural convection of the gas and the model for the second component (H<sub>2</sub>O) was density difference.
- Air inlet mass and momentum axial component along the axis of the tube was 12.73 m/s (considering an air flow of 60 L/min passing through a circular section of 10 mm diameter).The water droplets are assumed to have the same velocity as the air 12.73 m/s. The static temperature of the water was 313 K. The droplets mass flow rate was  $22.0 \times 10^{-6}$  Kg/s (taking into consideration 1/8 of the structure).
- The size distribution of the droplets was set using discrete diameter values and associated fractions of the droplet mass flow rate. The results of these experiments are shown in section 3.3.3. Uniform droplet size of 5  $\mu$ m was also assumed for the simulations.
- The wall of the cylinder was considered to have a heat transfer coefficient of 0.036 W/(m<sup>2</sup>K) as example and the outside temperature was set to 300 K.

### **5.3.6 RESULTS**

Figures 5-11, 5-12 and 5-13 show the results for the simulation when all the droplets were assumed to be 5  $\mu\text{m}$  diameter. The air initial temperature was 25, 50 and 100 $^{\circ}\text{C}$  respectively.

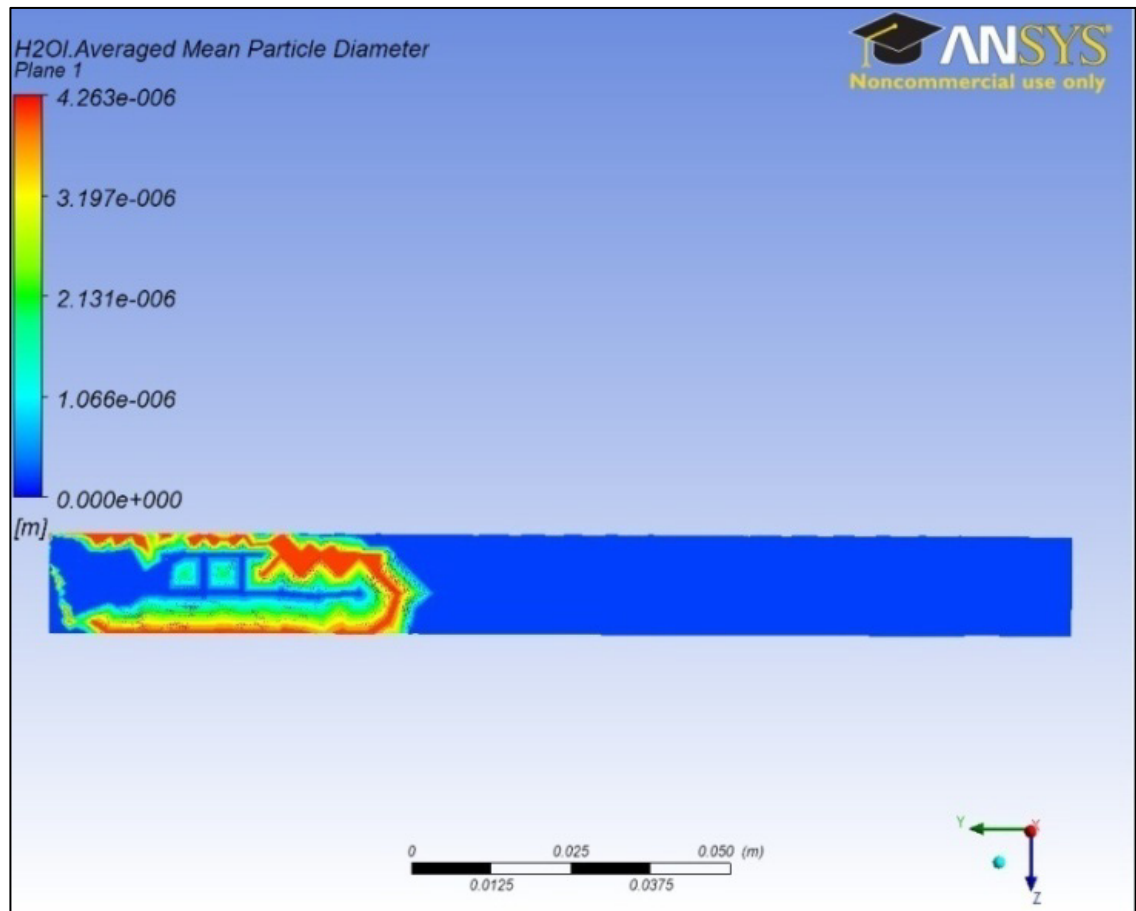


**Figure 5-11: Result of the simulation with initial droplets of 5  $\mu\text{m}$ , water temperature of 50 $^{\circ}\text{C}$  and air temperature of 25 $^{\circ}\text{C}$ .**

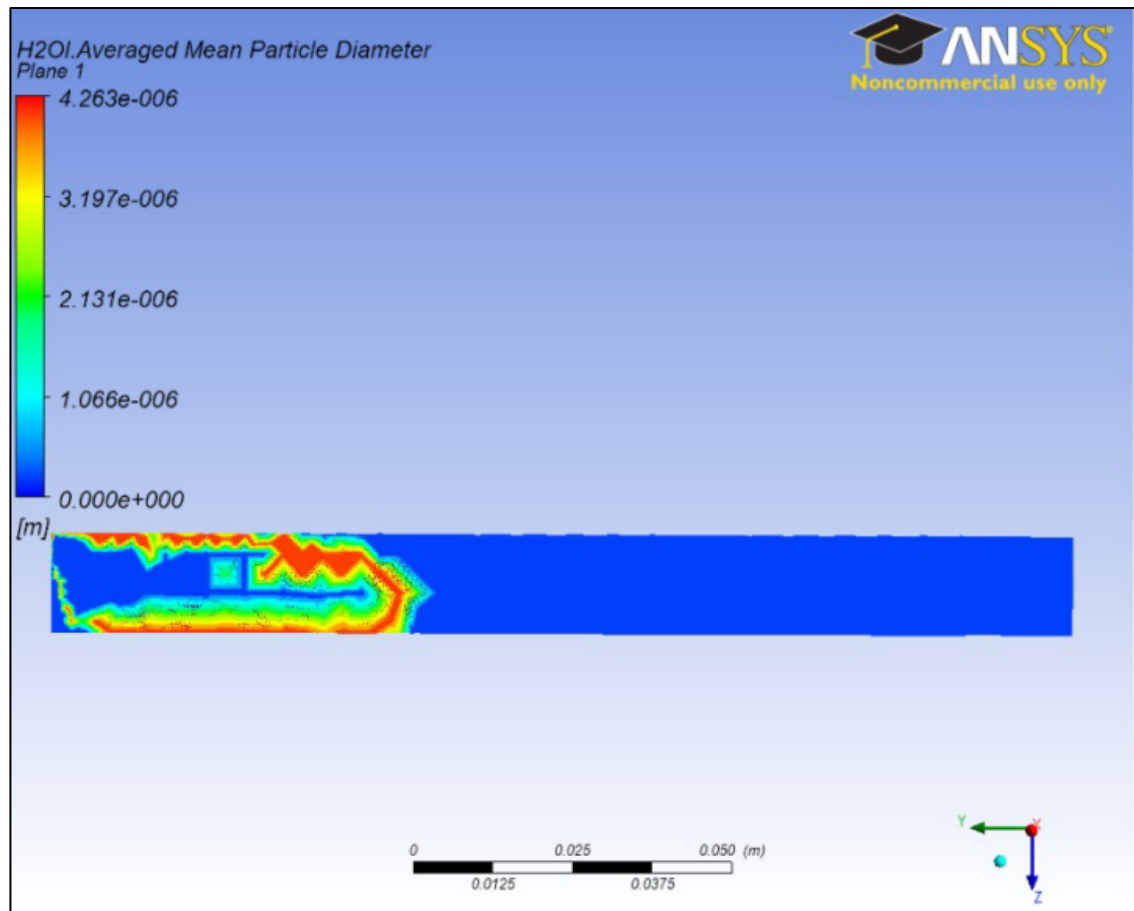


**Figure 5-12: Result of the simulation with initial droplets of 5  $\mu\text{m}$ , water temperature of 50°C and air temperature of 50°C.**

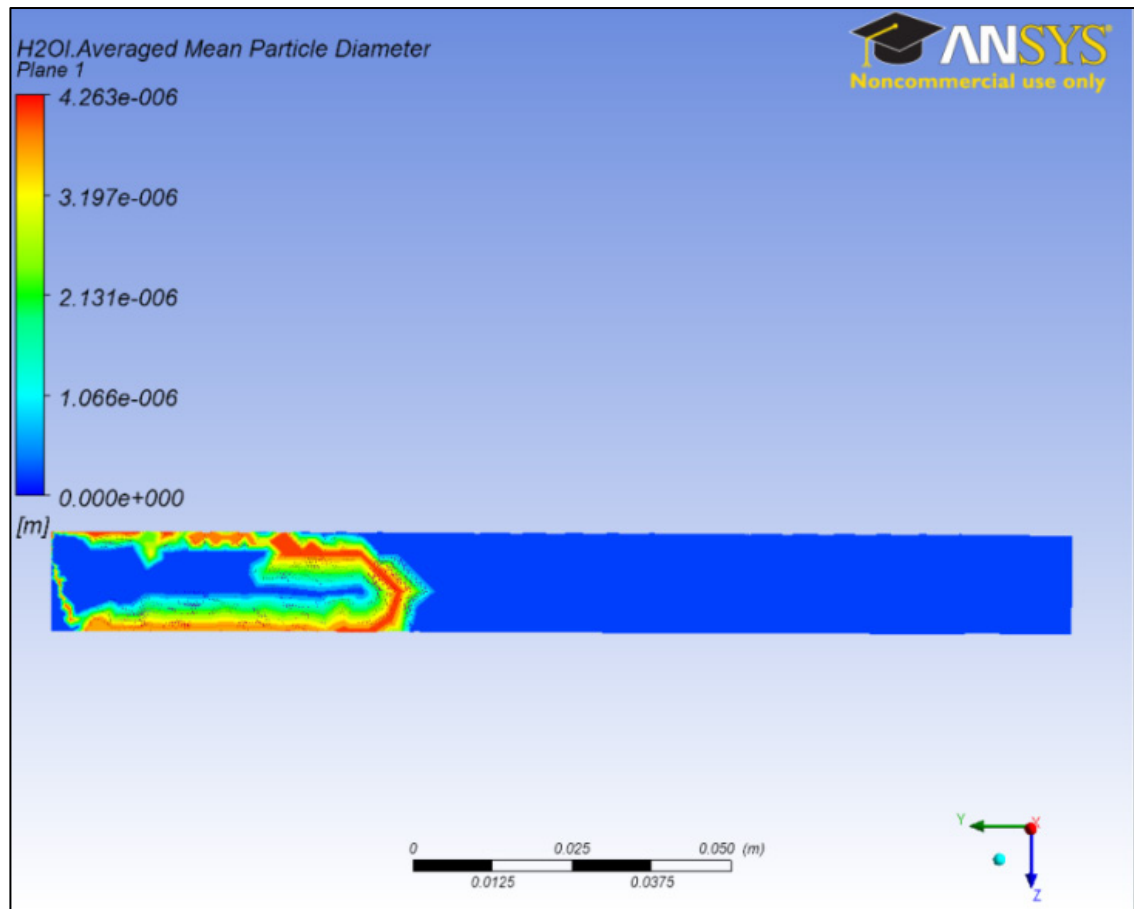


**Figure 5-13: Result of the simulation with initial droplets of 5  $\mu\text{m}$ , water temperature of 50°C and air temperature of 100°C.**

It can be seen that there was a complete evaporation at  $\sim 5.5$  cm from the input of water and air. The results were similar regardless of the temperature of the input air. Nevertheless, it is possible to see a faster evaporation as the air temperature increases.

Figures 5-14, 5-15, 5-16, 5-17 and 5-18 show the results for the simulation when the initial droplet size distribution was equal to the one obtained from the atomization of water with transducers of 1.5, 1.7, 2.1, 2.6 and 3.0 MHz in section 4.4.3.

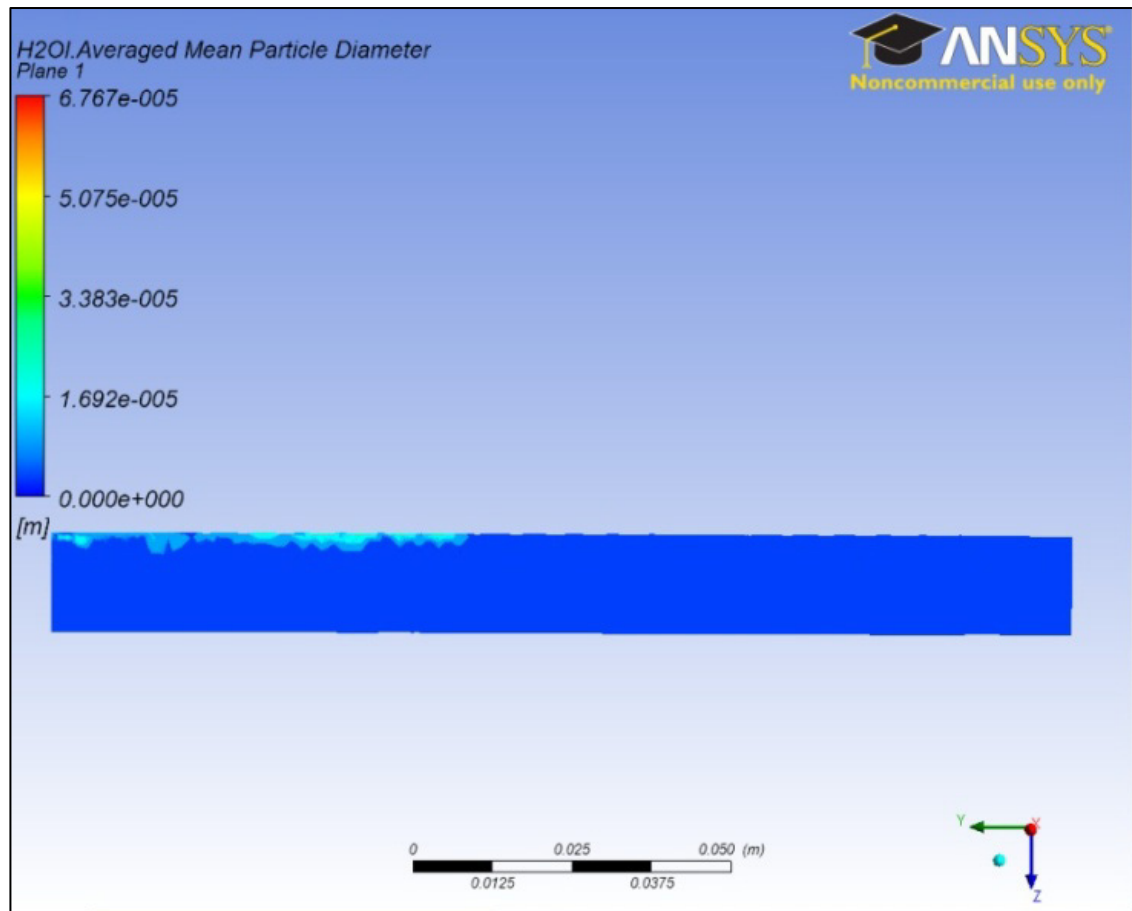


**Figure 5-14: Result of the simulation with initial droplet size distribution characteristic of a 1.5 MHz transducer, water temperature of 50°C and air temperature of 25°C.**

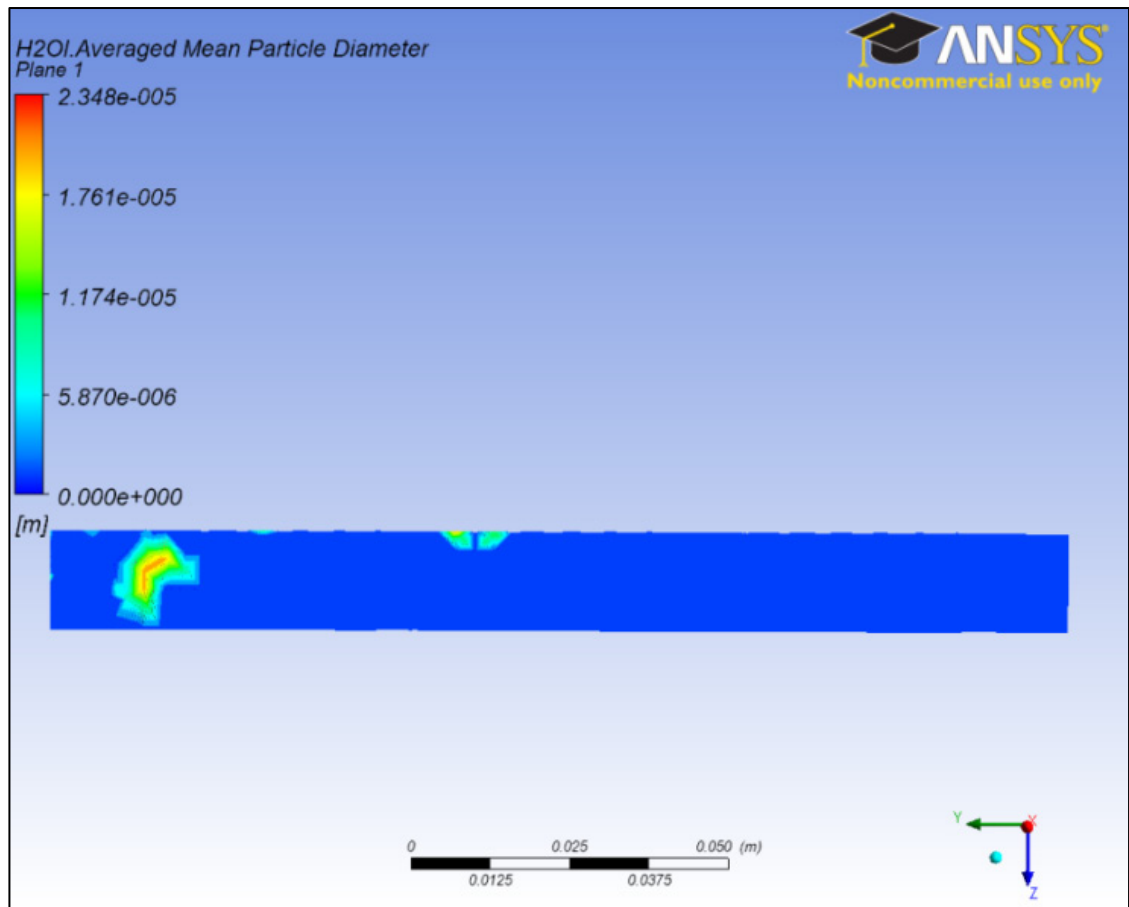


**Figure 5-15: Result of the simulation with initial droplet size distribution characteristic of a 1.7 MHz transducer, water temperature of 50°C and air temperature of 25°C.**

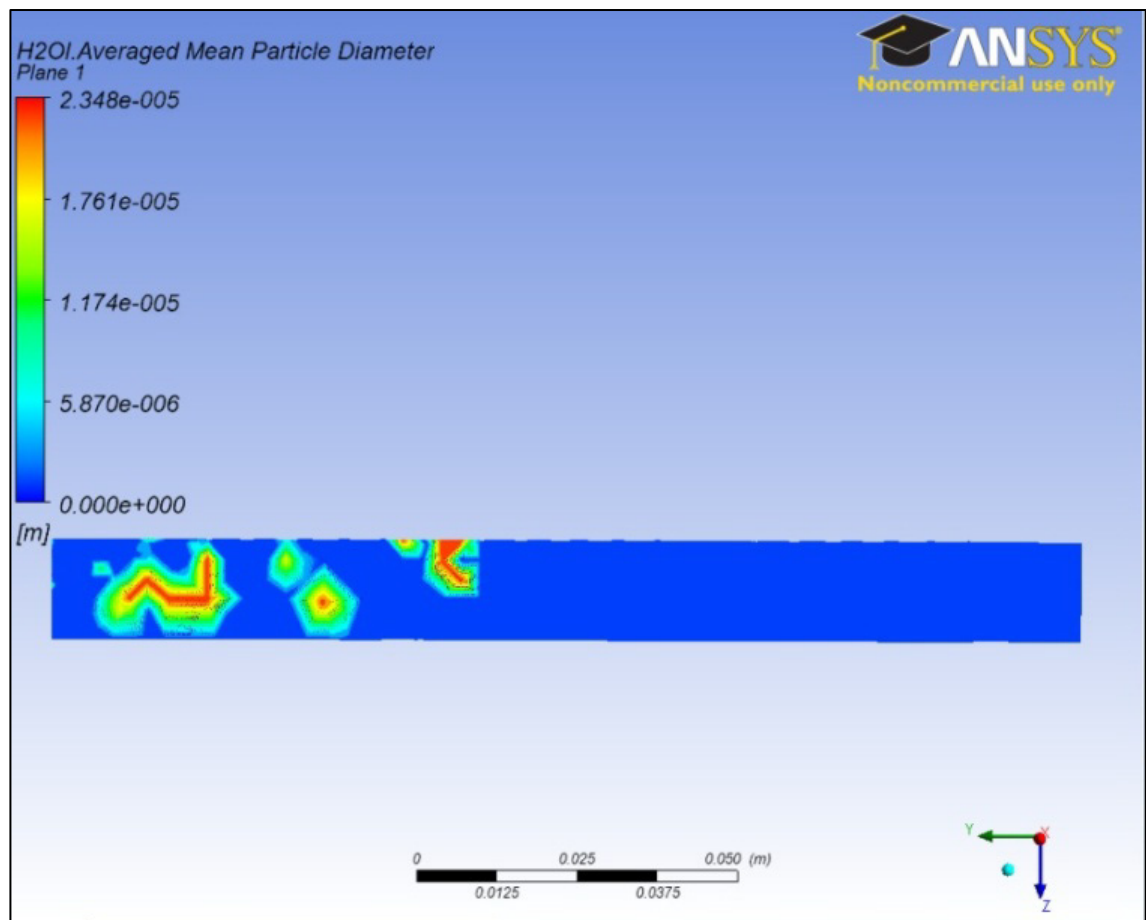


**Figure 5-16: Result of the simulation with initial droplet size distribution characteristic of a 2.1 MHz transducer, water temperature of 50°C and air temperature of 25°C.**

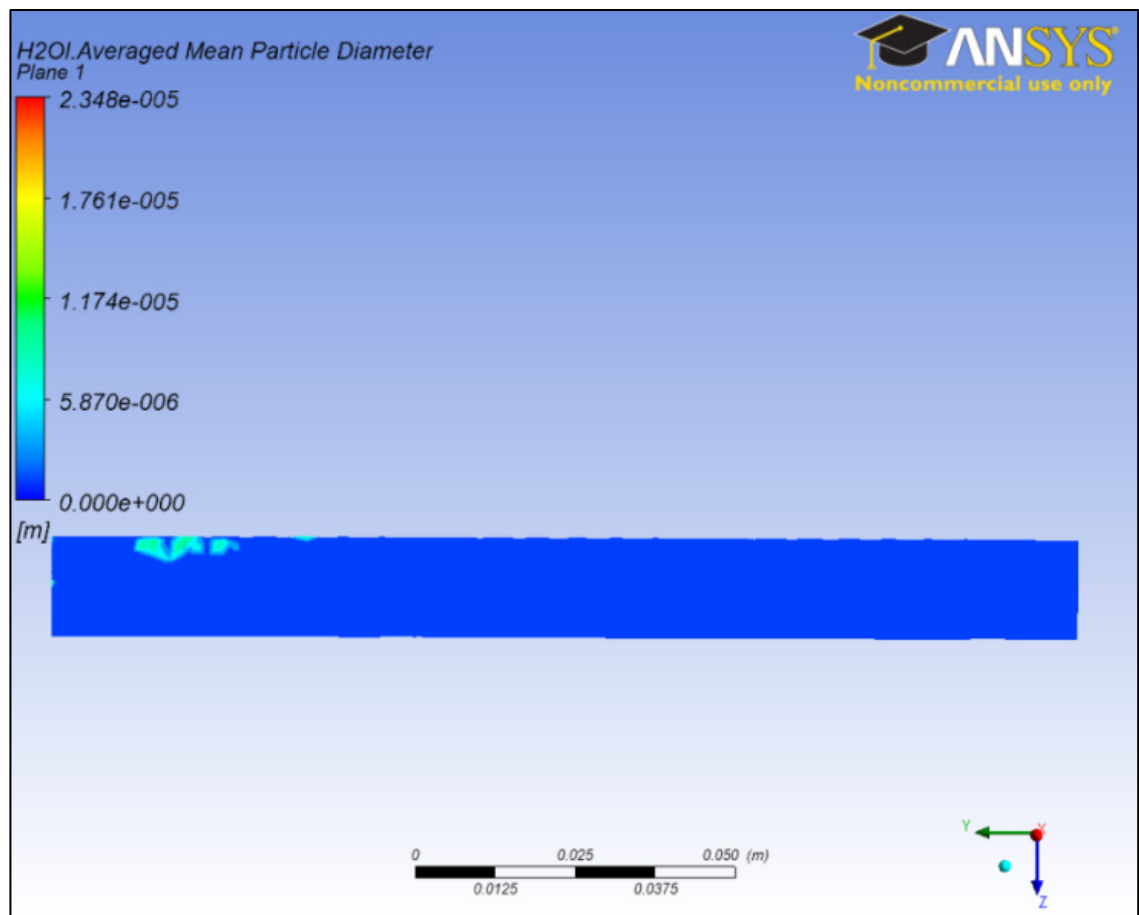


**Figure 5-17: Result of the simulation with initial droplet size distribution characteristic of a 2.6 MHz transducer, water temperature of 50°C and air temperature of 25°C.**



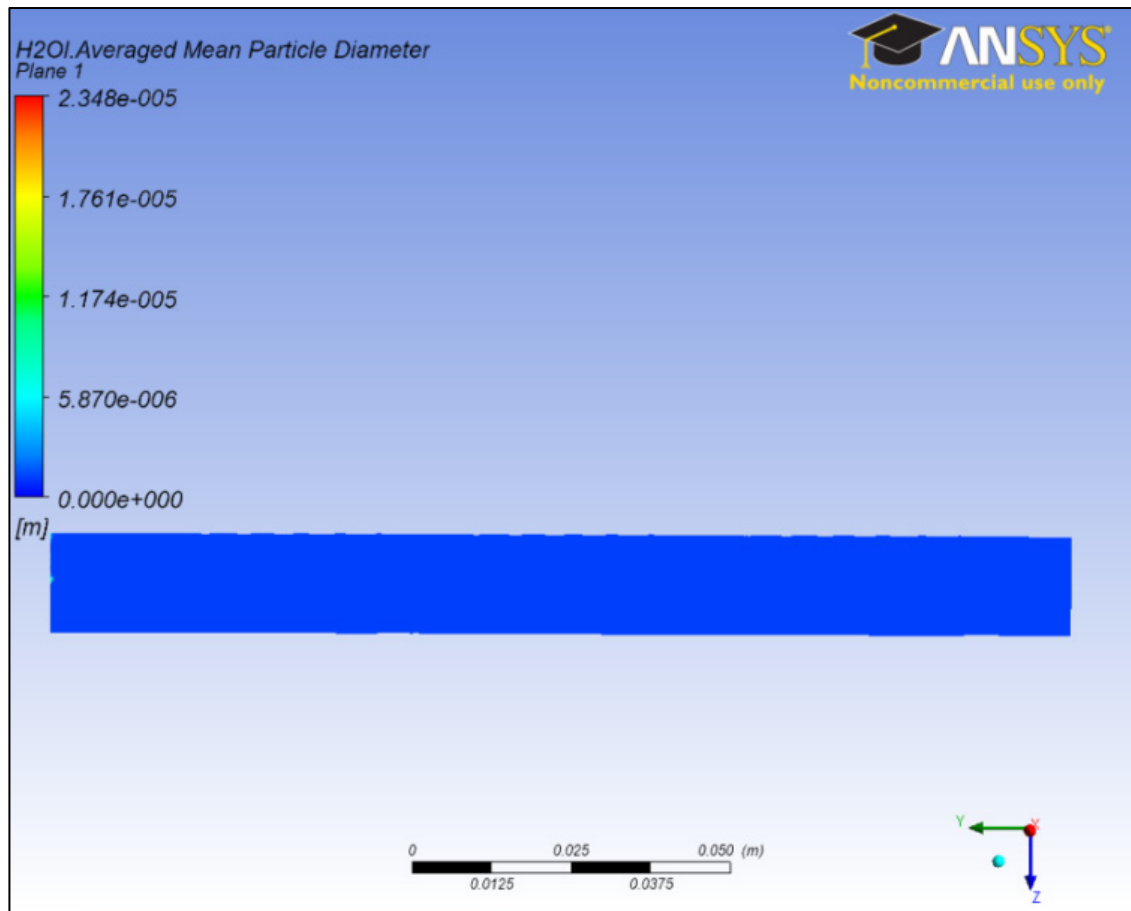


**Figure 5-18: Result of the simulation with initial droplet size distribution characteristic of a 3.0 MHz transducer, water temperature of 50°C and air temperature of 25°C.**

Quick evaporation is seen when the initial droplet size distribution is like that generated by the ultrasonic transducers tested in section 4.4.3. These results suggest that the air does not need to be heated above the ambient temperature to achieve the full evaporation of the droplets before they reach the patient.

## **CHAPTER 6: DISCUSSION AND CONCLUSION**

### **6.1 INTRODUCTION**

This chapter will discuss the literature review presented in Chapter 2, the experimental results obtained in Chapter 4 and the theoretical simulations from chapter 5. Additionally, the conclusion of this thesis will be presented as well as recommendations for future work.

### **6.2 ATOMIZATION PROCESS SELECTION**

The atomization principles have been classified into six categories in this thesis and discussed in section 2.2. They were centrifugal, pressure, two-fluid, electrostatic, ultrasonic and combinations of these methods.

Centrifugal atomizers have low energy consumption but the droplets are ejected from the atomizer at high speed and are likely to impinge on any close surface. This condition limits the miniaturization of such atomizers.

Pressure atomizers can work in any orientation. The main drawback of this method is the possible clogging of the hole/nozzles. Nevertheless, this problem could be solved by using distilled water.

Two-fluid atomizers require a compressed air source which would difficult to miniaturize.

The Electrohydrodynamic atomizers reviewed in the literature survey were not able to atomize the quantity of water required for this application. Another weakness is the need of a high voltage for its operation.

Ultrasonic atomizers, as shown in table 2-1, have a good relation between atomization rate and power consumption. They are small sized and commercially available.

### **6.3 PERFORMANCE OF ULTRASONIC ATOMIZERS**

In this thesis, an extended experimentation has been performed on flat ultrasonic transducers with five frequencies (1.5, 1.7, 2.1, 2.6 and 3.0 MHz).

The transducers were excited with bursts of pulses of sine and square shape. These bursts were sent at different rates to cause different duty cycles

Atomization rate was not affected by the number of pulses per burst. However, it visibly increased with increments of duty cycle. Sine pulses were more effective than square pulses in terms of power consumption.

It was not possible to determine if the number of pulses per bursts had an effect or not on the heating of the transducer. The duty cycle did have an important effect as it was expected (considering that the higher the duty cycle, the higher the power consumption). Although these transducers consumed less power when they were excited with sine pulses, they generated as much heat as when excited with square pulses.

Photographic and impact methods were attempted for the measurement of the droplet size distribution of the spray generated by the transducers. None of these methods gave consistent results due to the presence of droplets of different planes than the focal plane in the image. Different filters were used to eliminate these out of plane and have a clear image but these were unsuccessful. For the same reason, a Malvern Spraytec Laser Diffractometer was used for the measurement of the droplet size distribution. The spray produced by ultrasonic transducers of different frequencies had similar droplet size distribution and the Sauter mean diameter did not follow Lang's predictions (refer to section 4, Table 4-3, pg 56). Nevertheless, the Sauter mean diameters were all in the range of 3-7  $\mu\text{m}$ . These values were similar for every transducer regardless of whether

they were excited with square or sine pulses. Hence, the characteristics of the transducer had more effect on the Sauter mean diameter than its frequency or the shape of the excitation pulses. Likewise, the droplet size distribution and Sauter mean diameter were not affected by the power delivered to the transducer but the atomization rate was affected as stated by Barreras et al. [46, 56]. Moreover, the droplet size distribution and Sauter mean diameter were not affected by the number of pulses per burst, duty cycle or the shape of the pulses.

The complexity of the driving circuit increases as the frequency increases, and the performance of the transducers in terms of droplet size distribution, atomization rate, power consumption present slight changes. The use of transducers of 1.5 MHz is recommended for this application. This transducer's excitation with sine pulses would require less power than with square pulses and they should be supplied in bursts in order to not overheat the transducer. The number of pulses per burst does not have visible effect on the performance and the frequency at which the bursts are sent should be the minimum that achieve the atomization rates desired.

## **6.4 VAPORIZATION OF WATER DROPLETS**

Ideally, there should be no water droplets on the air supplied to the patient. Once they are added to the airflow, they should be fully evaporated before reaching the patient mask.

In order to facilitate the evaporation of the droplets in a short tube distance, the big droplets produced by the ultrasonic transducer should be avoided. For this reason, a housing structure has been designed, mathematically modelled and experimentally tested. This structure maximized the mixing of the droplets with the air and kept the big droplets (which do not move with the air flow) in the atomization chamber. With this design, the big droplets hit the walls and fall back to the ultrasonic transducer. Its performance has been assessed by measuring the droplet size distribution of a water

spray passing and without passing through the structure. In the first case, there was a higher concentration of the volume in droplets of small diameter than when the spray had not pass by the structure.

In order to determine the conditions required for the evaporation of the droplets, a mathematical model has been presented which was validated through experiments. Assuming 60 L/min of air at 25°C, and taking droplets of 5 µm diameter into a tube of 1 cm diameter, the droplets evaporated in approximately 5 cm. The result was similar when the initial size distribution was the characteristic for transducers of 1.5, 1.7, 2.1, 2.6 and 3.0 MHz. Hence a heater would not be necessary to achieve the fully evaporation of the water droplets before the air reaches the patient.

## **6.5 GENERAL OBSERVATIONS**

There is a high risk of upper airway infection when a CPAP machine is used (with or without humidifier). Pre-treated water is recommended when an atomizer is used to humidify the air. The use of hydrophobic filters between the humidifier and mask is the only method that would stop any microorganism and minerals dispersed by an atomizer from passing to the patient. Hygroscopic filters would also retain water and help to increase the pressure drop.

The container for the water storage also does not need to be rigid. Since this humidifier is aimed to be used in portable devices, a flexible container such as a sachet would be more suitable. A sachet has a small volume when it is empty and, when full, it could be put on the wall at a higher position than the atomizer. An electronically controlled valve can regulate the flow of water to the atomization chamber.

## 6.6 CONCLUSIONS

The purpose of this thesis was to develop a novel humidifier by selecting an appropriate atomizer, characterizing it through experimentation, designing a structure to adapt its output, analyzing the evaporation of the droplets generated and defining global characteristics of the whole system. This thesis has met these objectives. The findings of this thesis suggest that:

- a) Pressure and Ultrasonic atomization are the more suitable methods for this application. Pressure atomizers have a narrow droplet size distribution and are not position sensitive. However, ultrasonic atomizers showed the best relation between atomization rate and power consumption.
- b) Ultrasonic transducers of 5 frequencies have been tested under pulsed excitation with different burst frequencies (duty cycles) and wave-shapes. The results show that the performance is higher with sine pulses and the number of pulses per burst does not have a visible effect on the atomization rate nor the droplet size distribution. Contrarily, the duty cycle did have a proportional relationship with the atomization rate and the temperature of the transducers raised as the duty cycle increased. Regarding the frequency of the transducer, the droplet size distribution did not have a significant change with the frequency in the range of 1.5 to 3.0 MHz and, considering that the complexity of the driving circuit increases with the frequency, 1.5 MHz is recommended for this application.
- c) A structure was designed, mathematically modelled and experimentally tested to prevent large water droplets from entering the air stream to the patient and maximize the mixing of the droplets in the airflow.
- d) The evaporation of water droplets moving with the airflow in a 10 mm diameter tube was theoretically and experimentally analyzed. Fully evaporation was reached in approximately 5 cm and the heating of the air would not be necessary for the fully evaporation.

- e) Hydrophobic filters are recommended to reduce the risk of contamination of the air by any particle or microorganism. The maximum filter size should be at most as  $0.02\ \mu\text{m}$  that could deposit in the airways without retaining water as hygroscopic filters.
- f) The use of a flexible water container would be optimum for portable devices due to its small volume when is not being used.
- g) A humidifier based in an ultrasonic atomizer such as the one explained in this thesis would be significantly smaller and power efficient than current heating-type humidifiers used in CPAP systems.

## **6.7 FUTURE WORK**

In order to complete the development of this humidifier, work needs to be done in the design and implementation of the driving and control circuit. Since these ultrasonic atomizers can be overheated if they run without water on top of them, a proper water level detector must form part of the control system. In addition to this, pressure atomizers should be also considered for a possible replacement of the ultrasonic transducer since they can be operated in any position (not only horizontal). This is a desirable characteristic in portable equipment.

## APPENDIXES

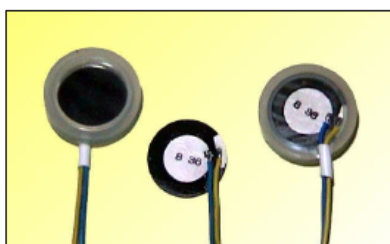


## APPENDIX A

### APPENDIX A.1

Datasheet of ultrasonic transducer of 1.65 MHz

#### Ultrasonic Atomizing Transducers



Pro-Wave has dedicated in ultrasonic field over 19 years since 1980 and earned a worldwide reputation for his specialty, flexibility and sincerity in the past decades.  
The ultrasonic atomizing transducers using our factory made high Q hard type piezoelectric ceramic element is ideal for atomizing liquids. A very fine mist having a particle diameter of only a few microns can be generated.  
We are not only supply atomizing element but also entire assembled transducer unit with silicone rubber holder.

#### Features

- Piezoelectric ceramic element clad with stainless steel for erosion resistance.
- Fine and consistent particle size of less than  $3\mu\text{m}$
- High atomizing efficiency  $>400\text{ cc/hr}$
- Less power consumption
- High stability and durability

#### Applications

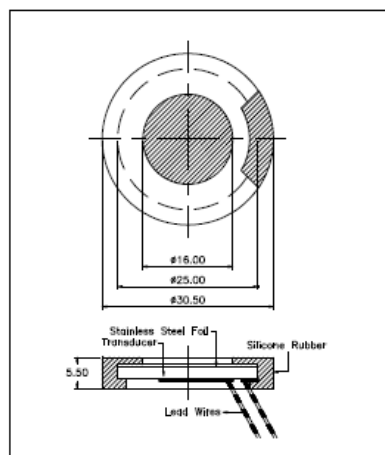
- Humidification in refrigerated food displays and storage, living environments, and air conditioning plants.
- Inhalation and disinfecting equipment
- Humidification in industrial process control for lubrication, coating and etc.

#### Specification

|                                   |                             |
|-----------------------------------|-----------------------------|
| <b>MI65D25</b>                    | 25mm Dia.                   |
| <b>Resonance Frequency</b>        | $1.65\pm 0.05\text{MHz}$    |
| <b>Resonance Impedance</b>        | $2.0\Omega\text{ max.}$     |
| <b>Capacitance at 1Khz</b>        | $\pm 20\%$ 2,000 pF         |
| <b>Dissipation Factor at 1Khz</b> | 0.5% max.                   |
| <b>Operation Duration (hour)</b>  | $>6,000$                    |
| <b>Atomizing Quantity</b>         | 400 cc/hr                   |
| <b>Water Level</b>                | 45 mm                       |
| <b>Input Power (maximum)</b>      | 30 Watt                     |
| <b>Operation Temperature</b>      | 0 to $45^{\circ}\text{C}$   |
| <b>Storage Temperature</b>        | -20 to $65^{\circ}\text{C}$ |

All specification is typical at  $25^{\circ}\text{C}$ .  
Other frequency and diameter element can be supplied upon request.

#### Dimensions



As supplied by Midas Components Ltd 01493 602602 [www.midascomponents.co.uk](http://www.midascomponents.co.uk)

# APPENDIX A.2

Datasheet of ultrasonic transducers of 1.4, 2.0, 2.5 and 3.0 MHz.



北京东方金荣超声电器有限公司  
BEIJING DONGFANG JINRONG ULTRASONIC ELECTRICAL EQUIPMENT CO.,LTD.

## Introduction

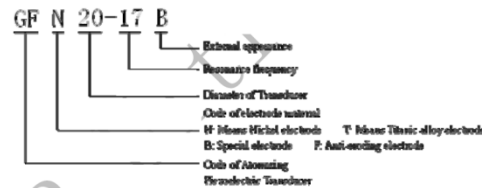
### Ultrasonic Atomizing Transducer

GF Series

#### 1. Main Applications

Humidifiers  
Inhalators  
Medical nebulizers

#### 2. Model



Note:  
(1) External appearance  
A: Means including cord and air tight seal ring.  
B: Means including cord and framework.  
C: Means including cord, air tight seal ring and metal cover.  
No letter means naked vibrator wafer.  
(2) Resonance frequency  
"17" shows the frequency is 1700 KHz

#### 3. Specifications

| Model   | F       | Resonance impedance | Kt      | Co        | Power | water level | water temp | Water quality | Fog output | Fog diameter | Life time | electrode | Appearance |
|---------|---------|---------------------|---------|-----------|-------|-------------|------------|---------------|------------|--------------|-----------|-----------|------------|
|         | KHz     | (Ω) max             | (%) min | (PF) ±20% | W     | mm          | ° C        |               | ± 50 ml/h  | μ m          | H/ml      |           |            |
| GF25-14 | 1400±50 | 2.3                 | 42      |           | 30    | 45          | 0~50       | drinking      | 450        | 5            | 5000      | T、N、      | A、C        |
| GF12-20 | 2000±50 | 2.0                 | 42      | 800       | 15    | 30          | 0~50       | drinking      | 150        | 4            | 3000      | T、N       | A、C        |
| GF12-25 | 2500±50 | 1.5                 | 42      | 925       | 13    | 30          | 0~50       | drinking      | 100        | 3            | 3000      | T、N       | A、C        |
| GF12-30 | 3000±50 | 1.5                 | 42      | 1050      | 8     | 20          | 0~50       | drinking      | 80         | 2            | 3000      | T、N       | A、C        |

## APPENDIX B

MATLAB<sup>TM</sup> code for the subtraction of images and conversion to binary values in the calculation of droplet diameters in photographic and impact methods

```
clear
clc
close all

%%%Loading images
A= imread('D:\P_01_AUT\Projects (not complete)\Droplet Size
Measurement\2010-01-25 TEMP24.5 HUM64\165mhz 400x 10.tif');
B= imread('D:\P_01_AUT\Projects (not complete)\Droplet Size
Measurement\2010-01-25 TEMP24.5 HUM64\Background 400x.tif');

D= A-B;

figure(1), imshow(A), title('Background');
figure(2), imshow(B), title('Image with droplets');
figure(3), imshow(D), title('Droplets without background');

%%%%%%%%%
Threshold= 10;
[rows,columns,deep]= size(D)
for i= 2:rows-2;
    for j= 2:columns-2;
        if D(i,j)>Threshold && D(i,j+1)>Threshold;
            D(i,j)= D(i,j);
        else
            D(i,j)= 0;
        end
    end
end
end
%%%%%%%%%

bw= im2bw(D,0.24);%graythresh(D));
figure(4), imshow(bw), title('Droplets in white');
L= bwlabel(bw);

stats= regionprops(L);
j= 1;
for i= 1 : length(stats)
    if stats(i).Area > 1
        Areas(j)= stats(i).Area;
        j= j+1;
    end
end
end
```

```

figure(5), hist(Areas,70)
xlabel('Droplet Areas (pixel)')
ylabel('Number of droplets');

Diameters= 2*sqrt(Areas/pi);%D32 (Sauter Mean Diameter) cannot be
calculated since there is no information of the volume
%%Scaling
Readings=[44 101 158 216 273 330 388 446 504 562 620 678 736 794 852
909 968 1026 1085 1143 1201 1259 1317];
for i= 1 : length(Readings)-1
    q(i)= Readings(i+1)-Readings(i);
end
Pixels_in_10_um= sum(q)/22;%the scale had divisions every 10[um]
One_pixel= 10/Pixels_in_10_um;%in [um]
Diameters_in_um= Diameters*One_pixel;
figure(6), hist(Diameters_in_um,70)
xlabel('Droplet Diameter (um)')
ylabel('Number of droplets');

%%Relating diameter and percentage in volume of every droplet
for i= 1 : length(Diameters_in_um);
    Volumes(i)= 4/3*pi*(Diameters_in_um(i)/2)^3;
end
Total_volume= sum(Volumes);
[n,xout]= hist(Diameters_in_um,70);
for i= 1: length(n)
    Percentage_in_volume(i)=
n(i)*4/3*pi*(xout(i)/2)^3/Total_volume*100;%quantity of droplets *
volume of the droplets
end
figure(7), bar(xout,Percentage_in_volume)
xlabel('Droplet Diameter (um)')
ylabel('Percentage in volume');

```

## APPENDIX C

MATLAB™ code for the calculation of water content in liquid and vapour state at different distances from the atomizer

```
clear;
close all;
valuesi= xlsread('1M5Hz.csv', 'c28:ag42');
valuesf= xlsread('1M5Hz.csv', 'c43:ag57');
%Outside the tube
Tai= mean(valuesi(:,29)); Ta= mean(valuesf(:,29)); %Ambient Temp [C]
RHai= mean(valuesi(:,31)); RHa= mean(valuesf(:,31)); %Ambient Rel Hum
%Above the transducer
T0i= mean(valuesi(:,1)); T0= mean(valuesf(:,1));
RH0i= mean(valuesi(:,3)); RH0= mean(valuesf(:,3));
% @ 2cm
T1i= mean(valuesi(:,5)); T1= mean(valuesf(:,5));
RH1i= mean(valuesi(:,7)); RH1= mean(valuesf(:,7));
% @ 4cm
T2i= mean(valuesi(:,9)); T2= mean(valuesf(:,9));
RH2i= mean(valuesi(:,11)); RH2= mean(valuesf(:,11));
% @ 8cm
T3i= mean(valuesi(:,13)); T3= mean(valuesf(:,13));
RH3i= mean(valuesi(:,15)); RH3= mean(valuesf(:,15));
% @ 16cm
T4i= mean(valuesi(:,17)); T4= mean(valuesf(:,17));
RH4i= mean(valuesi(:,19)); RH4= mean(valuesf(:,19));
% @ 32cm
T5i= mean(valuesi(:,21)); T5= mean(valuesf(:,21));
RH5i= mean(valuesi(:,23)); RH5= mean(valuesf(:,23));
% @ 50cm
T6i= mean(valuesi(:,25)); T6= mean(valuesf(:,25));
RH6i= mean(valuesi(:,27)); RH6= mean(valuesf(:,27));

%%%%%%%%%%%%%%%%%%%%%%%%%%%%%%%%%%%%%%%%%%%%%%%%%%%%%%%%%%%%%%%%%%%%%%%%
%Atmospheric conditions %%%%%%%%%%%%%%%%%%%%%%%%%%%%%%%%%%%%%%%%%%%%%%%%%%%%%%%%%%%%%%%%%%%%%%%%%
%%%%%%%%%%%%%%%%%%%%%%%%%%%%%%%%%%%%%%%%%%%%%%%%%%%%%%%%%%%%%%%%%%%%%%%%
Psa= 610.78*exp(Ta/(Ta+238.3)*17.2694); %Ambient water vapor
saturation pressure [Pa]

%RH= P/Ps *100
Pa= RHa/100*Psa; %Water vapor pressure [Pa]

Pa= Pa/101325; %Water vapor pressure [atm]

%P*V= n*R*T
%P*V= m/M *R*T
```

```

% $m = P \cdot V \cdot M / (R \cdot T)$ 
% $m[g] = P[atm] \cdot 1[L] \cdot 18[g/mol] / (.082[atm \cdot L / (mol \cdot K)] \cdot T[K])$ 
% $AH[g/L] = P[atm] \cdot 1[L] \cdot 18[g/mol] / (.082[atm \cdot L / (mol \cdot K)] \cdot T[K])$ 
AHa= Pa*1*18/(.082*(Ta+273)); %Absolute Humidity [g/L]

%%%%%%%%%%%%%%%%%%%%%%%%%%%%%%%%%%%%%%%%%%%%%%%%%%%%%%%%%%%%%%%%%%%%%%%%
%Situation after atomization @ 0cm %%%%%%%%%%%%%%%%%%%%%%%%%%%%%%%%%%%%%%%%%%%%%%%%%%%%%%%%%%%%%%%%%%%%%%%%%
%%%%%%%%%%%%%%%%%%%%%%%%%%%%%%%%%%%%%%%%%%%%%%%%%%%%%%%%%%%%%%%%%%%%%%%%
Atomization_rate= 0.2; %g/min
Flow_rate= 60; %in liters per minute
Time_of_exp= 5; %min

Water_added= Atomization_rate*Time_of_exp; %[g]
Vol_of_air= Flow_rate*Time_of_exp;

Water_added_per_L= Water_added/Vol_of_air; %[g/L]

Ps0= 610.78*exp(T0/(T0+238.3)*17.2694); %Water vapor sat pressure [Pa]

%RH= P/Ps *100
P0= RH0/100*Ps0; %Water vapor pressure [Pa]

P0= P0/101325; %Water vapor pressure [atm]

% $P \cdot V = n \cdot R \cdot T$ 
% $P \cdot V = m/M \cdot R \cdot T$ 
% $m = P \cdot V \cdot M / (R \cdot T)$ 
% $m[g] = P[atm] \cdot 1[L] \cdot 18[g/mol] / (.082[atm \cdot L / (mol \cdot K)] \cdot T[K])$ 
% $AH[g/L] = P[atm] \cdot 1[L] \cdot 18[g/mol] / (.082[atm \cdot L / (mol \cdot K)] \cdot T[K])$ 
AH0= P0*1*18/(.082*(T0+273)); %Absolute Humidity [g/L]

Vapour_state_0= AH0/(Water_added_per_L+AHa)*100;
Liquid_state_0= 100-Vapour_state_0;

%%%%%%%%%%%%%%%%%%%%%%%%%%%%%%%%%%%%%%%%%%%%%%%%%%%%%%%%%%%%%%%%%%%%%%%%
%Situation after atomization @ 2cm %%%%%%%%%%%%%%%%%%%%%%%%%%%%%%%%%%%%%%%%%%%%%%%%%%%%%%%%%%%%%%%%%%%%%%%%%
%%%%%%%%%%%%%%%%%%%%%%%%%%%%%%%%%%%%%%%%%%%%%%%%%%%%%%%%%%%%%%%%%%%%%%%%
Ps1= 610.78*exp(T1/(T1+238.3)*17.2694); %Water vapor sat pressure [Pa]

%RH= P/Ps *100
P1= RH1/100*Ps1; %Water vapor pressure [Pa]

P1= P1/101325; %Water vapor pressure [atm]

% $P \cdot V = n \cdot R \cdot T$ 
% $P \cdot V = m/M \cdot R \cdot T$ 
% $m = P \cdot V \cdot M / (R \cdot T)$ 
% $m[g] = P[atm] \cdot 1[L] \cdot 18[g/mol] / (.082[atm \cdot L / (mol \cdot K)] \cdot T[K])$ 
% $AH[g/L] = P[atm] \cdot 1[L] \cdot 18[g/mol] / (.082[atm \cdot L / (mol \cdot K)] \cdot T[K])$ 
AH1= P1*1*18/(.082*(T1+273)); %Absolute Humidity [g/L]

```

```
Vapour_state_1= AH1/(Water_added_per_L+AHa)*100;
Liquid_state_1= 100-Vapour_state_1;
```

```
%%%%%%%%%%%%%%%%%%%%%%%%%%%%%%%%%%%%%%%%%%%%%%%%%%%%%%%%%%%%%%%%%%%%%%%%
%Situation after atomization @ 4cm %%%%%%%%%
%%%%%%%%%%%%%%%%%%%%%%%%%%%%%%%%%%%%%%%%%%%%%%%%%%%%%%%%%%%%%%%%%%%%%%%%
%%%%%%%%%%%%%%%%%%%%%%%%%%%%%%%%%%%%%%%%%%%%%%%%%%%%%%%%%%%%%%%%%%%%%%%%
Ps2= 610.78*exp(T2/(T2+238.3)*17.2694); %Water vapor sat pressure [Pa]
T2= 25;
%RH= P/Ps *100
P2= RH2/100*Ps2;      %Water vapor pressure [Pa]

P2= P2/101325;      %Water vapor pressure [atm]
```

```
%P*V= n*R*T
%P*V= m/M *R*T
%m= P*V*M/(R*T)
%m[g]= P[atm]*1[L]*18[g/mol]/(.082[atm*L/(mol*K)]*T[K])
%AH[g/L]= P[atm]*1[L]*18[g/mol]/(.082[atm*L/(mol*K)]*T[K])
AH2= P2*1*18/(.082*(T2+273)); %Abslutive Humidity [g/L]
```

```
Vapour_state_2= AH2/(Water_added_per_L+AHa)*100;
Liquid_state_2= 100-Vapour_state_2;
```

```
%%%%%%%%%%%%%%%%%%%%%%%%%%%%%%%%%%%%%%%%%%%%%%%%%%%%%%%%%%%%%%%%%%%%%%%%
%Situation after atomization @ 8cm %%%%%%%%%
%%%%%%%%%%%%%%%%%%%%%%%%%%%%%%%%%%%%%%%%%%%%%%%%%%%%%%%%%%%%%%%%%%%%%%%%
%%%%%%%%%%%%%%%%%%%%%%%%%%%%%%%%%%%%%%%%%%%%%%%%%%%%%%%%%%%%%%%%%%%%%%%%
Ps3= 610.78*exp(T3/(T3+238.3)*17.2694); %Water vapor sat pressure [Pa]

%RH= P/Ps *100
P3= RH3/100*Ps3;      %Water vapor pressure [Pa]

P3= P3/101325;      %Water vapor pressure [atm]
```

```
%P*V= n*R*T
%P*V= m/M *R*T
%m= P*V*M/(R*T)
%m[g]= P[atm]*1[L]*18[g/mol]/(.082[atm*L/(mol*K)]*T[K])
%AH[g/L]= P[atm]*1[L]*18[g/mol]/(.082[atm*L/(mol*K)]*T[K])
AH3= P3*1*18/(.082*(T3+273)); %Abslutive Humidity [g/L]
```

```
Vapour_state_3= AH3/(Water_added_per_L+AHa)*100;
Liquid_state_3= 100-Vapour_state_3;
```

```
%%%%%%%%%%%%%%%%%%%%%%%%%%%%%%%%%%%%%%%%%%%%%%%%%%%%%%%%%%%%%%%%%%%%%%%%
%Situation after atomization @16cm %%%%%%%%%
%%%%%%%%%%%%%%%%%%%%%%%%%%%%%%%%%%%%%%%%%%%%%%%%%%%%%%%%%%%%%%%%%%%%%%%%
%%%%%%%%%%%%%%%%%%%%%%%%%%%%%%%%%%%%%%%%%%%%%%%%%%%%%%%%%%%%%%%%%%%%%%%%
Ps4= 610.78*exp(T4/(T4+238.3)*17.2694); %Water vapor sat pressure [Pa]

%RH= P/Ps *100
P4= RH4/100*Ps4;      %Water vapor pressure [Pa]
```

```

P4= P4/101325;          %Water vapor pressure [atm]

%P*V= n*R*T
%P*V= m/M *R*T
%m= P*V*M/(R*T)
%m[g]= P[atm]*1[L]*18[g/mol]/(.082[atm*L/(mol*K)]*T[K])
%AH[g/L]= P[atm]*1[L]*18[g/mol]/(.082[atm*L/(mol*K)]*T[K])
AH4= P4*1*18/ (.082*(T4+273));    %Absolute Humidity [g/L]

Vapour_state_4= AH4/(Water_added_per_L+AHa)*100;
Liquid_state_4= 100-Vapour_state_4;

%%%%%%%%%%%%%%%%%%%%%%%%%%%%%%%%%%%%%%%%%%%%%%%%%%%%%%%%%%%%%%%%%%%%%%%%
%Situation after atomization @32cm %%%%%%%%%%%%%%%%%%%%%%%%%%%%%%%%%%%%%%%%%%%%%%%%%%%%%%%%%%%%%%%%%%%%%%%%%
%%%%%%%%%%%%%%%%%%%%%%%%%%%%%%%%%%%%%%%%%%%%%%%%%%%%%%%%%%%%%%%%%%%%%%%%
Ps5= 610.78*exp(T5/(T5+238.3)*17.2694); %Water vapor sat pressure [Pa]

%RH= P/Ps *100
P5= RH5/100*Ps5;      %Water vapor pressure [Pa]

P5= P5/101325;        %Water vapor pressure [atm]

%P*V= n*R*T
%P*V= m/M *R*T
%m= P*V*M/(R*T)
%m[g]= P[atm]*1[L]*18[g/mol]/(.082[atm*L/(mol*K)]*T[K])
%AH[g/L]= P[atm]*1[L]*18[g/mol]/(.082[atm*L/(mol*K)]*T[K])
AH5= P5*1*18/ (.082*(T5+273));    %Absolute Humidity [g/L]

Vapour_state_5= AH5/(Water_added_per_L+AHa)*100;
Liquid_state_5= 100-Vapour_state_5;

%%%%%%%%%%%%%%%%%%%%%%%%%%%%%%%%%%%%%%%%%%%%%%%%%%%%%%%%%%%%%%%%%%%%%%%%
%Situation after atomization @50cm %%%%%%%%%%%%%%%%%%%%%%%%%%%%%%%%%%%%%%%%%%%%%%%%%%%%%%%%%%%%%%%%%%%%%%%%%
%%%%%%%%%%%%%%%%%%%%%%%%%%%%%%%%%%%%%%%%%%%%%%%%%%%%%%%%%%%%%%%%%%%%%%%%
Ps6= 610.78*exp(T6/(T6+238.3)*17.2694); %Water vapor sat pressure [Pa]

%RH= P/Ps *100
P6= RH6/100*Ps6;      %Water vapor pressure [Pa]

P6= P6/101325;        %Water vapor pressure [atm]

%P*V= n*R*T
%P*V= m/M *R*T
%m= P*V*M/(R*T)
%m[g]= P[atm]*1[L]*18[g/mol]/(.082[atm*L/(mol*K)]*T[K])
%AH[g/L]= P[atm]*1[L]*18[g/mol]/(.082[atm*L/(mol*K)]*T[K])
AH6= P6*1*18/ (.082*(T6+273));    %Absolute Humidity [g/L]

Vapour_state_6= AH6/(Water_added_per_L+AHa)*100;
Liquid_state_6= 100-Vapour_state_6;

```



## APPENDIX D

### APPENDIX D.1

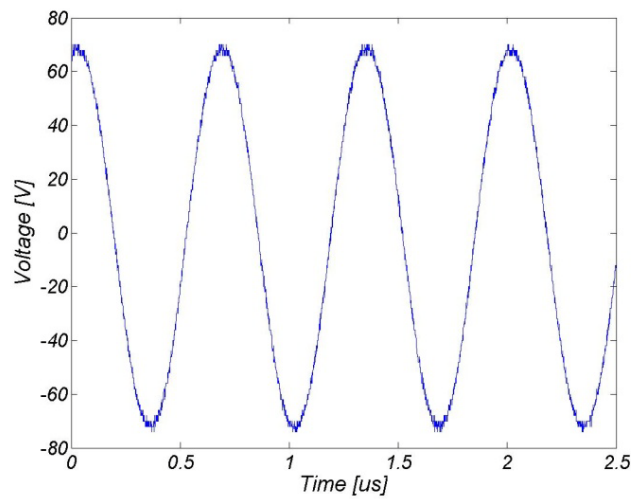


**Figure D-1: Voltage on the terminals of a 1.5 MHz transducer when a sine wave is applied.**

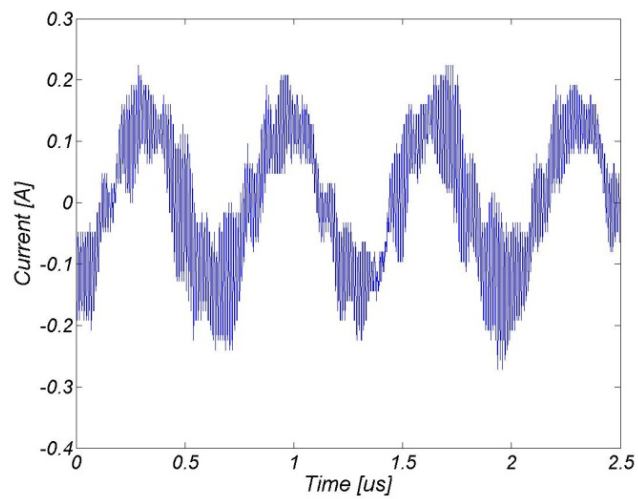


**Figure D-2: Current on a 1.5 MHz transducer when a sine wave is applied.**

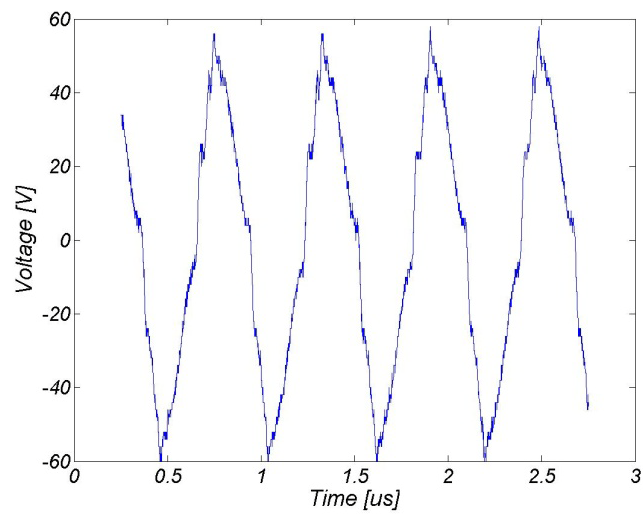


**Figure D-3: Voltage on the terminals of a 1.7 MHz transducer when a square wave is applied.**

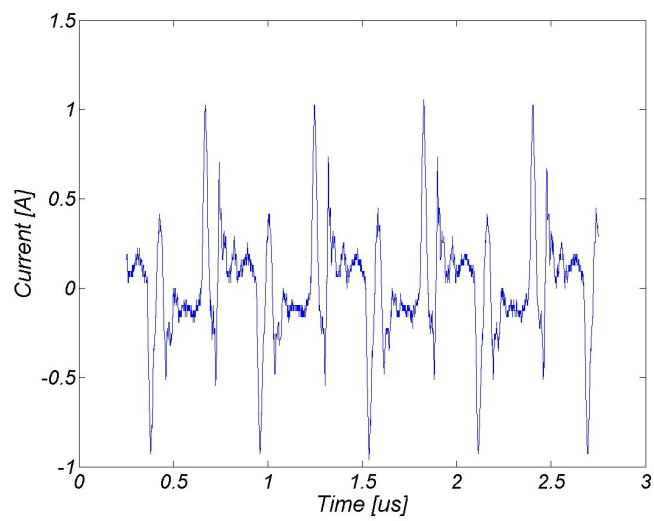


**Figure D-4: Current on a 1.7 MHz transducer when a square wave is applied.**

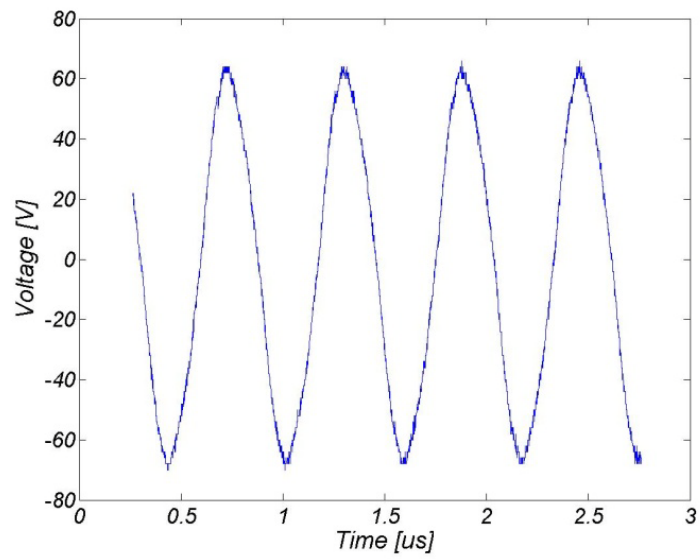


**Figure D-5: Voltage on the terminals of a 1.7 MHz transducer when a sine wave is applied.**

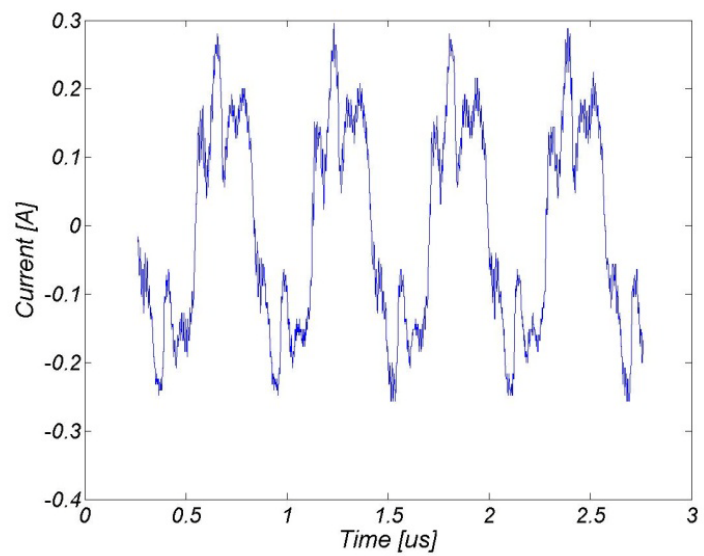


**Figure D-6: Current on a 1.7 MHz transducer when a sine wave is applied.**

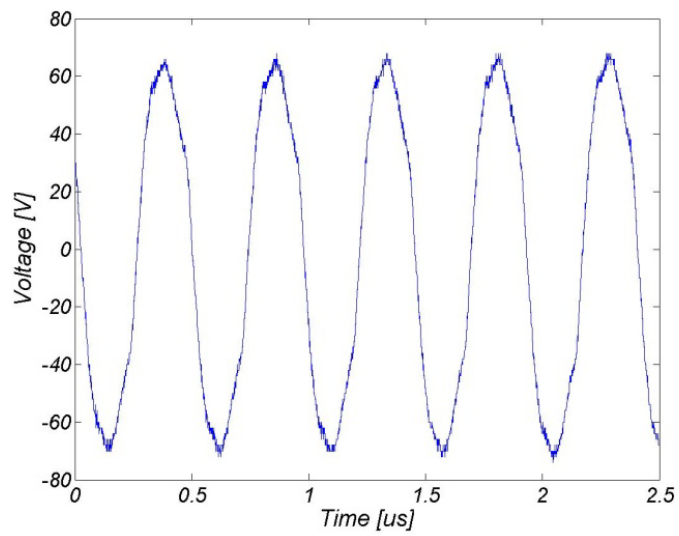


**Figure D-7: Voltage on the terminals of a 2.1 MHz transducer when a square wave is applied.**

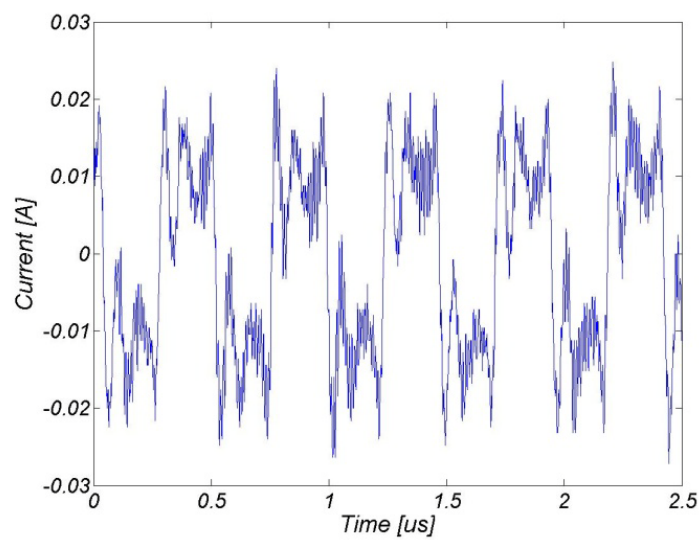


**Figure D-8: Current on a 2.1 MHz transducer when a square wave is applied.**

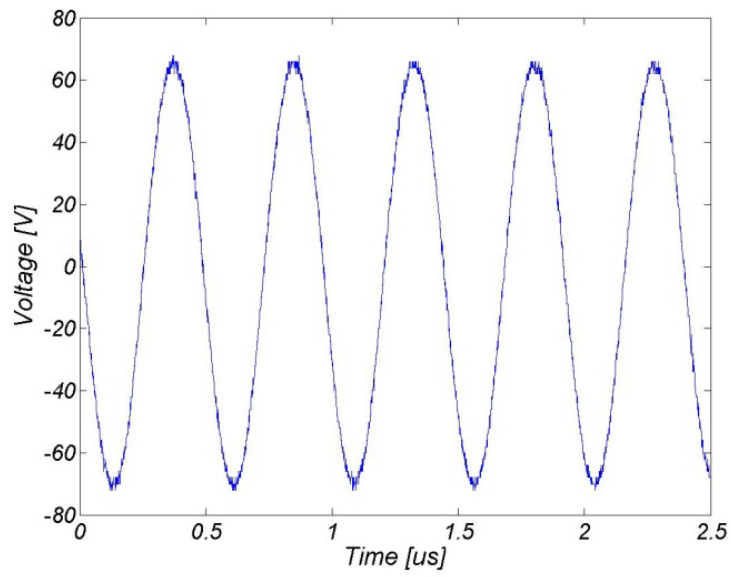


**Figure D-9: Voltage on the terminals of a 2.1 MHz transducer when a sine wave is applied.**

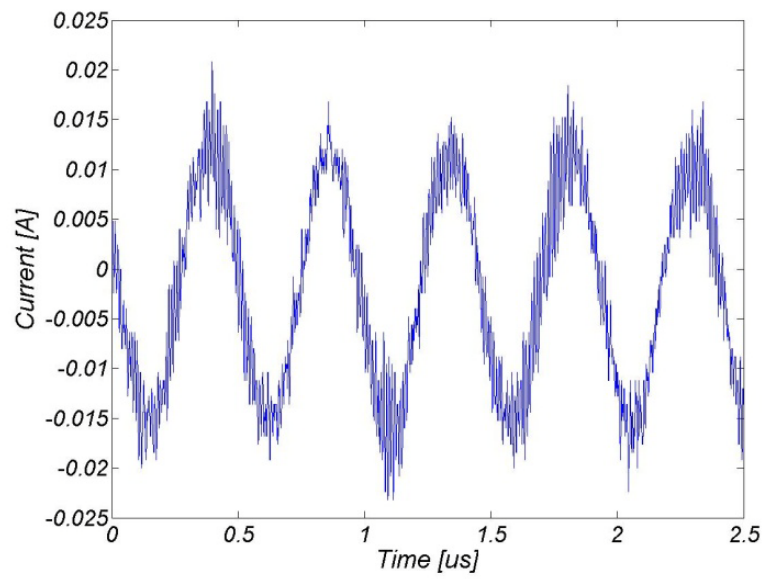


**Figure D-10: Current on a 2.1 MHz transducer when a sine wave is applied.**

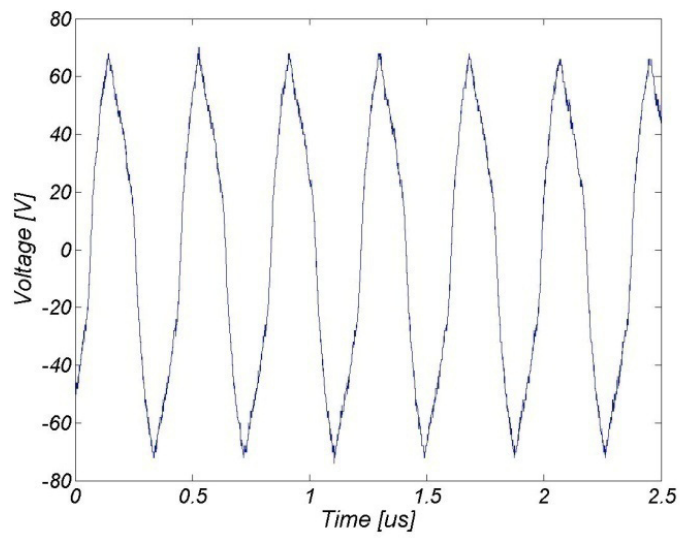


**Figure D-11: Voltage on the terminals of a 2.6 MHz transducer when a square wave is applied.**

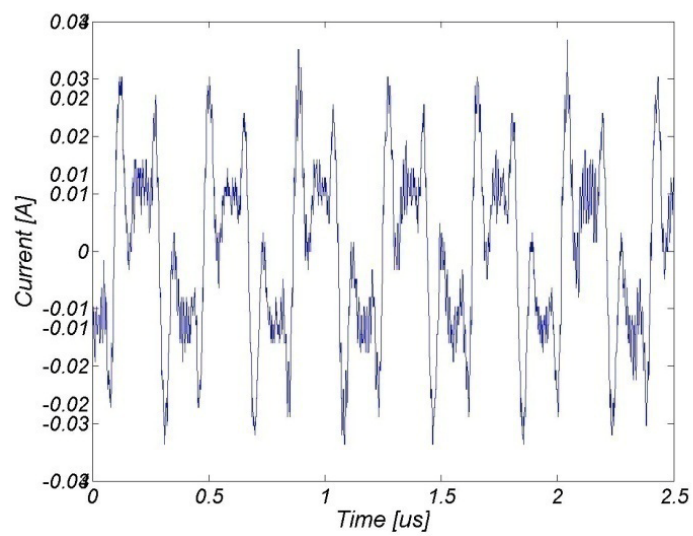


**Figure D-12: Current on a 2.6 MHz transducer when a square wave is applied.**

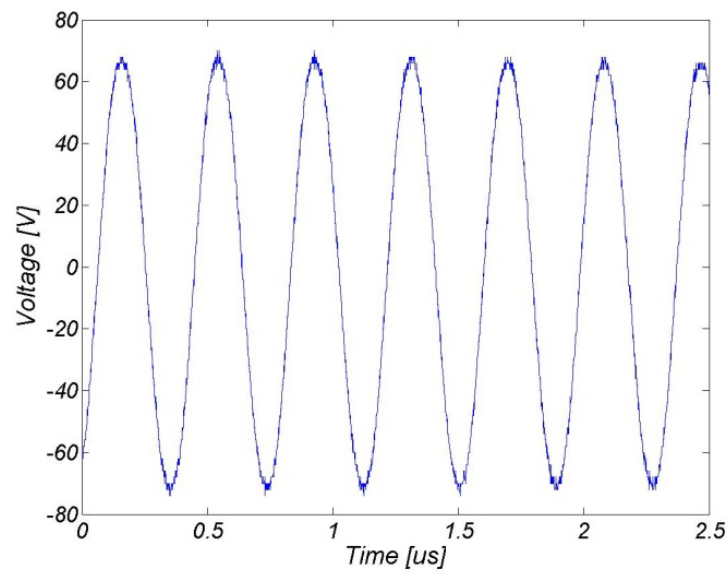


**Figure D-13: Voltage on the terminals of a 2.6 MHz transducer when a sine wave is applied.**

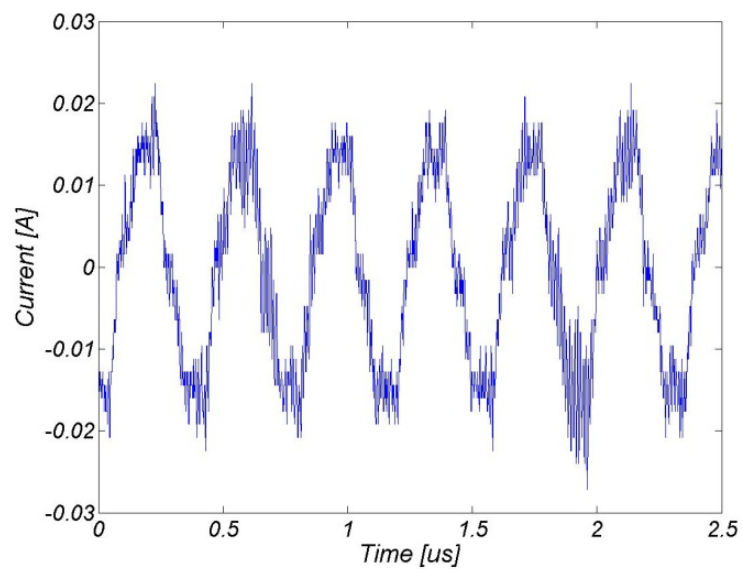


**Figure D-14: Current on a 2.6 MHz transducer when a square wave is applied.**

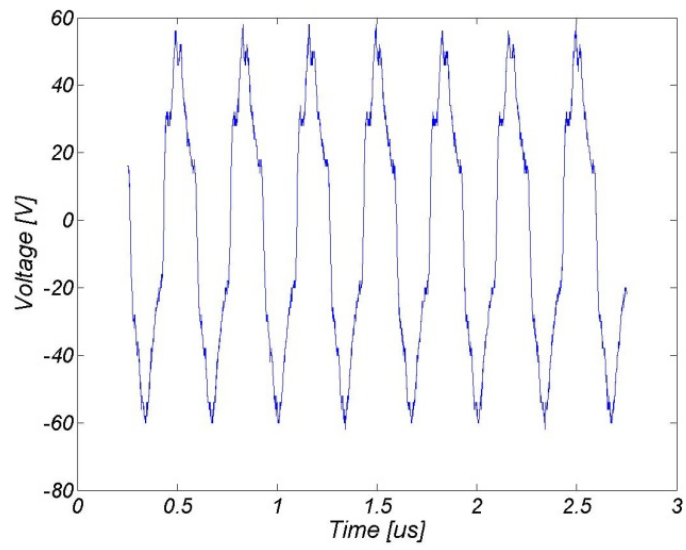


**Figure D-15: Voltage on the terminals of a 3.0 MHz transducer when a square wave is applied.**

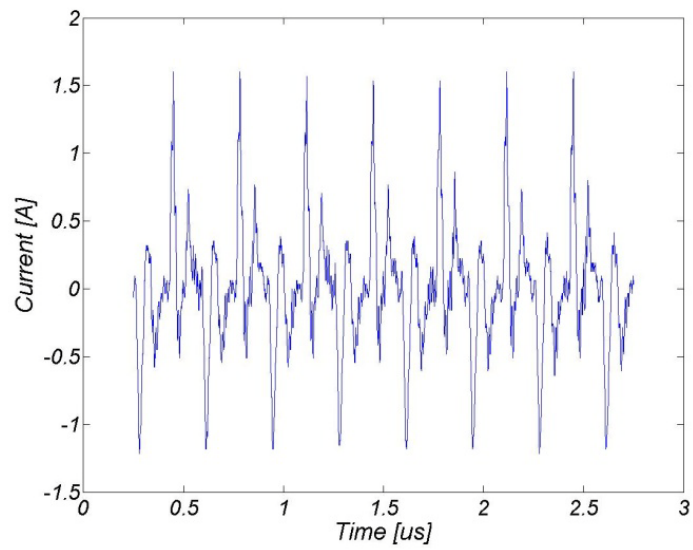


**Figure D-16: Current on a 3.0 MHz transducer when a square wave is applied.**



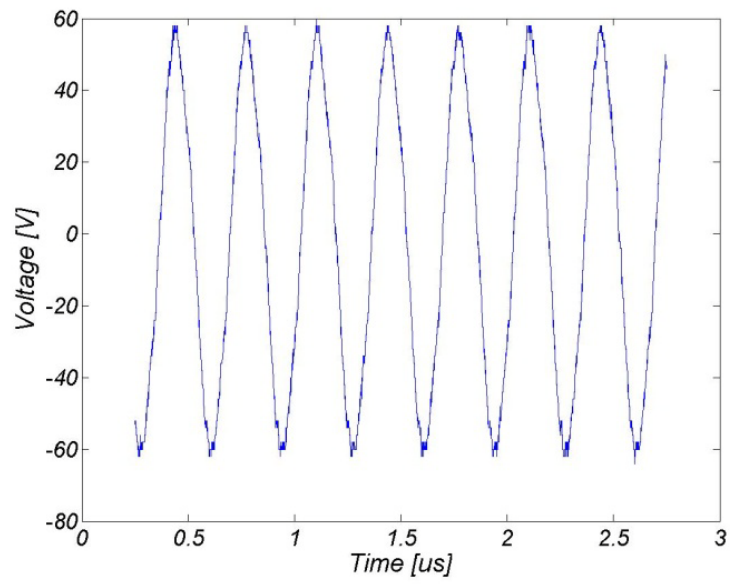


**Figure D-17: Voltage on the terminals of a 3.0 MHz transducer when a sine wave is applied.**

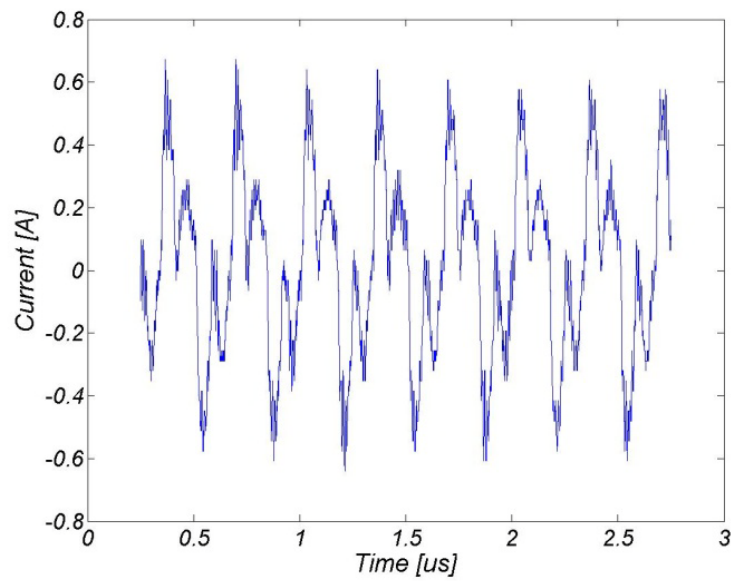


**Figure D-18: Current on a 3.0 MHz transducer when a sine wave is applied.**

## APPENDIX D.2

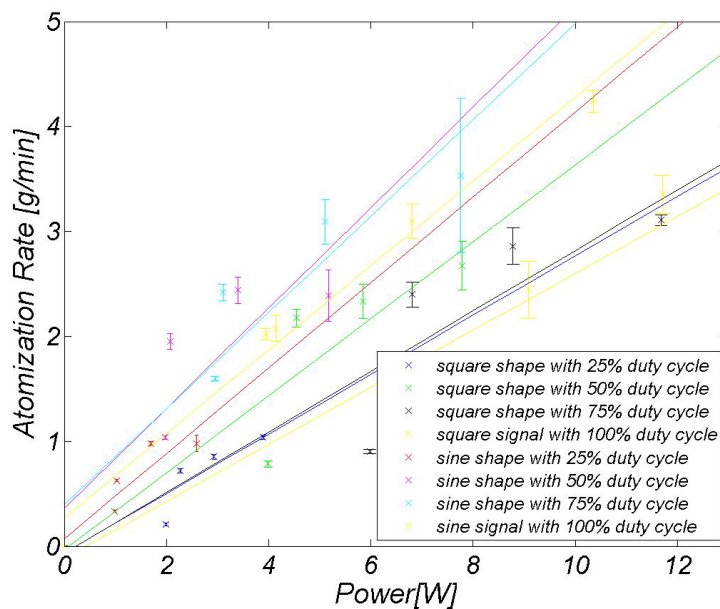


**Figure D-19: Atomization rate versus power consumption of a 1.7 MHz transducer excited at different duty cycles. Bars indicate standard deviation.**

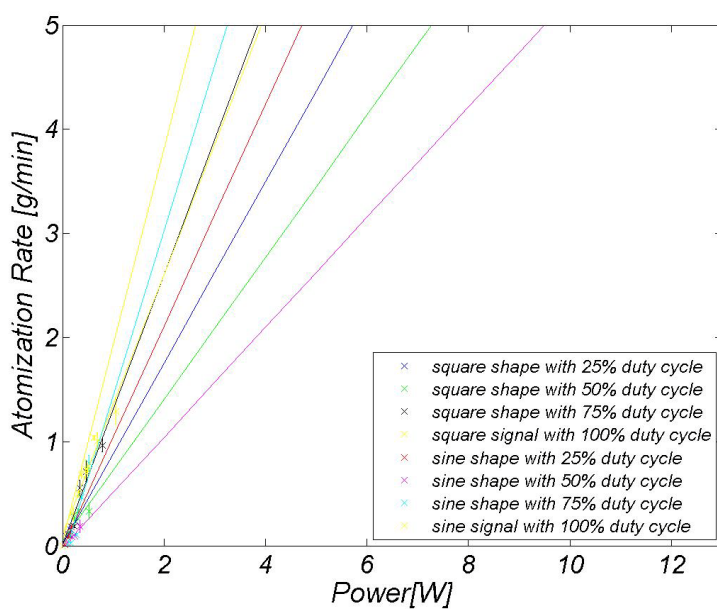


**Figure D-20: Atomization rate versus power consumption of a 2.1 MHz transducer excited at different duty cycles. Bars indicate standard deviation.**

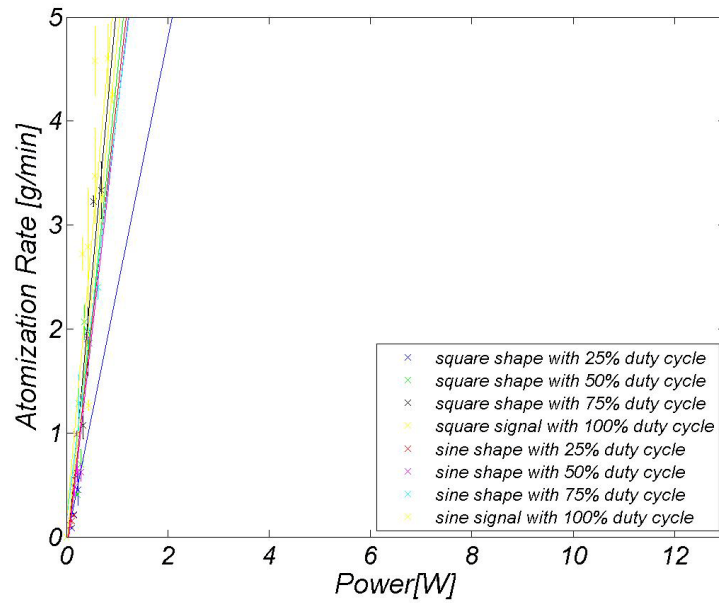


**Figure D-21: Atomization rate versus power consumption of a 2.6 MHz transducer excited at different duty cycles. Bars indicate standard deviation.**

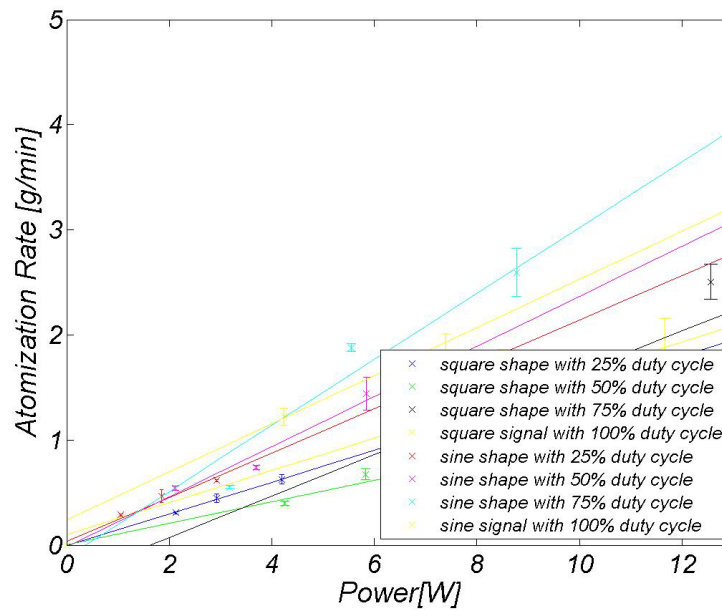


**Figure D-22: Atomization rate versus power consumption of a 3.0 MHz transducer excited at different duty cycles. Bars indicate standard deviation.**

## APPENDIX D.3

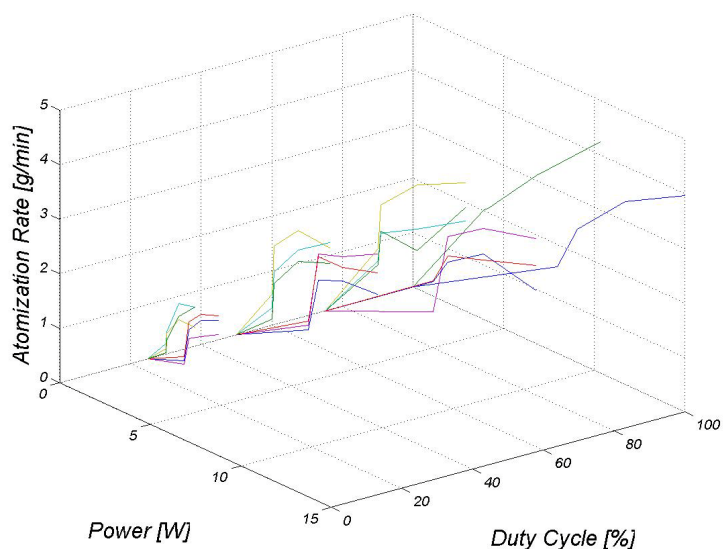


**Figure D-23: Atomization rate versus power consumption for a 1.7 MHz transducer excited with bursts of 5000 sine pulses (green), 10000 sine pulses (cyan), 20000 sine pulses (brown), 5000 square pulses (blue), 10000 square pulses (red) and 20000 square pulses (magenta) of different duty cycles.**

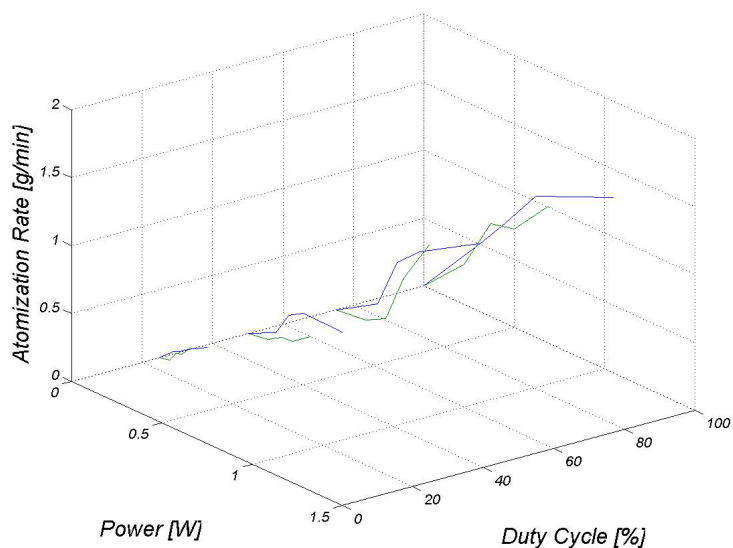


**Figure D-24: Atomization rate versus power consumption for a 2.1 MHz transducer excited with sine (blue) and square (green) pulses at four duty cycles.**

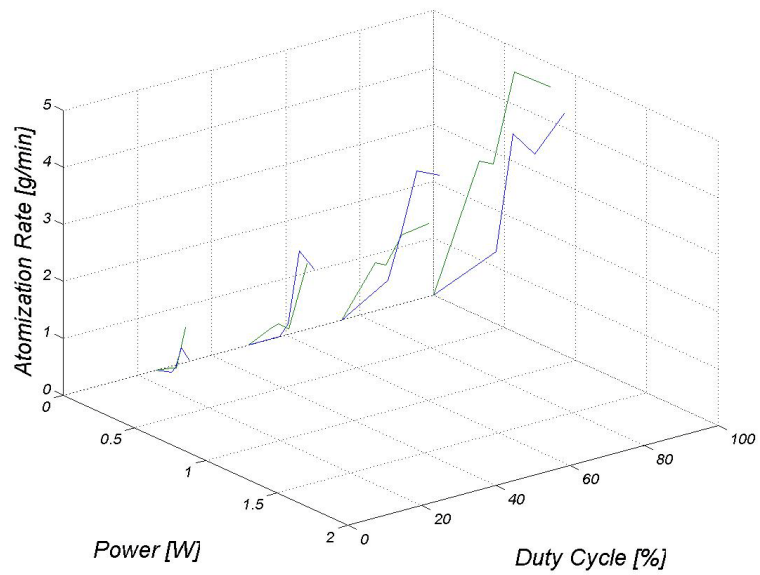


**Figure D-25: Atomization rate versus power consumption for a 2.6 MHz transducer excited with sine (green) and square (blue) pulses at four duty cycles.**

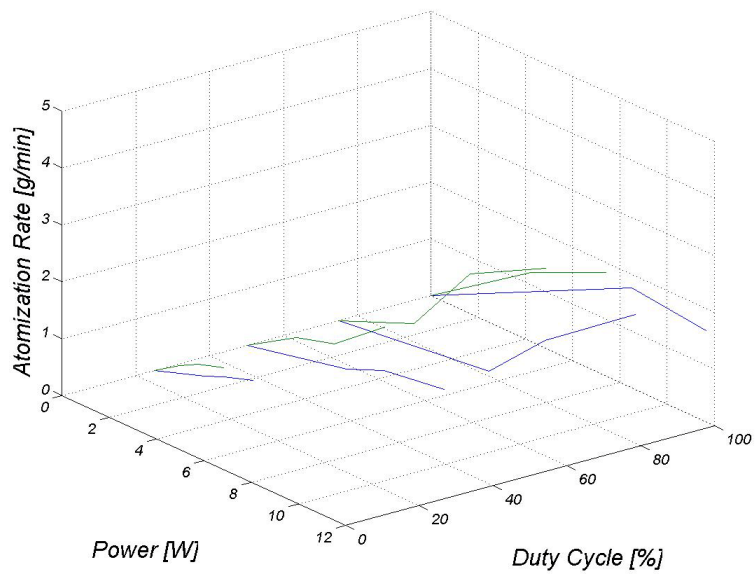


**Figure D-26: Atomization rate versus power consumption for a 3.0 MHz transducer excited with sine (green) and square (blue) pulses at four duty cycles.**

## APPENDIX D.4

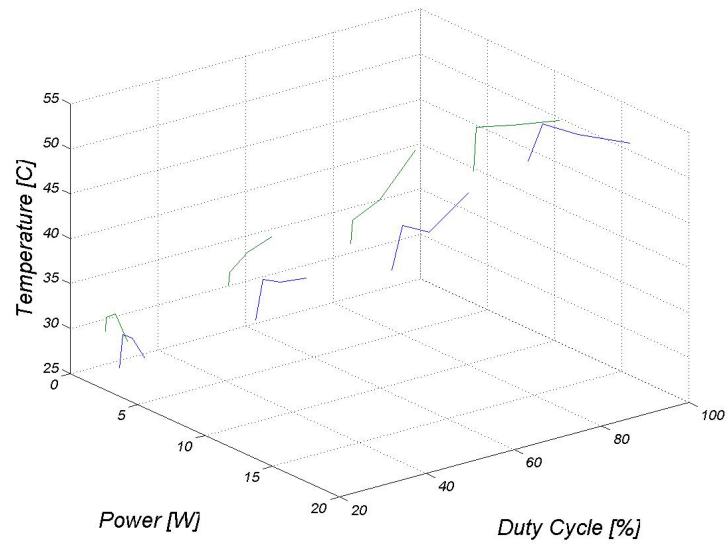


**Figure D-27: Temperature of a 1.7 MHz transducer when it was excited with sine (green) and square (blue) pulses at different powers and duty cycles.**

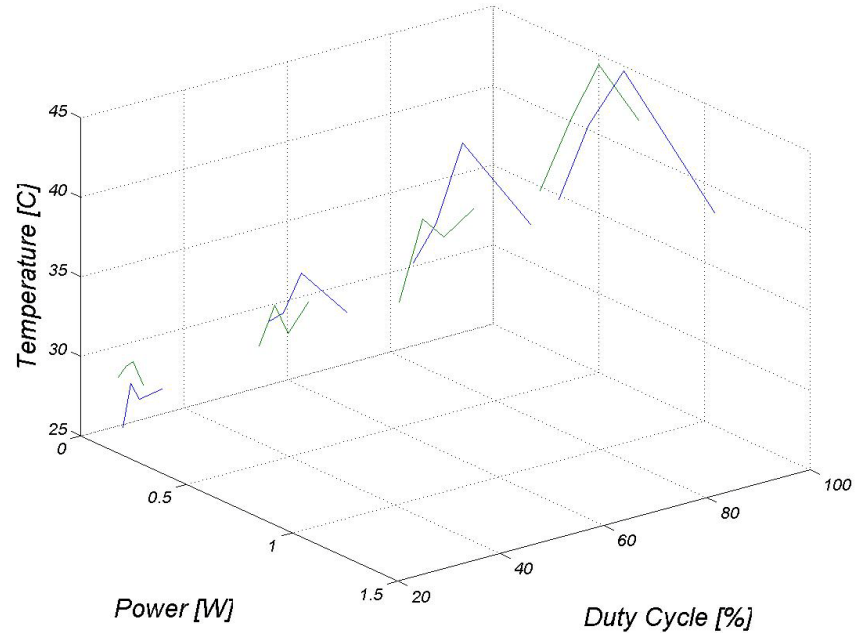


**Figure D-28: Temperature of a 2.1 MHz transducer when it was excited with sine (green) and square (blue) pulses at different powers and duty cycles.**

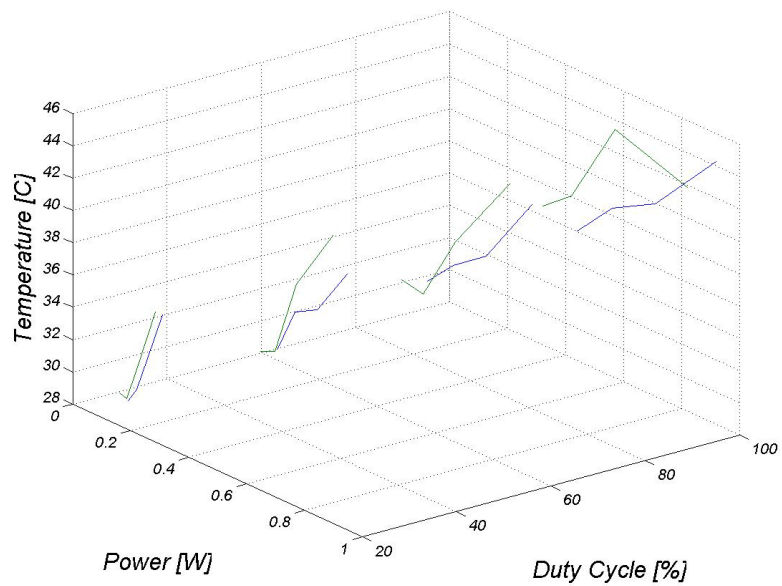


**Figure D-29: Temperature of a 2.6 MHz transducer when it was excited with sine (green) and square (blue) pulses at different powers and duty cycles.**

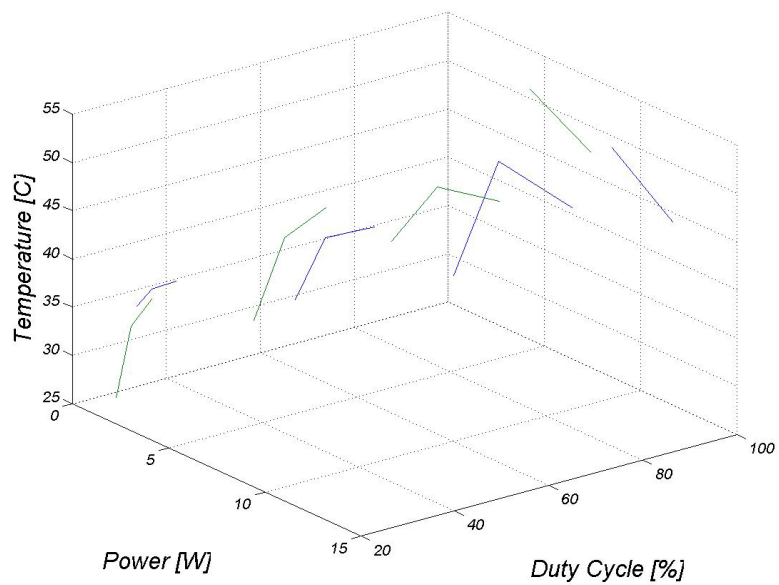


**Figure D-30: Temperature of a 3.0 MHz transducer when it was excited with sine (green) and square (blue) pulses at different powers and duty cycles.**

## APPENDIX D.5

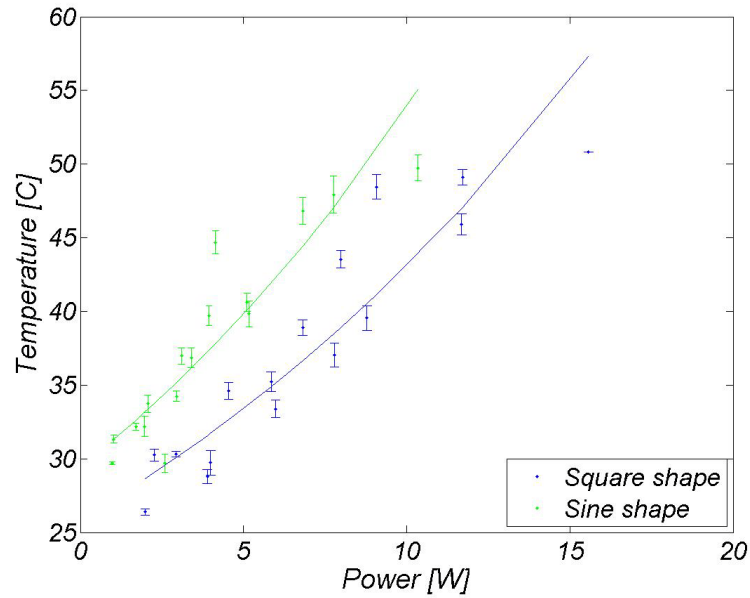


**Figure D-31: Temperature versus power consumption of a 1.7 MHz transducer. Bars indicate standard deviation.**

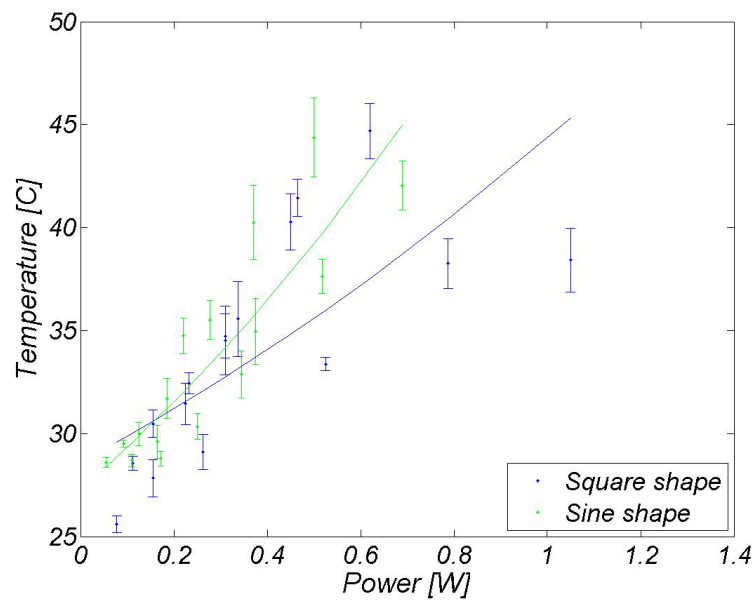


**Figure D-32: Temperature versus power consumption of a 2.1 MHz transducer. Bars indicate standard deviation.**



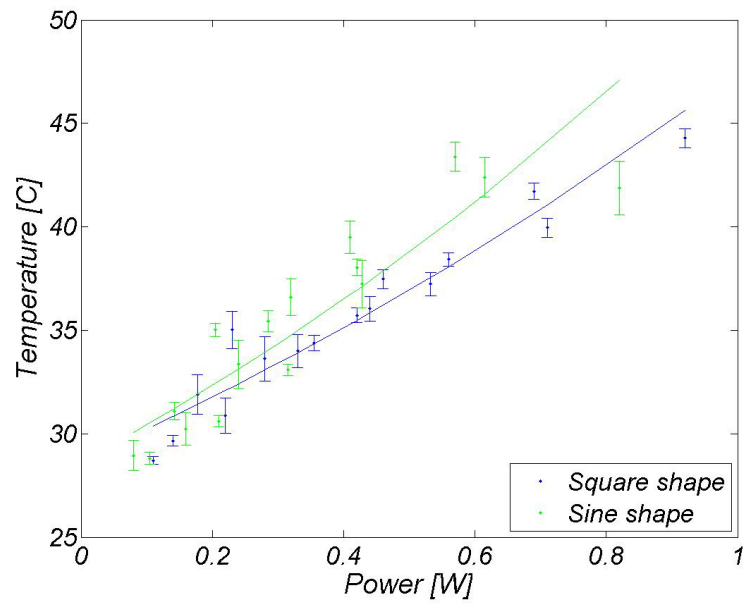


**Figure D-33: Temperature versus power consumption of a 2.6 MHz transducer.**  
**Bars indicate standard deviation.**

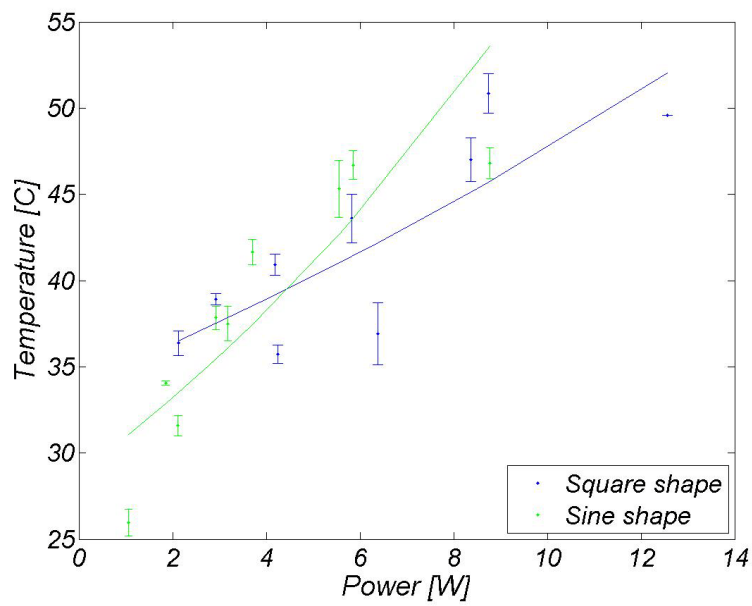


**Figure D-34: Temperature versus power consumption of a 3.0 MHz transducer.**  
**Bars indicate standard deviation.**

## APPENDIX D.6

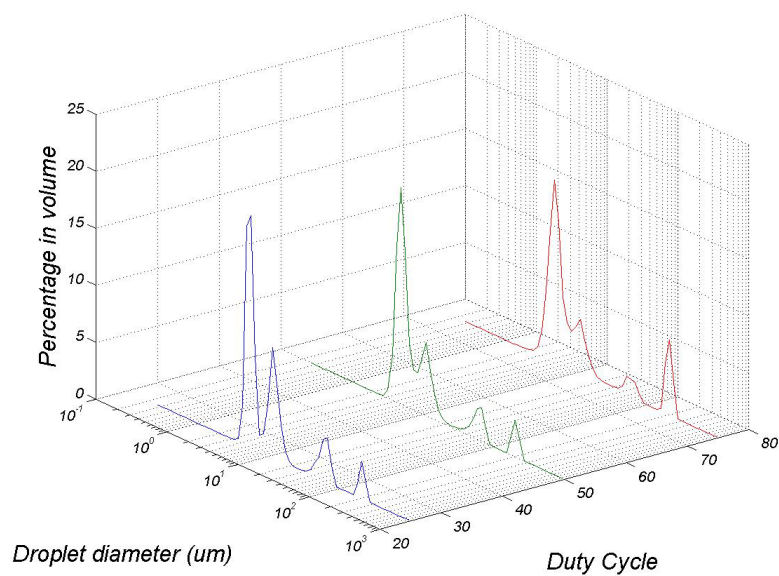


**Figure D-35: Droplet size distribution of a 1.7 MHz transducer excited with bursts of 10000 sine-shaped pulses.**

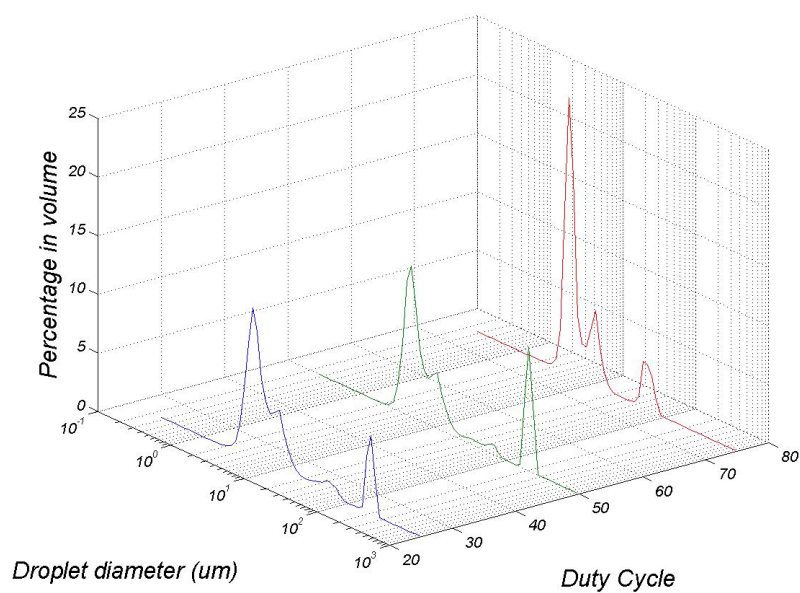


**Figure D-36: Droplet size distribution of a 1.7 MHz transducer excited with bursts of 20000 sine-shaped pulses.**

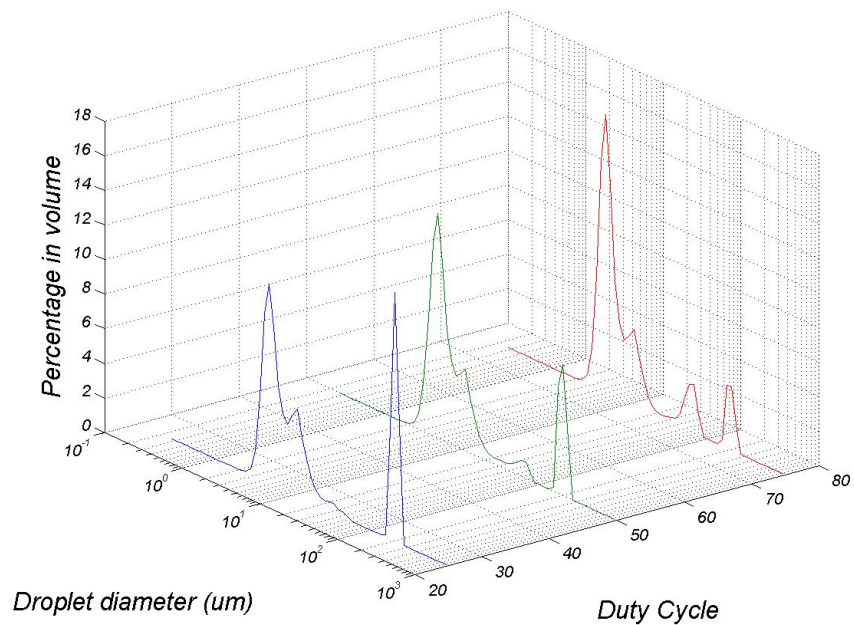


**Figure D-37: Droplet size distribution of a 1.7 MHz transducer excited with bursts of 5000 square-shaped pulses.**

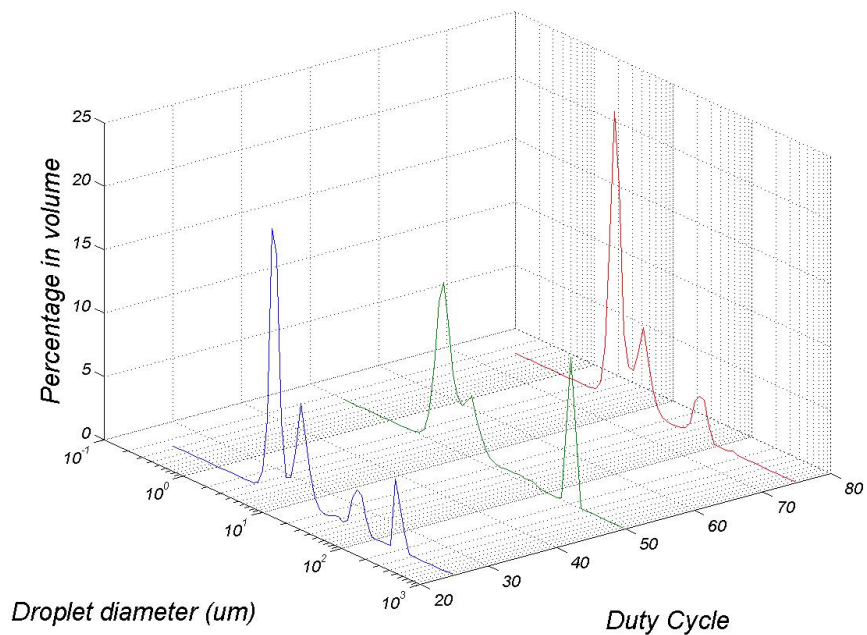


**Figure D-38: Droplet size distribution of a 1.7 MHz transducer excited with bursts of 10000 square-shaped pulses.**

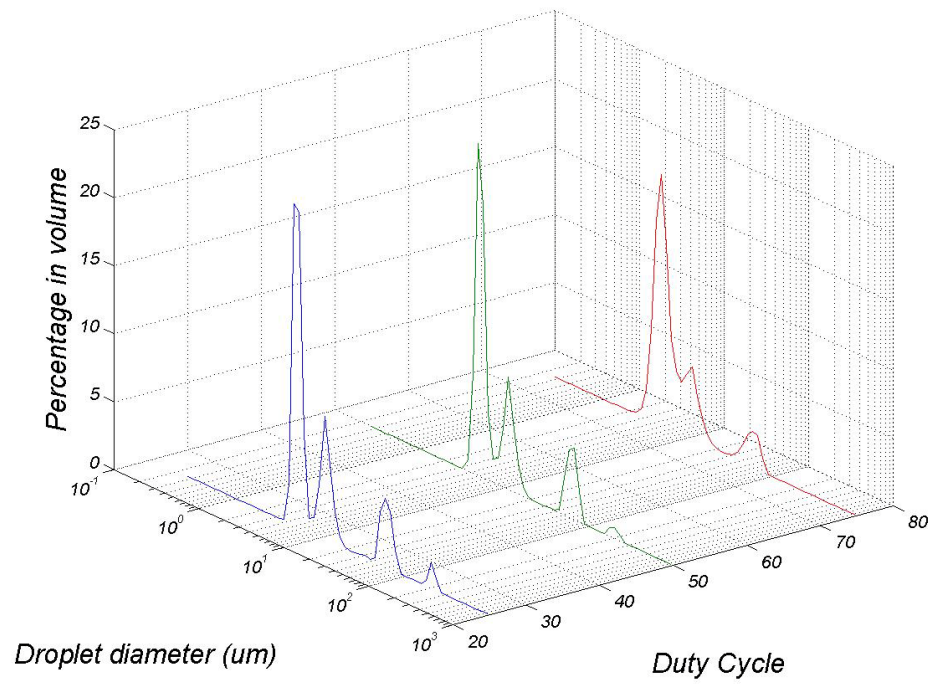


**Figure D-39: Droplet size distribution of a 1.7 MHz transducer excited with bursts of 20000 square-shaped pulses.**

## APPENDIX D.7

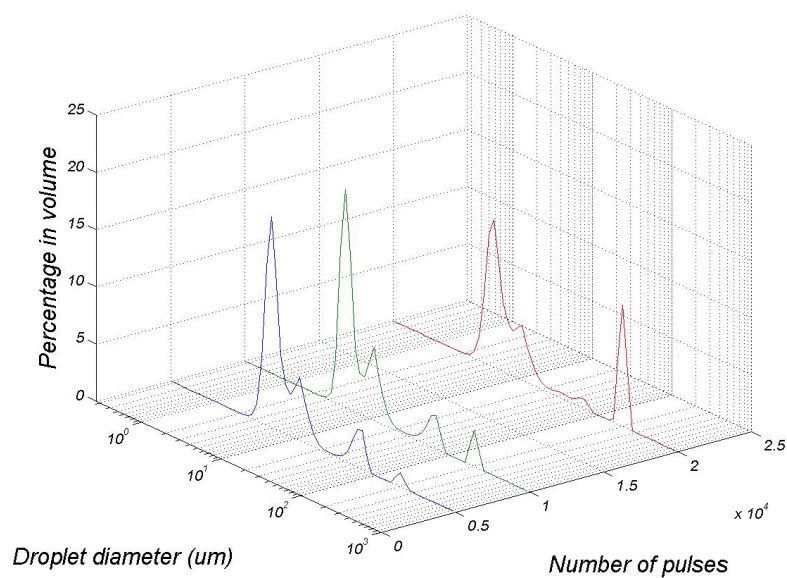


**Figure D-40: Droplet size distribution of a 1.7 MHz transducer excited with bursts of sine pulses. The duty cycle was 50%.**

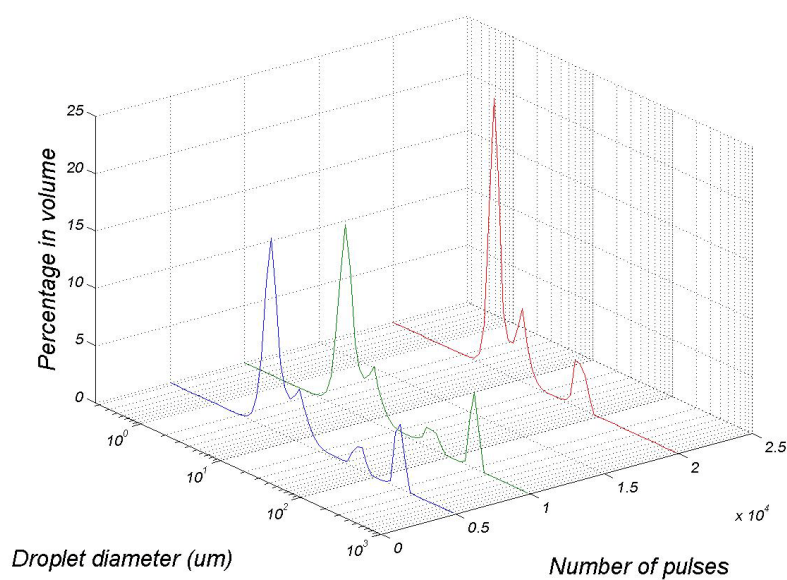


**Figure D-41: Droplet size distribution of a 1.7 MHz transducer excited with bursts of sine pulses. The duty cycle was 75%.**



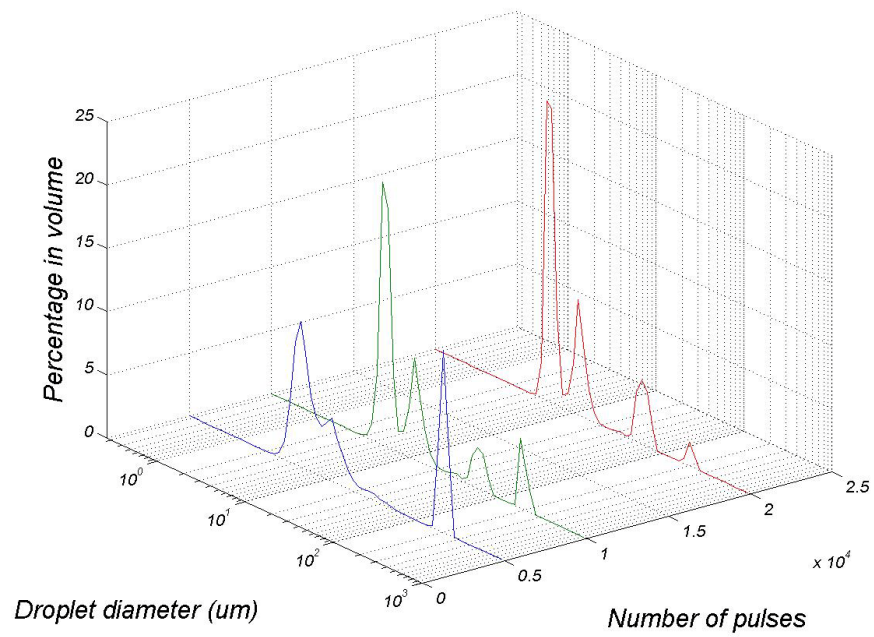


**Figure D-42: Droplet size distribution of a 1.7 MHz transducer excited with bursts of square pulses. The duty cycle was 25%.**

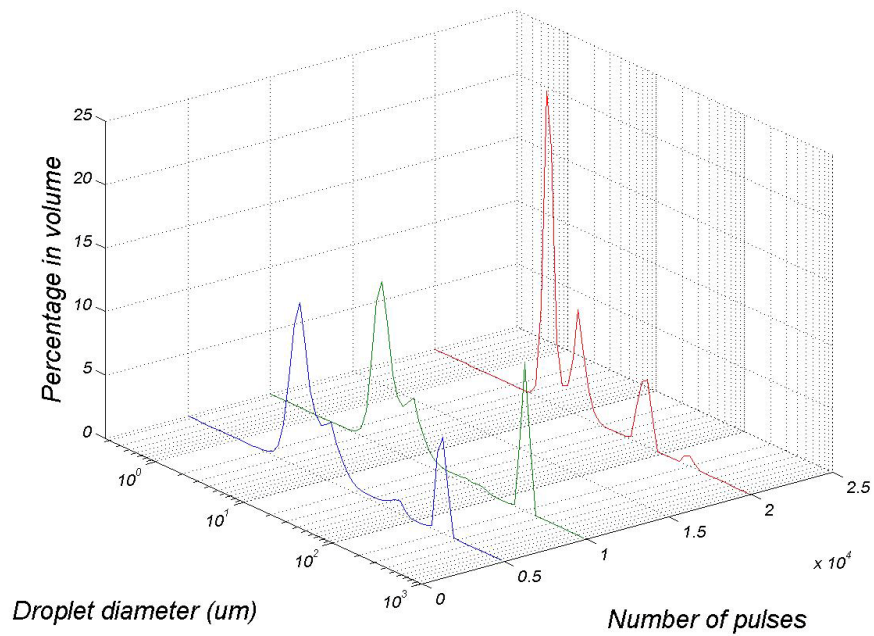


**Figure D-43: Droplet size distribution of a 1.7 MHz transducer excited with bursts of square pulses. The duty cycle was 50%.**

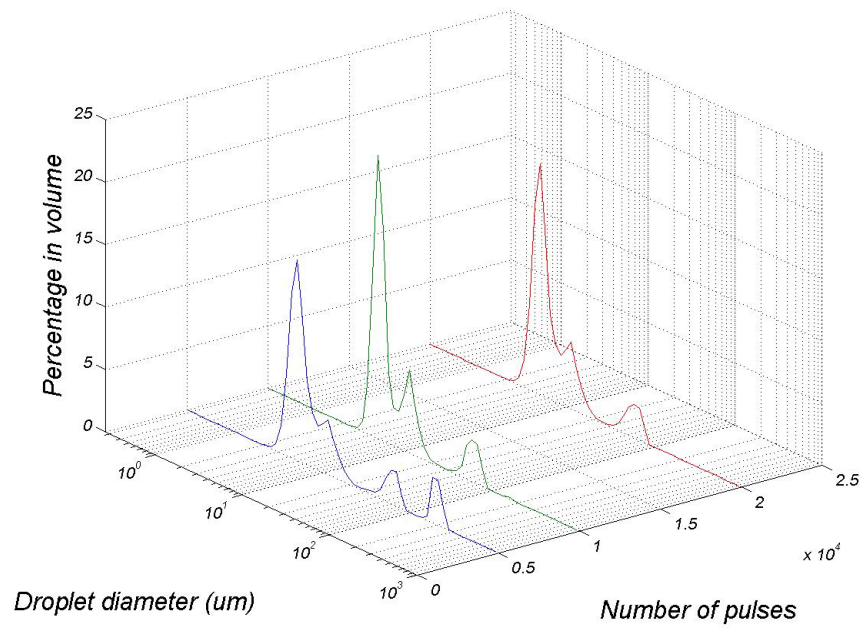


**Figure D-44: Droplet size distribution of a 1.7 MHz transducer excited with bursts of square pulses. The duty cycle was 75%.**

# APPENDIX E

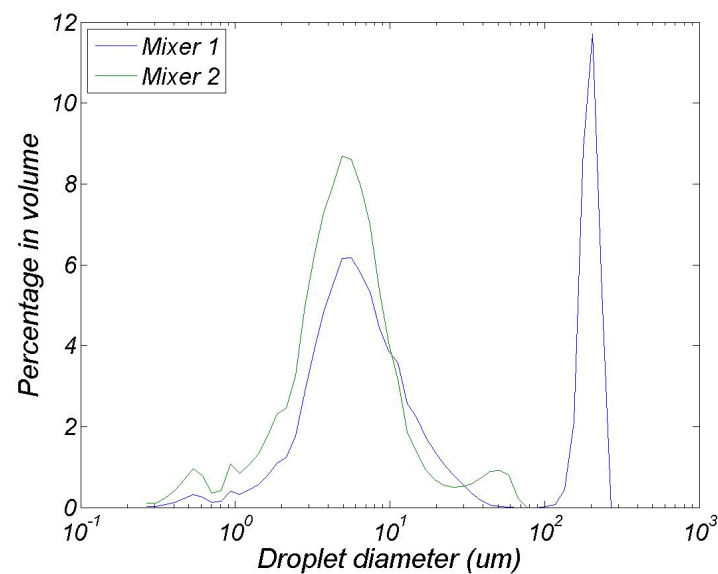


**Figure E-1: Droplet size distribution of a spray generated by a 1.5 MHz transducer using a mixer.**

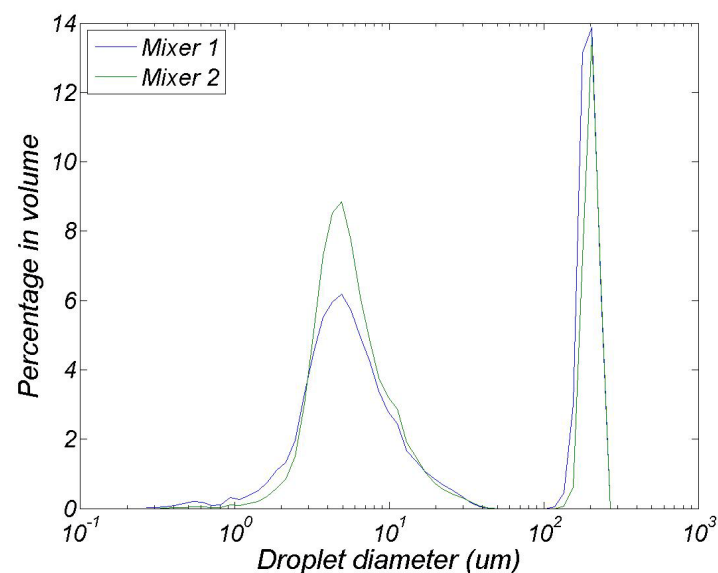


**Figure E-2: Droplet size distribution of a spray generated by a 1.7 MHz transducer using a mixer.**



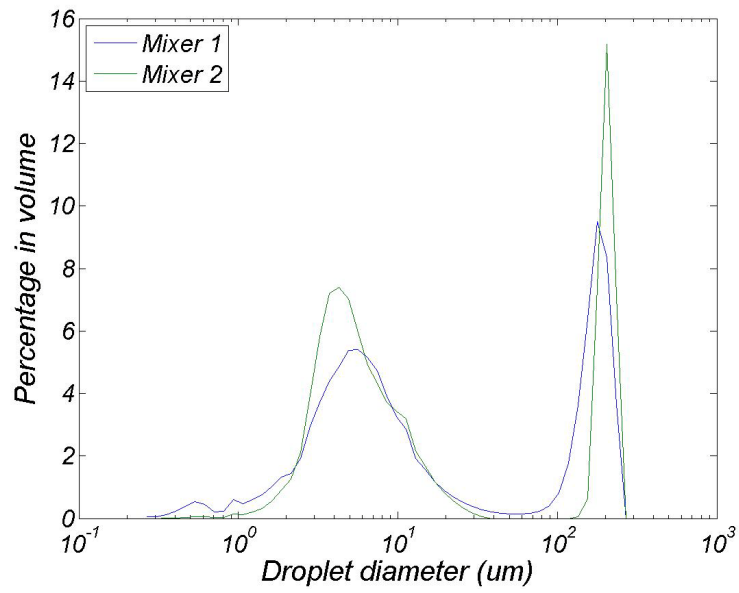


**Figure E-3: Droplet size distribution of a spray generated by a 2.1 MHz transducer using a mixer.**

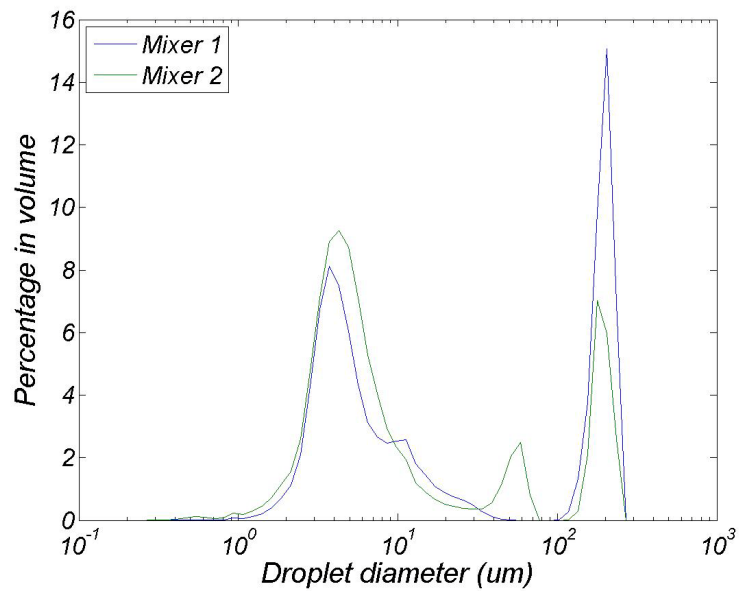


**Figure E-4: Droplet size distribution of a spray generated by a 2.6 MHz transducer using a mixer.**

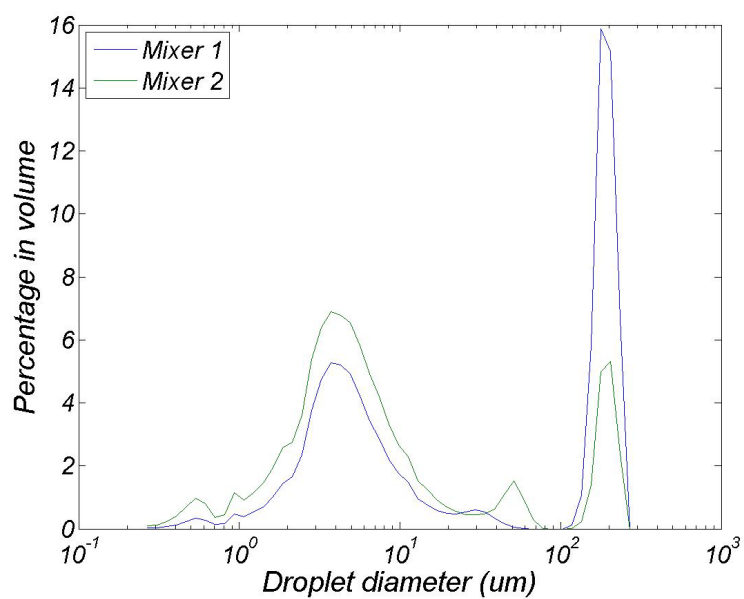


**Figure E-5: Droplet size distribution of a spray generated by a 3.0 MHz transducer using a mixer.**

## REFERENCES

1. Young, T., et al., *The occurrence of sleep-disordered breathing among middle-aged adults*. New England Journal of Medicine, 1993. **328**(17): p. 1230-1235.
2. Lam, B., D.C.L. Lam, and M.S.M. Ip, *Obstructive sleep apnoea in Asia*. International Journal of Tuberculosis and Lung Disease, 2007. **11**(1): p. 2-11.
3. Ip, M.S.M., et al., *A Community Study of Sleep-Disordered Breathing in Middle-Aged Chinese Women in Hong Kong: Prevalence and Gender Differences*. Chest, 2004. **125**(1): p. 127-134.
4. Udawadia, Z.F., et al., *Prevalence of Sleep-disordered Breathing and Sleep Apnea in Middle-aged Urban Indian Men*. American Journal of Respiratory and Critical Care Medicine, 2004. **169**(2): p. 168-173.
5. McNicholas, W.T. and M.R. Bonsignore, *Sleep apnoea as an independent risk for cardiovascular disease: Current evidence, basic mechanisms and research priorities*. European Respiratory Journal, 2007. **29**(1): p. 156-178.
6. Pandi-Perumal, S.R. and J.M. Monti, *Clinical Pharmacology of Sleep*. 2006: Birkhäuser Verlag.
7. Lee-Chiong, T. and M. Hirshkowitz, *Positive Airway Pressure Therapy for Obstructive Sleep Apnea*. Sleep Medicine Clinics, 2006. **1**(4): p. 527-531.
8. Blumenfeld, M. and J.J. Strain, *Psychosomatic Medicine*. 2006: Lippincott Williams & Wilkins.
9. Butkov, N. and T. Lee-Chiong, *Fundamentals of Sleep Technology*. 2007, Philadelphia, USA: Lippincott Williams & Wilkins.
10. Mintz, M.L., *Disorders of the Respiratory Tract: Common Challenges in Primary Care*. 2006: Humana Press.
11. Hanley, M.E. and C.H. Welsh, *Current Diagnosis & Treatment in Pulmonary Medicine*. 2003: McGraw-Hill.
12. Carney, P.R., R.B. Berry, and J.D. Geyer, *Clinical Sleep Disorders*. 2004: Lippincott Williams & Wilkins.

13. Mortimore, I.L., A.T. Whittle, and N.J. Douglas, *Comparison of nose and face mask CPAP therapy for sleep apnoea*. Thorax, 1998. **53**(4): p. 290-292.
14. Pepin, J.L., et al., *Side effects of nasal continuous positive airway pressure in sleep apnea syndrome: Study of 193 patients in two French sleep centers*. Chest, 1995. **107**(2): p. 375-381.
15. Sanders, M.H., C.A. Gruendl, and R.M. Rogers, *Patient compliance with nasal CPAP therapy for sleep apnea*. Chest, 1986. **90**(3): p. 330-333.
16. Schumann, S., et al., *Moisturizing and Mechanical Characteristics of a New Counter-Flow Type Heated Humidifier*. British Journal of Anesthesia, 2007: p. 8.
17. Liu, H., *Science and Engineering of Droplets - Fundamentals and Applications*. 2000: William Andrew Publishing/Noyes.
18. *Ultrasonic Humidifiers*. 1998, Oak Ridge National Laboratory for The U.S. Department of Energy. p. 20.
19. Lefebvre, A.H., *Atomization and Sprays*. 1989: CRC Press.
20. Crowe, T., ed. *Multiphase Flow Handbook*. 2006, CRC Taylor & Francis Group: Boca Raton.
21. Dombrowski, N. and T.L. Lloyd, *Atomisation of liquids by spinning cups*. The Chemical Engineering Journal, 1974. **8**(1): p. 63-81.
22. Alcock, R. and D. Froehlich, *Analysis of Rotary Atomizers*. American Society of Agricultural Engineers, 1986. **29**(6): p. 6.
23. Masayuki, S., *Formation of Uniformly Sized Liquid Droplets Using Spinning Disk Under Applied Electrostatic Field*. IEEE Transactions on Industry Applications, 1991. **27**(2): p. 7.
24. Teunou, E. and D. Poncelet, *Rotary Disc Atomisation for Microencapsulation Applications-Prediction of the Particle Trajectories*. Journal of Food Engineering, 2005. **71**(4): p. 9.
25. Willauer, H.D., et al., *Critical evaluation of rotary atomizer*. Petroleum Science and Technology, 2006. **24**(10): p. 1215-1232.

26. *Putting some spin into atomisation*. Metal Powder Report, 2005. **60**(11): p. 28-30.
27. Lin, S.P. and R.D. Reitz, *Drop and spray formation from a liquid jet*, in *Annual Review of Fluid Mechanics*. 1998. p. 85-105.
28. Faeth, G.M., L.P. Hsiang, and P.K. Wu, *Structure and breakup properties of sprays*. International Journal of Multiphase Flow, 1995. **21**(Suppl): p. 99-127.
29. Wijshoff, H. *Drop formation mechanisms in piezo-acoustic inkjet*. in *2007 NSTI Nanotechnology Conference and Trade Show - NSTI Nanotech 2007, Technical Proceedings*. 2007.
30. Wang, Y. and J. Bokor, *Ultra-High-Resolution Monolithic Thermal Bubble Inkjet Print Head*. Journal of Microlithography, Microfabrication, and Microsystems, 2007. **6**(4): p. 10.
31. Le, H.P., *Progress and trends in ink-jet printing technology*. Journal of Imaging Science and Technology, 1998. **42**(1): p. 49-62.
32. Meacham, J.M., et al., *Micromachined ultrasonic droplet generator based on a liquid horn structure*. Review of Scientific Instruments, 2004. **75**(5 PART 1): p. 1347-1352.
33. Perçin, G. and B.T. Khuri-Yakub, *Piezoelectrically Actuated Flexensional Micromachined Ultrasound Droplet Ejectors*. IEEE Transactions on Ultrasonics, Ferroelectrics, and Frequency Control, 2002. **49**(6).
34. Dhand, R., *Nebulizers that use a vibrating mesh or plate with multiple apertures to generate aerosol*. Respiratory Care, 2002. **47**(12): p. 1406-1416; discussion 1416.
35. Waldrep, J.C. and R. Dhand, *Advanced nebulizer designs employing vibrating mesh/aperture plate technologies for aerosol generation*. Current Drug Delivery, 2008. **5**(2): p. 114-119.
36. Lacas, F., et al., *Design and performance of an ultrasonic atomization system for experimental combustion applications*. Particle and Particle Systems Characterization, 1994. **11**(2): p. 166-171.
37. Gañán-Calvo, A.M. and A. Barrero, *A novel pneumatic technique to generate steady capillary microjets*. Journal of Aerosol Science, 1999. **30**(1): p. 117-125.

38. Snyder, H.E. and R.D. Reitz, *Direct droplet production from a liquid film: A new gas-assisted atomization mechanism*. Journal of Fluid Mechanics, 1998. **375**: p. 363-381.
39. Snyder, H.E. and R.D. Reitz, *Development of micro-machining techniques for air-assisted liquid atomization*. Experimental Thermal and Fluid Science, 1999. **20**(1): p. 11-18.
40. Wang, S.H., J.S. Chang, and A.A. Berezin, *Atomization characteristics of electrohydrodynamic limestone-water slurry spray*, in *7th International Conference on Electrostatics*, J.o. Electrostatics, Editor. 1993. p. 235-246.
41. Okuda, H. and A.J. Kelly, *Electrostatic atomization-experiment, theory and industrial applications*, in *37th Annual Meeting of the Division of Plasma Physics of the American Physical Society*, P.o. Plasmas, Editor. 1996, AIP, USA: Louisville, KY, USA p. 2191-2196.
42. Kim, M.C., S.Y. Lee, and W. Balachandran, *Change of atomization performance with selection of nozzle materials in electrohydrodynamic spraying*. Atomization and Sprays, 2004. **14**(2): p. 175-190.
43. Rosell-Llompart, J. and J. Fern  ndez de la Mora, *Generation of monodisperse droplets 0.3 to 4  $\mu$ m in diameter from electrified cone-jets of highly conducting and viscous liquids*. Journal of Aerosol Science, 1994. **25**(6): p. 1093-1119.
44. Lastow, O. and W. Balachandran, *Novel low voltage EHD spray nozzle for atomization of water in the cone jet mode*. Journal of Electrostatics, 2007. **65**(8): p. 490-499.
45. Rodes, C., et al., *Measurements of the Size Distribution of Aerosols Produced by Ultrasonic Humidification*. Aerosol and Science Technology, 1990. **13**: p. 10.
46. Barreras, F., H. Amaveda, and A. Lozano, *Transient High-Frequency Ultrasonic Water Atomization*. Experiments in Fluids, 2002. **33**: p. 9.
47. Sindayihebura, D., M. Dobre, and L. Bolle, *Experimental Study of Thin Liquid Film Ultrasonic Atomization*, in *Department of Mechanical Engineering*. 1997, Universite Catholique de Louvain: Louvain, Belgium.
48. Lang, R.J., *Ultrasonic Atomization of Liquids*. The Journal of the Acoustical Society of America, 1962. **34**(1): p. 6-8.

49. Flament, M.P., P. Leterme, and A. Gayot, *Study of the technological parameters of ultrasonic nebulization*. Drug Development and Industrial Pharmacy, 2001. **27**(7): p. 643-649.
50. Yule, A.J. and Y. Al-Suleimani, *On droplet formation from capillary waves on a vibrating surface*. Proceedings of the Royal Society A: Mathematical, Physical and Engineering Sciences, 2000. **456**(1997): p. 1069-1085.
51. Dumouchel, C., D. Sindayihebura, and L. Bolle, *Application of the maximum entropy formalism on sprays produced by ultrasonic atomizers*. Particle and Particle Systems Characterization, 2003. **20**(2): p. 150-161.
52. Dobre, M. and L. Bolle, *Practical design of ultrasonic spray devices: Experimental testing of several atomizer geometries*. Experimental Thermal and Fluid Science, 2002. **26**(2-4): p. 205-211.
53. Tsai, S.C., et al. *Efficient atomization using MHz MEMS-based ultrasonic nozzles*. in *Materials Research Society Symposium Proceedings*. 2005.
54. Wolf-Dietrich Drews, L. and K. Klaus Van der Linden, *Ultrasonic MHz Oscillator, in Particular for Liquid Atomization*. 1990, Siemens Aktiengesellschaft: United States of America.
55. Paneva, R., et al., *Micromechanical ultrasonic liquid nebulizer*. Sensors and Actuators, A: Physical, 1997. **62**(1-3): p. 765-767.
56. Lozano, A., et al., *High-frequency ultrasonic atomization with pulsed excitation*. Journal of Fluids Engineering, Transactions of the ASME, 2003. **125**(6): p. 941-945.
57. Miller, C. and A. Hadjicostis, *Piezoelectric Mist Generation Design*. 2007: US.
58. Mitsui, S., M. Takahashi, and K. Watanabe, *Ultrasonic Wave Nebulizer Driving Circuit*. 1982, TDK Electronics Co.: United States.
59. Yang, C., et al., *Ultrasonic Nebulizer for Producing High-Volume Sub-Micron Droplets*. 2006: USA.
60. Zhang, G., et al., *High-frequency ultrasonic atomization for drug delivery to rodent animal models - Optimal particle size for lung inhalation of difluoromethyl ornithine*. Experimental Lung Research, 2008. **34**(5): p. 209-223.

61. Jungmyoung, J., et al., *High-Frequency Surface Acoustic Wave Atomizer*. Sensors and Actuators A (Physical), 2008. **145-146**: p. 41.
62. Chono, K., et al., *Novel Atomization Method Based On SAW Streaming*, in *2003 IEEE Ultrasonics Symposium - Proceedings*. 2003, Institute of Electrical and Electronics Engineers Inc. p. 1786-1789.
63. Kurosawa, M., A. Futami, and T. Higuchi, *Characteristics of Liquids Atomization Using Surface Acoustic Wave*, in *Proceedings of International Solid State Sensors and Actuators Conference (Transducers '97)*. 1997, IEEE, New York, NY, USA: Chicago, IL, USA. p. 801-804.
64. Kurosawa, M., T. Watanabe, and T. Higuchi. *Surface acoustic wave atomizer with pumping effect*. in *Proceedings of the IEEE Micro Electro Mechanical Systems*. 1995.
65. Soluch, W. and T. Wrobel, *Low Driving Power SAW Atomiser*. Electronics Letters, 2006. **42**(24): p. 1.
66. Shirley, C. and S. Chen, *Recent advances on ultrasound-modulated two-fluid (UMTF) atomization and its applications*, in *Molecular and Quantum Acoustics*. 2002. p. 13.
67. Tsai, S.C., et al., *Ultrasonic spray pyrolysis for nanoparticles synthesis*. Journal of Materials Science, 2004. **39**(11): p. 11.
68. Shen, S.C., Y.J. Wang, and Y.Y. Chen, *Design and fabrication of medical micro-nebulizer*. Sensors and Actuators, A: Physical, 2008. **144**(1): p. 135-143.
69. Bachalo, W.D. *Droplet Analysis Techniques: Their Selection and Applications*. in *ASTM Special Technical Publication*. 1984.
70. Zaidi, S.H., *Difficulties in measuring liquid droplet size distributions using laser diffraction technique*. Atomization and Sprays, 1998. **8**(4): p. 439-452.
71. Corcoran, T.E., et al., *Optical measurement of nebulizer sprays: A quantitative comparison of diffraction, phase Doppler interferometry, and time of flight techniques*. Journal of Aerosol Science, 2000. **31**(1): p. 35-50.
72. Azzopardi, B.J., *Measurement of drop sizes*. International Journal of Heat and Mass Transfer, 1979. **22**(9): p. 1245-1279.
73. Tate, T.W., *Immersion Sampling of Spray Droplets*. AIChE, 1961. **7**(4): p. 4.



74. Malot, H. and J.B. Blaisot, *Droplet size distribution and sphericity measurements of low-density sprays through image analysis*. Particle and Particle Systems Characterization, 2000. **17**(4): p. 146-158.
75. Hedrih, K., V. Babovi, and D. Sarkovi, *An auxiliary size distribution model for the ultrasonically produced water droplets*. Experimental Thermal and Fluid Science, 2006. **30**(6): p. 559-564.
76. Yuan, J., et al., *Measurement and analysis of water mist droplet size based on machine vision*. Guangxue Xuebao/Acta Optica Sinica, 2009. **29**(10): p. 2842-2847.
77. Agu, R.U., et al., *The lung as a route for systemic delivery of therapeutic proteins and peptides*. Respiratory Research, 2001. **2**(4): p. 198-209.
78. Crowe, C., M. Sommerfeld, and Y. Tsuji, *Multiphase flows with droplets and particles*. 1998: CRC Press LLC.
79. Reist, P., *Aerosol science and technology*. 1993: McGraw-Hill Inc.
80. Hinds, W., *Aerosol technology: properties, behavior, and measurement of airborne particles*. 1999: John Wiley & Sons, Inc.
81. Davis, E. and G. Schweiger, *The airborne microparticle: its physics, chemistry, optics and transport*. 2002: Springer.
82. Sanner, B.M., et al., *Effect of continuous positive airway pressure therapy on infectious complications in patients with obstructive sleep apnea syndrome*. Respiration, 2001. **68**(5): p. 483-487.
83. (CIBSE), C.I.o.B.S.E., *Building Control Systems*. 2000: Butterworth-Heinemann.
84. Steinhauer, K. and P. Goroncy-Bermes, *Investigation of the hygienic safety of continuous positive airways pressure devices after reprocessing*. Journal of Hospital Infection, 2005. **61**(2): p. 168-175.
85. Agency, U.S.E.P., *Use and Care of Home Humidifiers*, in *Indoor Air Facts N8*, A.a. Radiation, Editor. 1991. p. 3.
86. Kleinstreuer, C., Z. Zhang, and Z. Li, *Modeling airflow and particle transport/deposition in pulmonary airways*. Respiratory Physiology and Neurobiology, 2008. **163**(1-3): p. 128-138.

87. Crook, B. and J.L. Sherwood-Higham, *Sampling and assay of bioaerosols in the work environment*. Journal of Aerosol Science, 1997. **28**(3): p. 417-426.
88. Wenzel, M., et al., *Sterile water is unnecessary in a continuous positive airway pressure convection-type humidifier in the treatment of obstructive sleep apnea syndrome*. Chest, 2005. **128**(4): p. 2138-2140.
89. Rodriguez Gonzalez-Moro, J.M., et al., *Bacterial colonization and home mechanical ventilation: Prevalence and risk factors*. Arch Bronconeumol, 2004. **40**(9): p. 392-396.
90. Bartley, J. and D. Young, *Ultrasound as a treatment for chronic rhinosinusitis*. Medical Hypotheses, 2009. **73**(1): p. 15-17.
91. Ortolano, G.A., et al., *Filters reduce the risk of bacterial transmission from contaminated heated humidifiers used with CPAP for obstructive sleep apnea*. Journal of Clinical Sleep Medicine, 2007. **3**(7): p. 700-705.
92. *Insittec Technical Specifications Manual (Man0297)*, Malverin Instruments Ltd.
93. *Spraytec Installation Manual (Man0300)*. 1999, Malvern Instruments Ltd.
94. *Liquid Evaporation Model Tutorial. Release 1.2.1*. 2009, ANSYS Inc.

## DECLARATION BY APPLICANT

I declare that the information provided by me in this application is true and complete.

I have read and understand the conditions of candidature outlined in the current Postgraduate Handbook and am prepared to accept them in full.

This proposal has been discussed between my supervisors and myself and I therefore submit it for confirmation of my candidature.

**Applicant's signature:**

**Date:**

.....

.....